UNIVERSIDADE TÉCNICA DE LISBOA

INSTITUTO SUPERIOR TÉCNICO

Influence of Interference in UMTS Capacity for Simultaneous Operation of TDD and FDD Modes

Luís Carlos Barruncho dos Santos Gonçalves

(*Licenciado*)

Dissertation submitted for obtaining the degree of

Master in Electrical and Computer Engineering

Supervisor: Professor LUÍS MANUEL DE JESUS SOUSA CORREIA

Jury

President: Professor LUÍS MANUEL DE JESUS SOUSA CORREIA

Members: Professor AMÉRICO MANUEL CARAPETO CORREIA

Professor RUI MIGUEL HENRIQUES DIAS MORGADO DINIS

April 2008

UNIVERSIDADE TÉCNICA DE LISBOA

INSTITUTO SUPERIOR TÉCNICO

Influence of Interference in UMTS Capacity for Simultaneous Operation of TDD and FDD Modes

Luís Carlos Barruncho dos Santos Gonçalves

(*Licenciado*)

Dissertation submitted for obtaining the degree of

Master in Electrical and Computer Engineering

Supervisor: Professor LUÍS MANUEL DE JESUS SOUSA CORREIA

Jury

President: Professor LUÍS MANUEL DE JESUS SOUSA CORREIA

Members: Professor AMÉRICO MANUEL CARAPETO CORREIA

Professor RUI MIGUEL HENRIQUES DIAS MORGADO DINIS

April 2008

To Cláudia and my parents

Acknowledgements

Above all, I wish to express my deep and sincere gratitude to Professor Luís M. Correia for his friendship, unconditional support, enthusiasm, great help, corrections, productive ideas and discussions throughout this work. His discipline, constant work directives and guidelines proved of great value and were determinant to the completion of this thesis. A special thank you for giving me the opportunity to work under his guidance.

I am also grateful for having the opportunity to use the facilities from *Instituto de Telecomunicações* for several times, allowing me to develop my work in an exclusive technological environment.

Special thank you to all GROW members for their knowledge sharing and help, directly and indirectly, and for being there whenever their help and knowledge was necessary.

Thank you also to João Cardeiro and Daniel Sebastião for their help and support on several stages of this thesis.

A special gratitude to my parents, for their unconditional support, always present, not only during this work, but also in my whole live, allowing me to be able to develop this work of which I am so proud.

I am also grateful to all my friends that shared a little of this work with me, and for withstanding my moments of less presence.

A special thank you to Luís Pires, for all the ideas, all the help, good and bad moments, and all the support and work developed together.

Finally, to Cláudia for everything.

Abstract

This work focuses on the performance analysis of UMTS TDD, in the presence of interference. In order to account for interference effects, a model was developed, allowing interference estimation on real cellular network deployments.

In TDD, the degree and level of synchronism changes the complexity of interference scenarios. Two different interference studies are presented: in the presence and without network synchronisation. Two radio resource management algorithms were developed: code and timeslot interference management.

The concept of non-destructive interference, which does not delay permanently an interference victim, is introduced.

Interference studies addressing the asymmetric nature of the TDD frame and lack of synchronisation between adjacent cells are presented. Two asymmetries fit the network, 9D3U and 10D2U.

In general, the interference model is able to characterise any given cellular deployment, and generate outputs to feed an automatic network deployment algorithm, allowing automatic network topology generation based on interference analysis.

Finally, the interference model can be applied not only to UMTS TDD, but generally to TDD based systems.

Keywords

UMTS. TDD. FDD. Interference modelling. Resource Management.

Resumo

O presente trabalho centra-se na análise de desempenho em UMTS TDD, na presença de interferência. Para se modelar os seus efeitos, foi desenvolvido um modelo de estimação de interferência, posteriormente utilizado para análise de uma topologia de rede real.

Em TDD, o grau e nível de sincronismo de rede altera a complexidade dos cenários de interferência. Dois estudos de interferência são apresentados: com e sem a presença de sincronismo na rede. Dois algoritmos de gestão de recursos foram desenvolvidos: códigos e interferência por timeslot.

É introduzido o conceito de interferência não-destrutiva, que não atrasa permanentemente uma vítima de interferência.

São apresentados vários estudos de assimetria da trama TDD e de falta de sincronismo entre células adjacentes. Duas assimetrias seriam as ideais: 9D3U e 10D2U.

O modelo desenvolvido consegue caracterizar qualquer topologia celular e gerar resultados que possam ser passados a um processo de planeamento celular automático, permitindo a geração de uma topologia de rede baseada nos níveis de interferência.

Finalmente, o modelo de interferência pode ser aplicado a qualquer sistema baseado em TDD.

Palavras-chave

UMTS. TDD. FDD. Modelo de Interferência. Gestão de Recursos.

Table of Contents

List of Figures

List of Tables

List of Acronyms

ACIR	Adjacent Channel Interference Ratio
ACLR	Adjacent Channel Leakage Ratio
AMC	Adaptive Modulation and Coding
BS	Base Station
CDMA	Code Division Multiple Access
CN	Core Network
CS	Circuit Switched
C&S	Control and Signaling
DL	DownLink
DRNS	Drift RNS
FDD	Frequency Division Duplex
FDMA	Frequency Division Multiple Access
FTP	File Transfer Protocol
GGSN	Gateway GPRS Support Node
GIS	Geographic Information System
GPRS	General Packet Radio System
GMSC	Gateway MSC
GSM	Global Systems for Mobile Communications
HARQ	Hybrid Automatic Request
HBR	High Bit Rate
HCR	High Chip Rate
HHO	Hard HO
HLR	Home Location Register
HO	HandOver
HSDPA	High Speed DL Packet Access
HSUPA	High Speed UL Packet Access
LBR	Low Bit Rate

LCR	Low Chip Rate
LoS	Line of Sight
MAT	Medium Access Technology
MCL	Minimum Coupling Losses
ME	Mobile Equipment
MSC	Mobile Switching Centre
MT	Mobile Terminal
MUD	Multi User Detection
NB	Node B
NLoS	Non LoS
OVSF	Orthogonal Variable Spreading Factor
PC	Power Control
PS	Packet Switch
QoS	Quality of Service
RAB	Radio Access Bearer
RNC	Radio Network Controller
RNS	Radio Network Subsystem
RRM	Radio Resource Management
SF	Spreading Factor
SHO	Soft HO
SIR	Signal to Interference Ratio
SMS	Short Message Service
SRNS	Serving RNS
SSHO	Softer HO
TD-CDMA	Time-Division CDMA
TDD	Time Division Duplex
TDMA	Time Division Multiple Access
TS	Time Slot
UL	UpLink
UMTS	Universal Mobile Telecommunications System
USIM	UMTS SIM
UTRA	UMTS Terrestrial Radio Access
VoIP	Voice over IP

VLR	Visitor Location Register
WCDMA	Wideband CDMA
WiMAX	Worldwide interoperability for Microwave Access

List of Symbols

α	Orthogonality Factor
$\overline{\alpha}$	Average orthogonality factor in the cell
β	Interference Reduction Factor
δ_{offset}	Ratio between the asynchrony offset time and the TS duration
λ	Wavelength
Δh_b	Difference between the BS height and the mean building height
Δh_m	Difference between mean building height and MT height
η	Cell Load Factor
η_{DL}	DL Load Factor
η_{UL}	UL Load Factor
η_{DL}^{FDD}	DL Load Factor for FDD
η_{DL}^{TDD}	DL Load Factor for TDD
η_{UL}^{FDD}	UL Load Factor for FDD
η_{UL}^{TDD}	UL Load Factor for TDD
$\overline{\tau}_{delay}$	Mean data delay
υ	Activity factor
υ_j	Activity factor for MT j
Ψ	Street orientation angle
b	Building separation
B_i	Information Bandwidth
B_t	Transmitted Bandwidth
d	Distance between Transmitter and Receiver
$d_{Building}$	Average separation between rows of buildings
E_b	Bit energy
f	Frequency
F	Fraction of the inter-cell interference
F_{FM}	Fast fading margin

F_M	Fading margin
F_{SM}	Slow fading margin
G_p	Processing gain
G_{Per}	Lenght of the guard period
G_r	Maximum receiver antenna gain
G_t	Maximum transmitter antenna gain
G_{SH}	Soft-handover gain
h_{Base}	BS height
$h_{Building}$	Building height
h_{Mobile}	MT height
i	Inter-to intra-cell interferences ratio
I_{Intra}	Intra-cell interference
I_{Inter}	Inter-cell interference
k	Boltzmann constant
L_{Body}	User body loss
L_c	Cable losses
$L_{MT\text{-}MT}$	Path loss between MTs
L_{p_j}	Allowed path loss between BS and MT_j
L_x	Additional attenuations in a link
L_{Other}	Additional attenuations (e.g., car or bulding)
NF	Noise figure of the MT receiver front-end
M	Size of the symbol set
M_{int}	Interference margin
N_b	Number of blocked MTs
N_{cov}	Number of covered MTs
N_{CS}	Total number of CS calls
N_{CS_b}	Number of blocked CS calls
N_d	Number of delayed MTs
N_{ft}	Number of destructively interfered MTs
N_{low}	Number of non destructively interfered MTs
N_0	Spectral thermal noise density
N_{PoleUL}	Pole number of MTs in UL
N_{PoleDL}	Pole number of MTs in DL
N_{PS}	Number of PS connections

N_{PS_d}	Number of delayed PS connections
N_s	Number of served MTs
N_{Slots}	Number of slots used for a certain service
N_T	Total noise plus interference
N_U	Number of MTs on the system
P_b	Blocking probability
P_d	Delay probability
P_{ft}	Probability of forced termination
P_{low}	Probability of low quality access
P_{ncov}	Non-covered MT probability
P_{Rx}	Receiver-input power
P_r	Power at the antenna terminal
$P_{Rx\min}$	Receiver sensitivity for a given service bearer
P_s	Served probability
P_t	Transmission power (delivered to the antenna)
R	Transmitter-receiver separation
R_b	Bit rate
R_{bj}	Bit rate of MT *j*
R_c	Chip rate
R_{code}	Code rate
R_n	Service bit rate of the *n* RAB
R_x	Receive
S	Received Signal Power
SF	Spreading Factor
SIR_{UL}	UL Signal to Interference Ratio
SIR_{DL}	DL Signal to Interference Ratio
T	Temperature
T_f	Frame duration
t_{offset}	Offset time
$t_{timeslot}$	TS time
T_S	Slot duration
T_x	Transmit
w	Street width
x	Horizontal distance between the MT and the diffracting edges

Chapter 1

Introduction

This chapter gives a brief overview of the thesis. It starts with the work's scope and motivations, and finishes presenting the objectives. Also the current State-of-the-Art of the technology in which this work is based is presented. At the end of the chapter, the thesis structure is provided.

1.1 Overview

A long way has been left behind, since it was first heard about the 3rd Generation (3G) of mobile systems, namely IMT-2000 or even Universal Mobile Telecommunications System (UMTS). Many thoughts were put ahead inside standardisation committees, leading to the development of several standards and a variety of multiple radio access techniques. 3G is characterised by:

- converging to a common world standard;
- high speed data services;
- using the available spectrum more efficiently.

3G mobile communications networks were designed to support various service types, in a clear evolution to what was offered by older cellular network systems. By the end of 2004, there were approximately 17 million UMTS subscribers, whereas that number rose to almost 50 million by February 2006 [HoTo06].

With the enormous success of 3G mobile communication services, operators afforded huge investments for network infrastructures. Due to high costs and scarcity of radio resources, accurate and efficient mobile network planning is of outmost importance. With the rapid growth of networks and number of Mobile Terminals (MTs), efficient quantitative methods to support decisions for Base Station (BS) location have become essential. This need is now even more acute with the advent of 3G and 3rd and half Generation (3.5G) networks, such as UMTS High Speed Downlink Packet Access (HSDPA)/ High Speed Uplink Packet Access (HSUPA).

3G introduced packet-based applications in an efficient way. The most known are web browsing, music and games download, mobile-TV streaming, as well as real time video sharing. Additionally, push email services, online gaming and wireless broadband access became available. These services have all the characteristics that a network based on High Speed Packet Access (HSPA) or Time Division Duplex (TDD) must offer; the majority of them is packet based and need asymmetric frame structures. TDD attracted great attention for its capability of flexible and efficient usage of frequency resources in the transfer of highly asymmetric and bursty data traffic since it is best suited for this type of traffic, such as Internet or other data centred services, based on IP.

The air interface of the UMTS covers both Frequency and Time Division Duplex (FDD and

TDD) modes. These air interfaces use different multiple access technologies: Wideband Code Division Multiple Access (WCDMA) for FDD and a hybrid Time Divison Multiple Access/Code Division Multiple Access (TDMA/CDMA) for TDD. Both technologies allowed deploying new services, such as Video Telephony, Web Browsing/Wireless Internet, and Email downloading, among others. UMTS was clearly developed in order to provide better packet switched (PS) services instead of circuit switched (CS) ones, with former CS-based voice services to be replaced by VoIP. All these services have higher bit rates and their penetration rates are continuously increasing, but still VoIP has the higher penetration rates. At the limit, voice-like services, and Low Bit Rate (LBR) services decrease their penetration rates, opposite to High Bit Rate (HBR) ones; multimedia services will be very successful among the population, having the higher penetration rates. Despite this successful introduction of new services, the two UMTS modes are quite different. The HBR services have a different nature concerning traffic flow: considering, e.g., Web browsing or file transfer services, the traffic in Downlink (DL) is greater than in the opposite link. This may lead to bandwidth waste in FDD as its band pairs are fixed, and it may not be completely used in Uplink (UL). So, a question arises: what if the unused portion of the UL bandwidth could be allocated for DL, thus, increasing the overall DL bit rate? This question was the driver for the development of TDD.

TDD being of asymmetric nature, has the advantage of accommodating diverse variable bit rate services, which is possible by assigning a different number of Time Slots (TSs) in UL and DL. TDD presents itself as being more spectrum efficient and flexible, particularly due to the possibility of changing traffic patterns and/or how much traffic goes to or comes from individual MTs. Taking into consideration that spectrum is a very limited resource, the spectrum efficiency, and flexibility offered by TDD are very advantageous.

Some significant advantages of TDD over FDD are summarised as follows:

- TDD is more spectrum efficient than FDD, since the latter cannot be used in environments where the operator does not have enough bandwidth to provide the required guard band between transmit and receive channels;
- TDD is more flexible than FDD, fulfilling the needs to dynamically reconfigure the allocated upstream and downstream bandwidth in response to customer needs;
- TDD does not require a pair of frequency blocks, which is indispensable for FDD.

According to Release 99 of 3GPP, WCDMA should support 2 Mbps of bit rate for DL,

nowadays far away from the actual user's needs, and from the always-on behavior of all IP based services. Release 99 is technologically limited to 2 Mbps for TDD and 384 kbps for FDD in DL, not being possible to support higher bit rates.

More recently, HSDPA appeared (with different modulation schemes, up to 16-QAM) being a packet-based data service in WCDMA DL with nominal data rates up to 14.4 Mbps. HSDPA features Adaptive Modulation and Coding (AMC), Hybrid Automatic Request (HARQ), fast cell search, and advanced receiver design. 3GPP's Release 4 specifications provide efficient IP support, enabling provision of services through an all-IP core network, and Release 5 specifications focus on HSDPA to provide higher data rates to support packet-based multimedia services. HSDPA is backward compatible with Release 99 and current deployments support 1.8, 3.6, 7.2 and 14.4 Mbps in DL.

When this work started, FDD was beginning to be deployed and TDD was under a lot of research due to its capabilities to support HBR services. That was one of the main driving factors to develop this work based on a real network, as well as studying the impacts of deploying TDD on a network without changing the cellular deployment. Since then, technology evolved, and TDD was deployed only in a few countries, but never spread widely. So the question urges: why presenting a study on TDD, three years later, taking into consideration that TDD never was deployed by cellular operators, being replaced by a new cellular technology? The answer to this question resides on the Medium Access Technology (MAT) as well as this work's objectives. Underlying TDD, a TDMA MAT exists which is used not only for UMTS. Several other systems based on this technology exist, and several studies are still made over this MAT (e.g. WiMAX), mainly dynamic channel assignment schemes, and interference reduction algorithms. Interference is the main driver of this work: what impacts interference has on a UMTS-TDD network when deployed with the same cellular topology used for FDD? How does interference impact over the network's overall capacity? What techniques may be used to reduce interference effects? This work focuses on interference aspects of both FDD and TDD modes of UMTS, but mainly on the latter. Interference considerations and studies go down to the TS level, thus, being useful for other cellular networks based on TDMA. TDD being a hybrid network is limited by interference in the CDMA component, applied to the TS nature of TDMA.

This thesis is centred on the development of an interference model to be applied to a real TDD network topology. Most interference studies and models are derived from a theoretical scenario with two adjacent BS, but are not applied to a real network topology. The

interference model presented in the current work is applied to a real existing network, with interference calculations based on is numerical part. The developed interference model has an adaptive nature, as opposite to the classic studies and models, due to the fact that interference is seen not as a whole destructive phenomenon, but split into two different components: destructive and non-destructive. The model is adaptive because interference calculations depend on the Radio Resource Management (RRM) algorithm. With classic models, if an MT suffers from excessive interference, it is outaged due to interference, despite the fact that it may be using several TSs.

In a TDD system with HBR services, it makes no sense to simply outage or delay an MT based on the global interference that it suffers. The proposed model checks how many TSs each MT is using and calculates the E_b/N_o for each one, with interference effects accounted. If the E_b/N_o value of each TS is below the target one, the MT ceases servicing in that TS only, thus having its service bit rate reduced. This is the idea behind the concept of non-destructive interference. If on all TSs the MT does not meet the E_b/N_o target requirements, then it is destructively delayed due to interference. This is the idea behind the destructive interference concept. By not considering the number of TSs an MT is servicing on, an interference model does not represent the reality of TDD, therefore producing unrealistic results. The developed model is adaptive to interference conditions in every snapshot of the reference scenario and network topology. This is an important feature because this thesis objective is also to apply the developed interference model to a real network, and evaluate its interference levels.

In order to be able to allow this behavior an RRM algorithm is developed, depending directly on the interference of each TS. Taking into consideration that this model is to be applied to an existing network, the interference model must implement all interference calculations within a single operator network, but also allow the inter-operator interference calculations to be made, by simply adding an Adjacent Channel Leakage Ratio (ACLR) value [HoTo01]. Two other novelties of the developed interference model, more as a consequence of using a real network are that cell overlapping is considered, and all interference calculations take that into consideration and also that MTs distribution is non-uniform on the cells, on the contrary of the majority of interference studies.

Summing up, the current work introduces and focuses on the following concepts and key words:

- destructive and non-destructive interference;

- adaptive interference model;
- interference-dependent RRM algorithm;
- intra-operator interference modelling;
- TDD interference modelling;
- non uniform MT distribution on overlapping cellular network (interference hot-spots);
- interference studies on a real network topology.

TDD is attractive and eases asymmetric or uneven allocation of resources to UL and DL, which supports a more efficient exploitation of the existing spectrum bands. However, since the same frequencies are used for UL and DL, new interference situations that do not occur in FDD appear in TDD. Therefore, interference is a more challenging problem in TDD than in FDD. In FDD, taking into consideration that different frequencies are used for both links, there are two interference scenarios: BS to MT and MT to BS. In this mode, considering a simple scenario of two adjacent cells, all BSs and MTs produce the same kind of interference. In an FDD network, there is negligible interference among BSs and MTs since duplex frequency separation among UL and DL is relatively large. In FDD, therefore, only BS to MT and MT to BS interference exists.

When considering TDD, with shared frequencies for UL and DL, no duplex separation exists among the two links, thus, separation exists in the time domain. Also, adjacent cells or operators may not be synchronised in time, therefore, additional interference scenarios occur. MT to MT interference occurs when an MT is transmitting and another MT is receiving in specific TS mapped onto the same carrier frequency in an adjacent cell. BS to BS interference occur when a BS is transmitting and another BS is receiving at the same time in a given TS, in adjacent cells. BS to BS interference depends heavily on path loss between the two BS, but it can be reduced with the aid of a careful network planning. Due to the stochastic or statistical nature of MT's locations inside a cell, MT to MT interference cannot be completely avoided by network planning.

BS to BS interference is the most serious source of inter-cellular interference in a TDD/CDMA scenario. In order to reduce it, synchronism among adjacent BSs is required as well as the same frame asymmetry. In this work, inter-operator interference is not considered; therefore, all BSs are under control of the same operator, reducing the complexity of dealing with the different interference scenarios.

1.2 Challenge and Contents

The increasing number of MTs of modern mobile radio networks, particularly regarding 3G, 3.5G and 4th Generation (4G) mobile communications, requires tools for planning and analysis of network topologies.

Since all signals share the same spectrum in WCDMA, interference is key element regarding capacity and coverage. CDMA based networks are interference limited, hence, interference plays a major role in the global network analysis and planning. Interference depends greatly on the cellular deployment, and is proportional to the number of deployed BS. Especially in urban areas, more BSs exist, thus, more interference occurs. In 3G networks, BS power is the shared resource. HBR services are expected to grow in penetration rates and with it interference becomes a more serious problem. The majority of TDD interference studies present several interference calculation schemes based on theoretical two-BS based scenarios. The challenge behind the current work is to develop an interference model and apply it to a real network and study its interference levels and effects. Also, the development of two resource management algorithms and also a channel allocation algorithm that would complete the interference model is an important challenge. The major novelties of this work are the concept of destructive and non-destructive interference, the development of an adaptive interference model, interference-dependent RRM algorithms and lastly applying the model to a real network.

Chapter 2 focuses on the UMTS network, its architecture and description of the different services. Chapter 3 focuses on network planning, starting with general capacity aspects and description of the link budget calculations in UL/DL. It also includes a description of the existing FDD simulator and the new TDD simulator, developed from scratch. The chapter finishes with interference studies for both modes of UMTS, and with the developed interference model.

Chapter 4 focuses deeply on the description of the developed TDD simulator and the analysis of the interference model and its interference calculations. A detailed description of the interference model is provided and, ending the chapter, assessment studies are presented.

Chapter 5 provides an analysis of simulation results for all tested scenarios. It presents the studies and simulations made towards finding a reference scenario, and characterise it for FDD and TDD. This chapter finishes with the results of interference calculations as a function

of the frame asymmetry assuming that there is synchronisation among BSs and the results and effects of interference over the network when no synchronisation is considered. Chapter 6 presents the final conclusions and suggestions of future work to improve the developed interference algorithm.

Annex A provides a presentation of the used propagation models, the COST-231 Walfish-Ikegami model and interference specific propagation models. Annex B presents the link budget used in the developed simulator. Annex C presents the flowcharts of the most important parts of the simulator platform, and of the new algorithms developed for TDD and interference calculations, as well as the RRM algorithms. Annex D presents the validation studies for the general simulator, as well as interference specific validations. Annex E includes the statistical data that led to the choice of the reference scenario. Annex F supports Chapter 5 results, regarding the asymmetry studies that were developed and its effects on interference. Annex G presents additional statistics and results of the interference study when synchronism was not considered in the global network. Finally, Annex H presents the user's manual of the TDD simulator.

Chapter 2

General Aspects

This chapter provides an overview of UMTS, including its architecture, a brief description of the radio network system and RRM algorithms. At the end, an overview of services and applications is presented.

2.1 High Level Network Architecture

One of the biggest objectives in UMTS was the design of a network that could support a wide range of services, each one with its different needs in what concerns Quality of Service (QoS). This is one of the reasons why the system was design in a modular way, adopted by 3GPP, along with the possibility of evolving it to other more complex systems with great versatility.

As described in [3GPP00a], the UMTS architecture consists of a set of entities – the User Equipment (UE), the UMTS Terrestrial Radio Access Network (UTRAN), and the Core Network (CN). UTRAN consists of several Radio Network Subsystems (RNSs) connected to the CN by an interface called CN-UTRAN interface, *Iu*. The UE is connected to the UTRAN through the Radio Interface, *Uu*. Figure 2.1 depicts the network architecture.

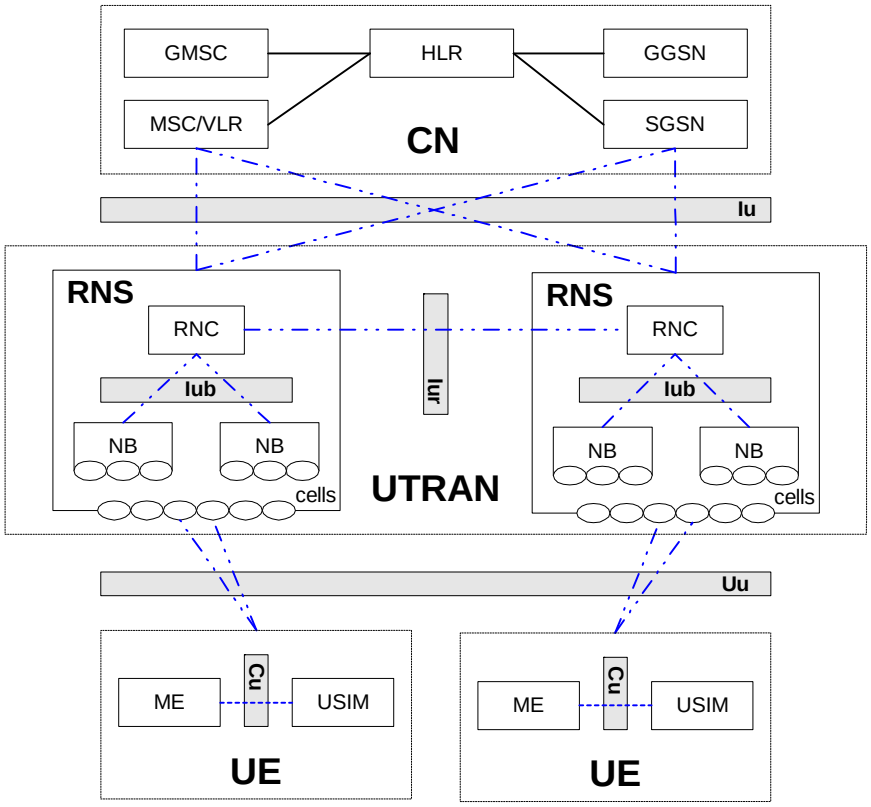

Figure 2.1 – UMTS High Level Architecture.

The CN is composed of two major domains: the CS and the PS. This two-dimensional architecture allows a smooth evolution from Global Systems for Mobile Communications/General Packet Radio System (GSM/GPRS) towards UMTS. The CN is formed by the following elements: the Home Location Register (HLR), Mobile Services Switching Centre/Visitor Location Register (MSC/VLR), GMSC (Gateway MSC), Serving

General Packet Radio System (GPRS) Support Node (SGSN) and the Gateway GPRS Support Node (GGSN).

CN functions may be summarised as follows:

- mobility management;
- operations, administration and maintenance;
- switching allowance;
- service availability;
- transmission of MT traffic between UTRAN(s) and/or fixed network(s).

Inside the UTRAN, each RNS is composed of the Radio Network Controller (RNC) and one or several Node Bs, generally known as BSs. The RNC is the entity that controls the radio resources in all the Node Bs connected to it. Besides the *Iu* and *Uu* interfaces, the Node Bs and their respective RNC are interconnected through the *Iub* interface. The Node B has the task to convert data between the *Uu* and *Iub* interfaces as well as contribute to RRM. RNSs are connected through their RNCs supported on another interface, *Iur*. Interfaces are further explained in the next subsection. UTRAN functions may be summarised as follows:

- handover;
- provision of radio coverage;
- RRM and control;
- system access control;
- security and privacy.

The Mobile Equipment (ME) and the UMTS Subscriber Identity Module (USIM) form the UE. Between the ME and the USIM there is a fifth interface, *Cu*. The ME is responsible for transmitting over the *Uu* interface, and, for each connection with the UTRAN, one and only one of the RNSs becomes the Serving RNS (SRNS), completing the interconnection between the *Iu* and *Uu* interfaces. If necessary, another RNS can support the Serving RNS (SRNS) by providing radio resources, becoming the Drift RNS (DRNS) [3GPP00a].

2.2 Radio System Description

In this section some of the most important aspects of the radio system are addressed.

UMTS was designed in order to support two different operation modes: TDD [3GPP03b] and FDD [3GPP03a]. For both modes, the original signal suffers a two-phase process, before

being transmitted. The first phase is known as channelisation in which the signal's bandwidth is increased by transforming each data symbol into a number of chips; the number of chips per data symbol is called the Spreading Factor (SF). After that, in the second phase, the spread signal is coded using a scrambling code [3GPP03c].

The independence between MT signals is achieved through the use of Orthogonal Variable Spreading Factor (OVSF) channelisation codes that preserve the DL orthogonality among MTs. This allows multiple services with variable bit rates to be carried over one physical resource. As the bit rate changes, the interface sees its power allocation adjusted in accordance to its needs, so that the QoS is guaranteed instantaneously. As referred before, there are two types of codes, channelisation and scrambling. The former perform channels separation in a single cell or in the MT, allowing different MTs to transmit simultaneously on the same channel. The latter are used to distinguish among cells and MTs, allowing multiples BSs on a same channel, whilst each MT is assigned a unique scrambling code [3GPP03e].

Each RF channel has a 4.4 MHz bandwidth, for both TDD and FDD. The wideband characteristic of WCDMA results in a performance gain compared to other cellular systems, by reducing the radio signal's fading. Another advantageous factor is the existence of fast Power Control (PC) in DL, which increases network performance, especially in indoor and low-speed outdoor environments, thus, increasing the overall system capacity. Table 2.1 shows a summary of the main FDD and TDD parameters.

Table 2.1 – Main FDD and TDD Parameters.

Main parameters	TDD	FDD
Multiple access method	CDMA / FDMA / TDMA	CDMA / FDMA
FDMA channel bandwidth [MHz]	4.4 (HCR) and three bands of 1.6 (LCR)	4.4
Frame duration [ms]	10	10
Number of TSs in UL	15	15
Number of TSs in DL	15	15
Chip rate [Mcps]	1.28 and 3.84	3.84
Modulation	QPSK	QPSK
Spreading factor UL	1 up to 16	4 up to 256
Spreading factor DL	1 up to 16	4 up to 512

FDD and TDD differ in the multiple-access technique. FDD uses direct sequence WCDMA (multiple-access based on CDMA/FDMA), while TDD uses Time Division CDMA (TD-

CDMA), which is a MAT based on CDMA/FDMA/TDMA. It can generally be said that the only place where FDD and TDD differ is the physical layer of the UTRAN protocol stack. All others protocols and system components are nearly the same.

The multiple access scheme used in FDD is adequate for services with symmetric traffic like voice. It is designed to be used in any kind of environment, namely in macro and micro cells with high mobility MTs. FDD frequency bands are [1920, 1980] MHz for UL and [2110, 2170] MHz for DL [3GPP03a]. Each timeslot is composed of 10 bits, with a corresponding length of 2 560 chips. The radio frame has a chip length of 38 400 chips. The number of slot bits may sometimes vary according to the different physical channels. Greater details on the frame structures for both UL and DL can be found in [3GPP00d].

TDD is advantageous for services with high-density asymmetric traffic, as IP based services, for instance. It is designed to be used mainly in indoor environments or in hot-spot areas with low mobility MTs.

The TDD frequency bands are [1900, 1920] and [2020, 2025] MHz [3GPP03b]. The TDMA is subdivided into 15 TSs of 2560 chips each, so that the TS duration is 666 μs, as shown in Figure 2.2. Each TS can be allocated to UL or DL (at least one in each link).

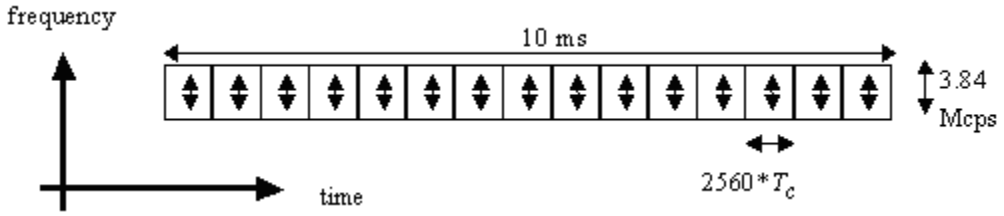

Figure 2.2 – TDD frame structure.

With such flexibility, TDD can be adapted to different environments and deployment scenarios [3GPP03d]. Figure 2.3 shows examples for multiple and single switching point configurations, as well as symmetric and asymmetric UL/DL allocations of the TDMA frame structure. Each TS comprises several (maximum 16) orthogonal spreading codes. The figure shows the frame structure, with emphasis on the multi point switching configuration examples it can support. Channel allocation can be symmetric or asymmetric and the asymmetry can range up to 14 TSs for DL and only 1 TSs for UL. The standard includes two different transmission modes at the physical layer, differing in the chip rate and bandwidth requirements: High Chip Rate (HCR) mode with 3.84 Mcps and a TDD Low Chip Rate (LCR) one with 1.28 Mcps. LCR provides the flexibility to be used for high spot or high density areas, enabling high speed data services or enhanced coverage. Table 2.2 summarises

the main differences between the two modes.

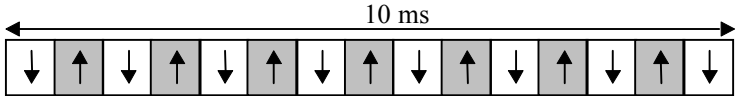

(a) Multiple-switching-point configuration (symmetric DL/UL allocation).

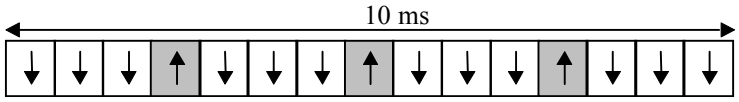

(b) Multiple-switching-point configuration (asymmetric DL/UL allocation).

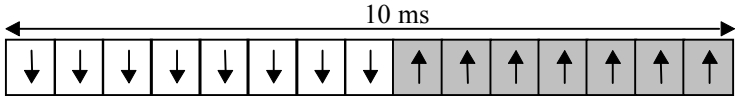

(c) Single-switching-point configuration (symmetric DL/UL allocation).

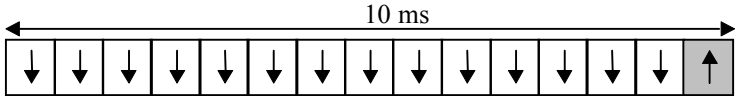

(d) Single-switching-point configuration (asymmetric DL/UL allocation).

Figure 2.3 – TDD HCR frame structure examples (extracted from [3GPP03d]).

With only a third part of the chip rate, LCR also needs only one third of the spectrum. In the HCR option, a frequency band with a bandwidth of 4.4 MHz is allocated to an operator, while in the LCR option, there are three frequency bands with a bandwidth of 1.6 MHz each.

Table 2.2 – Main parameters related to TDD HCR Mode and TDD LCR Mode.

Duplexing method	TDD (HCR)	TDD (LCR)
FDMA channel spacing [MHz]	5	1.6
TDMA frame duration [ms]	10	10 (divided in 2 sub-frames)
Slots/Frame UL	15	15 (7 timeslots/sub-frame)
Slots/Frame DL	15	15 (7 timeslots/sub-frame)
Chip rate [Mcps]	3.84	1.28
Modulation	QPSK	QPSK or 8PSK

In scenarios with low inter-cell interference, operation with a single channelisation code with

SF 1 is also possible for the DL physical channels to transmit high data rates. For UL physical channels, transmission with a single code and different SF in the range of 16 down to 1 is favorable, because this leads to a smaller peak-to-average transmission power ratio. In order to support higher data rates, different channelisation codes may be used in parallel, being called multicode operation.

The PC used in the TDD HCR mode is slower compared to the one in the FDD. Although such a PC is basically less specific, it makes sense because of the TDMA components in the multiple access technique of the HCR mode. It should be noted that fast PC is difficult to implement in HCR mode, since an MT only transmits for a fraction of the time frame, and the channel state can change significantly when an MT moves. Depending on the switching points selected within a time frame between UL and DL, the transmitter power can be changed once or several times in a time frame.

The LCR mode gives a faster PC functionality, which is advantageous, because LCR has less frequency diversity that can be compensated with faster control algorithms. PC for TDD is performed on a frame basis, i.e., one PC update per 10 ms, being done in different ways for UL and DL.

2.3 Radio Resource Management Features

RRM is responsible for guaranteeing QoS, maintaining the planned coverage area, and offering high capacity. RRM comprises handover, power control, admission control, and load control. These features are required to maximise the system's throughput with a mix of different bit rates, services and quality requirements. The following paragraphs address these features.

PC is the first one to be referred, and it is one of the most important features of UMTS. Since UMTS is a CDMA-based system where all MTs share a common frequency, interference control is a crucial issue, therefore, it is essential to keep the transmission power to a minimum. To accomplish this, WCDMA includes a set of features - commonly referred to PC - that consist in three different algorithms: Open Loop, Inner Loop and Outer Loop.

The Open Loop is responsible for setting the initial UL and DL transmission power when an MT is accessing the network. The Inner Loop PC allows the MT and BS to adjust their transmitted power based on the Signal to Interference Ratio (SIR) in order to compensate for

radio channel's fading, occurring at a frequency of 1 500 Hz. The Outer Loop has the aim of maintaining the quality of the communication link to a certain level, determined by the quality requirements of the corresponding bearer service, by producing adequate SIR for the Inner-Loop.

Another RRM feature is Handover (HO), which allows MTs to keep their connection active, maintaining a seamless communication with the network. In UMTS there are three different types of HO: Soft Handover (SHO), Softer Handover (SSHO) and Hard Handover (HHO). FDD supports intra-frequency, inter-frequency and intersystem HOs, whilst UTRA TDD supports inter-system and intra-system HOs (with UTRA FDD and with GSM), based on the HHO mechanism. The main difference between FDD and TDD is that TDD does not use SHO and SSHO.

The third RRM mechanism is call admission. When high network loading exists, before admitting a new connection, admission control needs to check if the service admittance does not sacrifice the existing coverage area or the existing connections' QoS. Admission control accepts or rejects requests to establish radio access to the network. MTs located on the edge of a cell require more BS power and, as they start servicing, required power creates additional interference on the existing MTs; hence, an admission mechanism is required so that those MTs' connections are rejected in order to achieve a more stable system. As the network rejects those calls, the major interferers are powered off, and an immediate interference decrease is achieved, allowing the system to reduce the BS transmit power, allowing other MTs to enter the cell. This is known as the cell breathing phenomena, i.e., a reduction or increase on the size of the cell to control interference.

2.4 Services and Applications

Different types of applications have different characteristics and performance requirements. 3GPP has grouped the large set of possible applications into four main categories of service classes, according to different QoS requirements [3GPP00b], which are described in more detail in the current section. In the next paragraphs each of these service classes is described in detail [3GPP00b], [FeCS00].

There are four main service classes to be considered: Conversational, Streaming, Interactive and Background. The most widespread application of Conversational is speech. With the new Internet and multimedia services, a number of new applications require this scheme, for

example VoIP. The real time conversation scheme is characterised by a low transfer time due to its conversational nature. The maximum transfer delay is given by the human perception of video and audio conversation, therefore, the limit for acceptable transfer delay is very strict, as failure to provide low enough transfer delay results in unacceptable low QoS. Traffic is assumed to be symmetric in this case.

The streaming class is one of the new schemes regarding data communication, which rises a number of new requirements in data communication systems. When the MT is using real-time video or listening to audio, the scheme of real-time streams applies. Multimedia streaming is a technique for transferring data such that it can be processed as if it was a steady continuous stream (*e.g.*, a client browser can start displaying data before the entire file has been received). Streaming services are mostly unidirectional with very asymmetric applications. At the receiver side, a suitable media player application or a browser plug-in plays the streaming data. This service class must preserve the time relations among different MTs within a flow, although it does not have as strict requirements on low transfer delay. But the delay variation of the end-to-end flow must be limited, to preserve the time relation between MTs of the stream. Normally, the data stream is time aligned at the MT, which means that highest acceptable delay variation over the transmission media is given by the capability of the time alignment function of the media player application. Thus, acceptable delay variation is much greater than the delay variation accepted in the Conversational class. Streaming class traffic is asymmetric.

When the MT, either a machine or a human, is on-line requesting data from remote equipment (*e.g.*, a server), the Interactive class applies. Examples of human interaction with the remote equipment are: web browsing, data base retrieval, and server access. Examples of machines interaction with remote equipment are polling for measurement records, and automatic data base enquiries (tele-machines). Interactive traffic is a classical data communication scheme, on an overall level being characterised by the request response pattern of the MT. At the message destination there is an entity expecting the message (response) within a certain time, round trip delay time, therefore being one of the key attributes. Another characteristic is that the content of the packets must be transparently transferred (with low bit error rate). Traffic is assumed to be asymmetric in this class.

According to the 3GPP approach, when the MT, typically a computer, sends and receives data-files in Background, this scheme applies. As application examples one has background delivery of Emails, Simple Messaging System (SMS), File Transfer Protocol (FTP), among

others. Background traffic is one of the classical data communication schemes that on an overall level is characterised by the destination not expecting the data within a certain time (they do not require immediate action). Thus, the scheme is more or less delivery time insensitive. Delay may vary from seconds to minutes, or even hours. Background class traffic is asymmetric. Table 2.3 summarises and compares the service classes' characteristics.

Table 2.3 – UMTS Service Classes (adapted from [3GPP00b] and [FeCS00]).

Class	Conversational	Streaming	Interactive	Background
Fundamental characteristics/ requirements	Preserve time relation (variation) among information entities of the stream. Conversational pattern (stringent and low delay).	Preserve time relation (variation) among information entities of the stream.	Request response pattern within a certain time; round-trip delay time is therefore a key attribute. Preserve payload content: packets must be transparently transferred with low bit error rate.	Destination is not expecting the data within a certain time. Preserve payload content: packets must be transparently transferred with low bit error rate.
Transfer delay	Minimum Fixed	Minimum Variable	Moderate Variable	Large Variable
Nature of traffic	Symmetric	Asymmetric	Asymmetric	Asymmetric
Bandwidth	Guaranteed bit rate	Guaranteed bit rate	No guaranteed bit rate	No guaranteed bit rate
Service examples	Speech VoIP Video Telephony	VoD AoD Media Broadcast	WWW Location Based Interactive Games FTP	SMS Email

The main distinguishing factor among these classes is how delay sensitive traffic is: Conversational is meant for traffic that is very delay sensitive, while Background is the most delay insensitive traffic class.

Although there are other approaches in what concerns service classes, e.g., the UMTS Forum one ([UMTSFo98a] and [UMTSFo98b]), due to standardisation efforts that have been conducted by 3GPP, this latter approach is followed from now on, although taking into account that other approaches are referred when necessary. Following the 3GPP approach, the different services were chosen in accordance to the different QoS classes, keeping in mind that their characteristics should be the most heterogeneous possible, in order to exemplify the service multiplicity present in UMTS. Six services and applications were chosen, Table 2.4.

Table 2.4 – Selected services and applications (adapted from [FeCS00] and [HoTo01]).

Service Class	Services and selected applications
Conversational	Speech Telephony Voice Call - Advanced speech service and traditional voice service. VoIP in the future when IPv6 is deployed.
	Video Telephony Video Call - Service that allow simultaneous transfers of voice and video between two end-MTs.
Streaming	Video Streaming Video on Demand - One-way video and sound streaming. Content delivery service on a unicast or multicast basis.
Interactive	Multimedia Service Web Browsing (WWW) - Access to the Internet and MT-to-MT data transfer. Session based communication and data transfer. Data contains text, extensive graphics, video and audio sequences.
Background	Background Messaging Email – Electronic message exchange, which can be plain text or include video clips, images and/or sound.
	Unrestricted Data Retrieval Service FTP – Data transfer regardless of any specific format. File transfers and server retrieval. It allows the transfer of any type of data file between different types of computers or networks.

Chapter 3

Interference Modelling

This chapter starts with brief considerations about interference and capacity in FDD and TDD, followed by an analysis of the link budget for both modes. After that, some interference studies concerning inter- and intra-cellular interferences are presented. This chapter ends with the development of an interference model that is used to calculate system's interference.

3.1 Capacity Aspects

Network capacity represents the maximum number of MTs that a netwok can support. The need for studying capacity on both UL and DL exists, and the most restrictive connection must be identified, as well as the limiting factors. In TDD, traffic channels are allocated to different TSs and each one may be either code or interference limited. The capacity of a cell depends on UL and DL load factors, which are characterised in what follows.

The UL load factor for FDD is given by [HoTo01]:

$$\eta_{UL}^{FDD} = \sum_{j=1}^{N_U} \frac{(E_b/N_{0[\mathrm{dB}]})_j}{R_{c[\mathrm{chip/s}]}/R_{b\,j[\mathrm{bps}]}} \cdot \upsilon_j \cdot (1+i) \tag{3.1}$$

Taking into account the characteristic of TSs, present in TDD, the UL load factor is estimated on a per TS basis:

$$\eta_{UL}^{TDD} = \frac{E_b/N_{0[\mathrm{dB}]}}{R_{c[\mathrm{chip/s}]}/R_{b[\mathrm{bps}]}} \cdot \upsilon \cdot (1+i) \tag{3.2}$$

where,

- i Normalised inter- to intra-cell interferences ratio (ranging from 0 to 1);
- R_{bj} Service bit rate of MT *j;*
- υ_j Activity factor of MT *j* at physical level (ranging from 0 to 1);
- E_b/N_o Equivalent Signal-to-Noise Ratio (SNR) required to meet a predefined QoS;
- R_c Chip Rate (3.84 Mcps for FDD and TDD HCR and 1.28Mcps for TDD LCR).

The transmitted power in UL leads to an interference increase in adjacent cells, whereas the power received by an MT is considered as interference on all other MTs in the same TS.

The higher the system load, the higher the interference, which implies that the receiver noise level is larger in a highly loaded system. Also, it should be considered that the BS power delivered to each MT must be the minimum amount of power necessary to establish the connection, as it becomes interference from other MTs point of view. The BS power may be expressed by [HoTo01]:

$$P_{BS\ [\mathrm{W}]}^{TX} = \frac{N_{rf} \cdot R_{c[\mathrm{chip/s}]} \cdot \sum_{j=1}^{N} \upsilon_j \cdot \frac{\left(E_b / N_{0[\mathrm{dB}]}\right)_j}{R_{c\,[\mathrm{chip/s}]} / R_{j[\mathrm{bps}]}} \cdot \overline{L_{p_j[\mathrm{dB}]}}}{1 - \overline{\eta_{DL}}} \tag{3.3}$$

where,

- $\overline{L_{p_j}}$ Average attenuation between BS and MT$_j$ *;*
- $\overline{\eta_{DL}}$ DL Load factor (average value across the cell);
- N_{rf} Spectral noise density of the MT receiver front-end.

The spectral noise density of the MT receiver is defined by:

$$N_{rf[\mathrm{dBm}]} = -174 + F_{N[\mathrm{dB}]} \tag{3.4}$$

where,

- F_N Noise figure.

The DL load factor, also defined in [HoTo01], can be approximated by its average value across the cell for FDD mode:

$$\eta_{DL}^{FDD} = \sum_{j=1}^{N} \upsilon_j \cdot \frac{\left(E_b / N_{0[\mathrm{dB}]}\right)_j}{R_{c\,[\mathrm{chip/s}]} / R_{bj[\mathrm{bps}]}} \cdot \left[\left(1 - \overline{\alpha_j}\right) + \overline{i_j}\right] \tag{3.5}$$

and for TDD:

$$\eta_{DL}^{TDD} = \upsilon \cdot \frac{E_b / N_{0[\mathrm{dB}]}}{R_{c\,[\mathrm{chip/s}]} / R_{b[\mathrm{bps}]}} \cdot \left[\left(1 - \overline{\alpha}\right) + \overline{i}\right] \tag{3.6}$$

where,

- $\overline{\alpha}$ Average orthogonality factor in the cell (depends on the multipath propagation, ranging from 1, fully orthogonal, to 0; the values considered hereafter correspond to 60 % for vehicular and 90 % for pedestrian).

The capacity in DL is directly determined by the required transmission power. As the BS transmission power increases, more interference exists on the network, and less capacity is available. In order to overcome this limitation, it is necessary to reduce the BS transmitted power per link as much as possible, leading to an interference reduction and an increase in

system's capacity.

Capacity depends more on DL load than UL, since DL maximum transmission power is shared among MTs, while in UL each additional MT has its own power amplifier. Therefore, even with low load in DL, coverage decreases as a function of the number of MTs. Basically, coverage is limited in UL, while capacity is DL limited.

The processing gain, G_p, is expressed in terms of the information bit rate, R_b, and the code chip rate R_c,

$$G_{P[\mathrm{dB}]} = 10\log\left(\frac{R_{c[\mathrm{chips/s}]}}{R_{b[\mathrm{bps}]}}\right) \tag{3.7}$$

For TDD, the processing gain is calculated differently, since its slotted structure must be taken into account. In TDD there are 15 TSs and the information is transmitted in one or several slots using one or more codes. G_p is calculated for data rates that can be supported by transmission in one or more slots, the following expression being used:

$$G_{P[\mathrm{dB}]} = 10\log\left(\frac{R_{c[\mathrm{chips/s}]}}{R_{b[\mathrm{bps}]}}\cdot\frac{k}{15}\cdot\frac{chips\,in\,slot - midamble - guard\ period}{chips\,in\,slot}\right) \tag{3.8}$$

where:

- k is the number of slots used for the service considered (i.e., voice service k=1, see Table 3.1).

In the context of the current thesis, (3.8) is simplified and as:

$$G_{p[\mathrm{dB}]} = \frac{R_{c[\mathrm{chips/s}]}}{R_{b[\mathrm{bps}]}}\cdot\frac{k}{15} \tag{3.9}$$

R_b being given by

$$R_{b[\mathrm{bps}]} = \frac{\log_2(M)\cdot R_{c[\mathrm{chip/s}]}\cdot\left(T_S\cdot R_{code} - G_{Per[\mathrm{chip}]}\right)}{SF\cdot T_f} \tag{3.10}$$

where M is the size of the symbol set (QPSK, i.e, 4), T_S is the slot duration (666.7μs), T_f is the frame duration (10 ms), R_{code} is the code rate (1/3), G_{Per} is the length of the guard period (96chips) and SF is the spreading factor. Assuming that burst type 1 is used for 12.2 kbps voice and burst type 2 is used for 128 kbps data, the parameters are as follows:

chips_in_slot=2560, midamble (burst type 1/2) = 512/256, guard period=96.

Examples of the processing gain for some services and the E_b/N_0 values considered in TDD link budget are given in [LaWN02]. The required E_b/N_0 values are substantially higher for DL than for UL, which stems mainly from the fact that no diversity scheme is included in DL. If that had been the case, link performance would improve, and balancing of the two links would be easier. However, since transmit diversity is not as efficient as receive diversity, there are higher requirements on DL E_b/N_0 values.

Three resources potentially limit FDD and TDD: BS power, load in DL and number of codes. In FDD, BS power and DL load limit the system, while in TDD, the number of codes is the limiting factor. In order to correctly evaluate network interference, it is necessary to compute the link budget in both UL and DL.

3.2 Link Budget

This section focuses mainly on the particular aspects of UMTS link budget. For the complete analysis, please refer to Annex B.

In addition to general parameters used in link budget estimations, there are some WCDMA-specific parameters that have to be taken in account [HoTo01]. The allowed propagation loss for the cell is given by:

$$L_{p[\mathrm{dB}]} = P_{t[\mathrm{dBm}]} + G_{t[\mathrm{dBi}]} + G_{r[\mathrm{dBi}]} + G_{SH[\mathrm{dB}]} - P_{Rx\min[\mathrm{dBm}]} - \sum L_{x[\mathrm{dB}]} - \sum F_{M\,[\mathrm{dB}]} \tag{3.11}$$

where,

- P_t Transmission power (delivered to the antenna);
- G_t Maximum transmitting antenna gain;
- G_r Maximum receiver antenna gain;
- G_{SH} Soft-handover gain;
- $P_{Rx\min}$ Receiver sensitivity for a given service bearer;
- L_x Additional attenuations in a link: MT body loss L_{Body}, cable losses L_c and others (car or building penetration losses) L_{Other};

- F_M Fading margins, i.e., fast fading F_{FM}, and slow fading F_{SM}.

The propagation losses obtained in both UL and DL are input parameters for the cell radius calculations. The COST 231 Walfisch-Ikegami propagation model [DaCo99] is adequate to calculate the maximum path loss in urban and micro-cell environments taking urban parameters like street and building dimensions into account. For the scenarios characterised in this work, this model satisfies the environment and system parameters conditions, thus, being used. For further details on the used propagation models refer to Annex A.

The minimum received power of an MT depends on its service and is given by:

$$P_{rmin[\mathrm{dBm}]} = \frac{E_b}{N_{0\,[\mathrm{dB}]}} - G_{P[\mathrm{dB}]} + N_{T[\mathrm{dBm}]} \tag{3.12}$$

where:

- E_b/N_0 is a relation between energy of bit and noise density, which depends of the service, mobile speed, receiver algorithms, and BS antenna structure;
- G_P is the processing gain obtained from (3.7) for FDD, and (3.9) for TDD;
- N_T is the total effective noise plus interference power, see Annex B.

TDD radio performance is characterised by synchronisation needs, asymmetry, and low cell breathing [LaWN02]. Load factors are not of particular interest in the TDD planning procedure, since power-based load control is not needed to ensure system stability and coverage, code limitation in each slot happens before coverage is badly affected.

In TDD, link budget has two parameters of some importance, the BS noise figure and fast fading margin. The first has been suggested as one way of counteracting the possibly severe interference problems that may arise. The idea is to make the receiver less sensitive to interfering signals coming from TDD and FDD MTs, and other TDD BSs located closely. However, this approach does not completely solve interference problems, and it also has negative effects by increasing the overall interference level in the own system, since the desired MTs must increase their output powers to compensate for the poorer UL reception performance. The second parameter is similar to the transmit PC headroom in FDD. It ensures that the Transmit Power Control (TPC) scheme has enough room to vary the power to compensate for fading effects. If TPC is not used, this parameter is set to zero.

In conclusion, absolute values of the maximum allowed propagation loss are lower for TDD than for FDD, due to TDD's slotted characteristics. However, another effect of this property is that coverage is also much more stable when load increases, i.e., cell breathing is much lower. Without DL transmit diversity, there is quite a large unbalance between maximum allowed propagation loss for UL and DL. LBR services are code limited in many cases, while HBR services are most often interference limited. A TS reuse factor of 1 may be possible for voice services, but probably not for data services with a speed of 64 kbps or more. However, the reuse factor may not have to be decided on a permanent basis, but it could potentially result from an 'average utilisation effect' from channel allocation decisions made by a dynamic channel allocation scheme. Delay requirements impact heavily upon the throughput obtainable. Non-delay sensitive services can reach a much higher throughput than delay ones.

The propagation models behind interference calculations, which are base of the developed interference model, are specifically related to interference, and were imported from [3GPP04], [QiWD00a]. Three models are used: one that models the path loss among MTs and BSs, which is used when the network is synchronised, and two others used when synchronism does not exist, modelling the path loss among MTs and among BSs.

3.3 TDD and FDD Interference Studies

This section offers a perspective of some studies that have been conducted regarding intra- and inter-cell interferences in the two modes of the UMTS. Also other interference studies, not directly related to these two kinds of interference, were analysed, because they are relevant to the interference analysis.

In [QiWD00a], a study about inter-cell interference for TDD is presented. The study considers specific interference scenarios, and presents a propagation model for each one. It presents a new approach, since the majority of interference studies use the same model for the two modes. This study assumes that there is perfect PC in the network. Another interesting aspect is the assumption that TDD frames between two adjacent cells have different asymmetries, and that there is an arbitrary offset to model imperfect frame synchronisation, which allows the development of a more realistic model, as in practice these two aspects may exist in the network. The study analyses the impact of asynchronised and differently asymmetric TDD connections on network capacity in both UL and DL. The simulation starts with a simple scenario consisting of two BSs, but afterwards it is generalised to seven and

nine cell clusters, investigating the contributions of each ring to the total interference over a single BS. MTs are uniformly distributed over the cell, and only the voice service is considered, which leaves room to the current work because data services are also considered. Shadowing is also considered.

The authors of that study also made an investigation on interference between TDD and FDD modes [QiWD00b]. Although the main objective of the current thesis is not interference calculation between the two modes, there are several important concepts that can be extracted from this study. As in the first study, the authors start by defining four interference scenarios in TDD and also one propagation model for each scenario. Shadowing is considered as well as Minimum Coupling Loss (MCL) due to the fact that BSs are always placed much higher than MTs. This work studies interference on both links, UL and DL, and also considers perfect PC. Regarding synchronisation, it is assumed that MTs have an offset to properly model the imperfections of the network. Having this in mind, the authors studied the influence of the distance between two adjacent BSs on the inter-system interference, considering different channel loads per slot. Simulations were made considering different channel loads in one TDD slot. Results are given considering the relation between the network capacity, the load of TDD cells, and the value of the Adjacent Channel Interference Ratio (ACIR). Once again, only voice is considered. On both studies, MT's mobility is not considered.

Another study, presented in [HSLT00] focuses on TDD, considering different interference scenarios and the network for the duration of single TS. It is assumed that TSs in different cells have a small offset concerning synchronisation, and considerations are made about the impact of higher or smaller offsets on interference. The simulation also considers that TDD frames may have different asymmetries, and studies intra- and inter-cell interferences. The scenario is assumed to be indoor, following the most probable application of TDD, which is not the object of the current thesis, as only outdoor scenarios are considered. Additionally, the study assumes that the second tier of cells does not contribute significantly to interference levels. As other studies, MTs are uniformly distributed over the entire cell, which is not assumed in the current thesis. The study presents interference for different loads per TS, the required cell area to fulfill E_b/N_o requirements, and some considerations on the placement of two adjacent BSs.

Another study, [Thom03], on UMTS networks ACIR, applies only to FDD and presents the common sources of ACIR. A model to estimate interference levels is developed, considering voice and three data services with different bit rates as the available services. The analysis is

made on both UL and DL, considering that MTs are spread uniformly on the cell with no mobility. No simulator was developed, instead, an existing one was used to analyse possible interference scenarios, and nevertheless, there are some interesting considerations about the usage of UMTS planning tools to identify potential dead zones due to ACIR. Some techniques on how to mitigate the ACIR problem are presented, e.g., the increase of channel separation between adjacent carriers of two different operators. The major conclusion is that ACIR is one of the biggest problems in UMTS network planning and that planning engineers from different operators must cooperate with each other in their site deployment in order to minimise ACIR. Since interference calculations in this thesis assume the existence of adjacent cells and their interaction, this study provides interesting concepts to be retained.

[SLHW02] presents an approximation for the calculation of inter-cell interference for UMTS, introducing the concept of feedback behavior on the cells, due to the response given when interference grows, by rising the transmit power. There is the need for having some kind of iterative behavior on the interference model. The study presents an analytical model for computation of interference levels using fixed-point equations. As others, this study assumes that MTs have no mobility and are uniformly distributed over the cell, with either voice or data service. The propagation model used in the study is the vehicular test environment found in [ETSI98], which is not used in the current thesis. After deriving the simplest model with one cell, the study is extended to a two-cell problem, and finally to the first and second ring of cells. The current work takes the interference of the six interferers into account, hence, the considerations made in [SLHW02] about cell tiers are of use.

[NgDa03] presents a study about the estimation of inter-cell interference in CDMA macro-cells. It assumes that there is perfect PC in UL and that DL power is the same at every BS. An interesting concept is introduced concerning the distribution of MTs, assuming that MTs are not uniformly distributed, but instead it assumes that they are distributed in small groups in the neighboring cells, thus, forming small congestion areas, with no mobility associated. These small groups located in hot spots enable the study of their influence in the inter-cell interference. Only the first tier of cells is considered, and it is assumed that fast fading does not affect the average signal power level, since the investigation is concerned about the average signal and interference, shadowing being not considered. The study presents results on SIR according to the distance of interfering MTs to the neighbor BS and also from the impact of the number of MTs.

[KwWa95] presents a study about the effect of adjacent cell interference on network capacity

for CDMA networks. This work introduces a new aspect related to the cell geometry: cells have circular geometry, beyond the normally considered hexagonal one. It presents a numerical method to calculate interference from the six adjacent cells considering the hexagonal structure, after which cells are considered to be circular and a closed form solution is obtained. Another interference calculation method is presented for irregular-shaped cells. The study provides a way to obtain the total interference from adjacent cells considering that MTs have no mobility and that they are uniformly distributed over the cell. This study also considers that optimum PC exists. The total interference received at a BS is modeled, formed by intra- and the inter-cell interferences from adjacent cells. A conclusion is that interference from cells farther away than the ninth tier is negligible, but that second to ninth tier of cells should be considered.

[LKCW96] presents a model to calculate inter-cell interference. Differently from other studies, it assumes that PC is not optimum, and that its errors impact on interference. The cell structure is considered to be hexagonal, with uniformly distributed MTs and no mobility. A propagation model is derived to allow the calculation of path loss, and shadowing is considered for both macro- and micro-cell scenarios. SHO and HHO are also considered to calculate their impact on interference. The authors consider four types of inter-cell interference: macro-to-macro, micro-to-micro, micro-to-macro and macro-to-micro. Each one of these interference types is simulated with its own model. This study refers only to UL and all conclusions are drawn as a function of the PC error. In the current thesis, perfect PC is assumed, thus, the majority of this work conclusions do not apply; nevertheless, the four interference scenarios may be used and four models can be derived according to the characteristics of each one.

[DaMo97] presents a work on the characterisation of the multi-access interference in a DS-CDMA voice and data network. It considers only FDD. The work addresses both UL and DL and outputs interference and SIR at the BS and MT. Two service classes are considered according to the services characteristics: stream mode services, with variable bit rate, for large amount of transmitted information with ON-OFF characteristic, and packet-based services, where transmission is discontinued at the end of the data burst. A simple model to calculate the short-term interference power is given as the sum of all signal powers of other interferers/MTs.

3.4 Conceptual Interference Model

The main goal of this thesis is to analyse intra- and inter-cell interferences of UMTS TDD. The first approach is to consider the simplest case of one BS, followed by the analysis of two adjacent BSs, and finally of the other tiers of interfering cells.

When both TDD and FDD coexist, a careful radio network planning is needed, due to ACIR. In a building or outdoor environments where FDD is already deployed, it is possible to increase the overall capacity by deploying co-localised TDD BSs. This leads to a complex interference environment that must be analysed. Also, MTs mutual interference depends on the location and type of service used. Inter-system interference is not considered in this work.

In FDD, interference can occur only among MTs or among BSs, due to the fact that there is a small guard band between adjacent UL and DL channels: DL channels interfere with other DL channels, and UL channels interfere with other UL ones, but UL and DL do not affect each other.

In TDD, interference analysis is more complex, because there are specific interference scenarios: the same carrier is used for both UL and DL, therefore MTs and BSs may interfere on each other, creating new possible BS-to-BS, BS-to-MT and MT-to-MT interference scenarios. A brief description of these scenarios follows.

- If all cells are TS synchronised and the same slot asymmetry is applied, i.e., the same slots are used for UL and DL in all cells and all MTs transmit and receive at the same time, they do not interfere with each other. The same applies to BSs. However, interference still exists, because one BS in one cell interferes with MTs from surrounding cells and MTs from one cell interfere with BSs in other cells. This leads to MT-to-BS and BS-to-MT interference.
- If all cells are TS asynchronised, UL and DL transmissions exist in the same TSs from different cells, an MT on one cell may be transmitting at the same time another MT from an adjacent cell is receiving, leading to MT-to-MT interference. The same situation occurs for BSs leading to BS-to-BS interference.

It is, therefore, important to be able to have a measurement of the levels of signal and interference powers among the network. A local mean SIR at cell level can be calculated by summing signals from other MTs. SIR_{UL} is calculated as follows [3GPP04]:

$$SIR_{UL} = \frac{G_P \cdot S}{(1-\beta)\cdot I_{Intra} + I_{Inter} + N_0} \tag{3.13}$$

where:

- G_p processing gain;
- S Received signal;
- I_{Intra} Intra-cell interference, generated by those MTs that are connected to the same BS that the reference MT;
- I_{Inter} Inter-cell interference, generated from other cells;
- N_0 Thermal noise, which may be neglected compared with interference levels;
- β Interference reduction factor due to the use of, for example, Multi-User Detection (MUD) in UL.

The ratio of the intra-cell interference to the total of interference is given by:

$$F = \frac{I_{Intra}}{I_{Intra} + I_{Inter}} \tag{3.14}$$

In DL, SIR can be expressed as [3GPP00a]:

$$SIR_{DL} = \frac{G_P \cdot S}{\alpha \cdot I_{Intra} + I_{Inter} + N_0} \tag{3.15}$$

Compared to a micro-cellular environment, a signal in macro-cellular one follows more complex paths, which is translated into a more multipath fading; because of these higher distances (more reflection and refraction points), the α factor in a macro-cellular environment is expected to be higher than in a micro-cellular one.

Regarding interference estimation, the modelling process can be divided into several phases:

- Gather information about interfering transmitters and victim receivers: the number of interferers must be known as well as their locations, and also the receiver characteristics. All this information includes also knowing certain parameters, as antenna gain, services' target E_b/N_o, physical scenario and other propagation model related information.

- Define geometry aspects: considering that this work analyses interference in a real radio network, the network layout must be fed to the algorithm with the BSs location, other radio planning parameters and MTs distribution.
- Provide other victim and interferer characteristics: slot symmetry, assumptions made in the interference model, the existence or inexistence of mobility, maximum allowed load and others.
- Compute interference: after having all the required inputs, intra- and inter-cell interferences in both TDD and FDD is calculated using an interference model, producing several outputs.
- Degradation metrics: as metric examples there are (besides interference levels) the network load, delay, the number of outage MTs, blocked MTs, interference caused blocked MTs, among others.

A simple input-output model can be constructed, as depicted in Figure 3.1. The interference model is developed in order to evaluate interference scenarios in TDD operation. Operation during one TS is considered and analysis is made at the frame and TS levels. The model must support studies when synchronism exists between adjacent cells and also when there is a time offset leading to asynchronism between adjacent cells. Also, the interference model must be applied to the real network topology presented in this work.

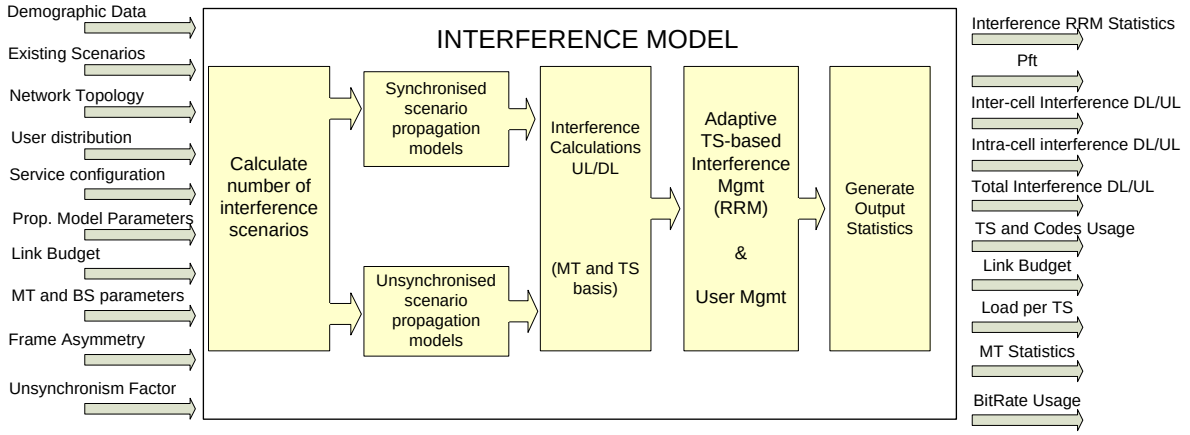

Figure 3.1 - Interference model block diagram.

Most studies assume that traffic generated by MTs is uniformly distributed inside the cell, not considering that in the same coverage area there may exist sets of MTs whose location cause heavier interference compared to other sets, e.g., as traffic hot-spots in [NgDa03]. In the current work, due to non-uniform distribution of users, traffic, load and interference hot-spots

exist, hence, being a more realistic scenario to study.

After having the values of intra- and inter-cell interferences, new values of E_b/N_o are calculated for all MTs, now taking interference into account. For all MTs whose E_b/N_o is below a given target value minus 0.5 dB, delay occurs and new delay probabilities are calculated considering interference [QiWD00a], [QiWD00b]. MTs with LBR services cause less interference than MTs with HBR services, when in the same location. This happens because HBR services require higher transmit powers, thus, causing higher interference powers on other MTs.

The developed RRM algorithm for interference analysis and evaluation is discussed in greater detail in Subsection 4.2.3, and it consists of introducing a new concept: non-destructive interference whenever an MT is servicing on more than one TS, which clearly benefits HBR MTs. These MTs see its service bit rate reduced in the presence of interference instead of simply being delayed and put out of service.

This idea appeared because it makes no sense that in a HBR services environment - where MTs suffer several degrees of interference – MTs may be put away from service just because they do not comply with the target E_b/N_o in some of their TSs. This way, an algorithm is added to the interference model that checks how many TSs each MT is using and calculates the corresponding E_b/N_o in the presence of interference for all of them. If a certain MT does not comply with its target E_b/N_o, in all used TSs, it becomes delayed, becoming a victim of destructive interference. However, if it does not comply with target values only on some of the used TS, it ceases service only on those TSs - leading to a bit rate reduction - but does not become outaged or totally delayed, thus, having suffered from non-destructive interference.

In TDD if adjacent cells or operators are not synchronised, interference paths appear among MTs (inter-MT) and also among BSs (inter-BS). This is illustrated in Figure 3.2 for the synchronised and asynchronised cases.

Inter-BS interference can be controlled by a correct radio network planning, and avoided if sufficient coupling loss exists among the BSs [HoTo01]. Inter-MT interference is statistical in time due to the fact that MTs location cannot be controlled, meaning that this kind of interference cannot be avoided by network planning. Inter-MT and Inter-BS interference existence is assumed, modeled and analysed.

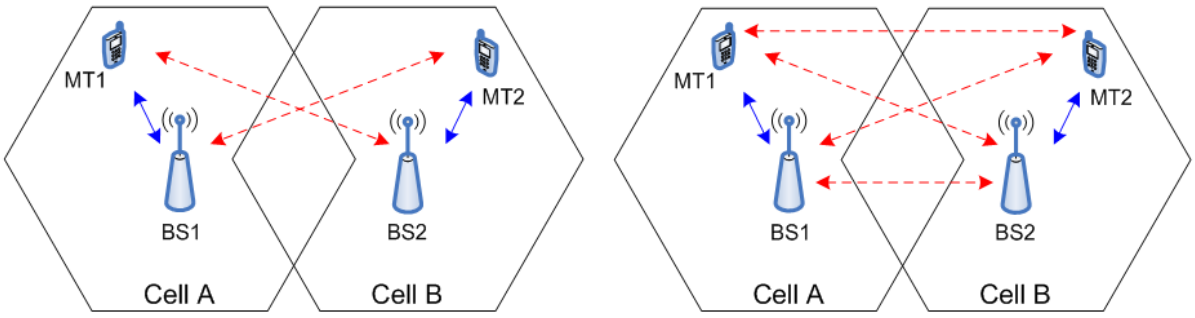

(a) With synchronisation. (b) Without synchronisation.

Figure 3.2 – Interference scenarios.

Concerning time synchronisation offset between two adjacent cells, a small offset corresponds to UL transmissions at the same time in adjacent cells, and no overlapping of UL and DL occurs. This leads to low inter-BS and inter-MT interferences, but higher MT to BS and BS to MT interferences. On the other hand, a higher offset results in higher inter-BS and inter-MT interferences and lower BS-to-MT and MT-to BS ones. The several interference scenarios and their effects are summarised on Table 3.1

Table 3.1 - Effects of frame offset (adapted from [HSLT00]).

	Interference scenario			
	BS-to-BS	MT-to-MT	BS-to-MT	MT-to-BS
Small offset	low	low	high	high
Large offset	high	high	low	low

The time offset is represented by a synchronisation factor, δ_{offset}, which is a percentage of the TS duration. For instance, an δ_{offset} value of 1 % means that there is an offset time between the BSs of 6.66 μs. The synchronised network is represented by an asynchonisation factor of δ_{offset}=0 (i.e., all BSs transmit and receive at the same TSs). The asynchronised network is represented by a synchronisation factor of δ_{offset}=1 (i.e., when one BS is transmitting, the other is receiving on the same TS). Between 0 and 1, TSs are not aligned and their timing is offset by this synchronisation factor.

When an MT does not meet the E_b/N_o requirements on a single or all used TSs, two performance metrics are introduced:

- Forced Termination Probability, P_{ft}. An MT data connection is dropped when, in the

presence of interference, the UL or DL E_b/N_o drops below the minimum target values;

- Low Quality Access Probability, P_{low}, quantifies the number of data connections, in UL or DL, that become reduced due to the presence of interference, thus, with less quality than it should have when interference is not considered.

3.5 Numerical Interference Model

The interference model is developed from a simple two-cell deployment, as show in Figure 3.2. This simple model assumes that there are two cells, each one with the respective BS and several MTs. In Figure 3.2, only two MTs are considered to exemplify the possible interference scenarios. In blue, the normal communication path among MTs and BSs and in red interference paths when synchronisation and asynchronisation exists. The current work includes the definition of a time offset to allow modelling asynchronism.

In the UL, BS1 is considered to be the victim of the interferers: MTs from both cells and the BS from the adjacent cell [QiWD00a]. In this case the inerference components are given by:

$$I_{Total_{UL}} = I_{Inter_{UL}} + I_{Intra_{UL}} \tag{3.16}$$

$$I_{Intra_{UL}}^{MTs_1 \to BS_1} = \sum_{i=1}^{N_1 - 1} P_{Tx_i}^{UL} \tag{3.17}$$

$$I_{Inter_{UL}} = I_{BS_2 \to BS_1} + I_{MTs_2 \to BS_1} \tag{3.18}$$

where,

- $P_{Tx_i}^{UL}$ is the transmit power of MT *i* from cell A;
- $I_{BS_2 \to BS_1}$ is the interference that BS_2 causes on BS_1;
- $I_{TOTAL_{UL}}$ is the total interference in UL;
- $I_{\mathrm{Inter}_{UL}}$ is the inter-cell interference in UL;
- $I_{\mathrm{Intra}_{UL}}$ is the intra-cell interference in UL;
- $I_{MTs_2 \to BS_1}$ is the interference that MTs from cell 2 cause on BS_1;
- $I_{Intra_{UL}}^{MTs_1 \to BS_1}$ is the intra-cell interference that MTs from cell 1 cause on BS_1;
- N_1 is the number of interfering MTs from cell 1.

In DL, MT1 is the victim, and interferers are the BS and MTs from cell B and the BS from its own cell:

$$I_{Total_{DL}} = I_{Inter_{DL}} + I_{Intra_{DL}} \tag{3.19}$$

$$I_{Inter_{DL}} = I_{BS_2 \to MT_1} + I_{MTs_2 \to MT_1} \tag{3.20}$$

$$I_{Intra_{DL}}^{BS_1 \to MTs_1} = \alpha \sum_{i=1}^{N_1 - 1} P_{Tx_i}^{DL} \tag{3.21}$$

where,

- $I_{BS_2 \to MT_1}$ is the interference that BS_2 causes on MT_1;
- $I_{MTs_2 \to MT_1}$ is the interference that MTs from cell 2 cause on MT_1;
- $I_{TOTAL_{DL}}$ is the total interference in DL;
- $I_{\text{Inter}_{DL}}$ is the inter-cell interference in DL;
- $I_{\text{Intra}_{DL}}$ is the intra-cell interference in DL;
- $I_{Intra_{DL}}^{BSs_1 \to MTs_1}$ is the intra-cell interference that BS_1 cause on MT_1;
- α DL orthogonality factor;
- $P_{Tx_i}^{DL}$ is the transmit power of BS *i* from cell B.

When considering the existence of asynchronism among adjacent BSs, two new interference scenarios appear, hence, new interference equations exist.

In UL, one has [QiWD00a]:

$$I_{Total_{UL}} = I_{Inter_{UL}} + I_{Intra_{UL}} \tag{3.22}$$

$$I_{Intra_{UL}}^{MTs_1 \to BS_1} = \sum_{j=i}^{T_S} \sum_{i=1}^{N_1} P_{Tx_i} \tag{3.23}$$

$$I_{Inter_{UL}} = \delta_{offset} \cdot I_{BS_2 \to BS_1} + \left(1 - \delta_{offset}\right) I_{MTs_2 \to BS_1} \tag{3.24}$$

$$I_{MTs_2 \to BS_1} = \sum_{i=1}^{N_2} P_{Tx_i} \tag{3.25}$$

where:

- T_S is the total timeslots in a frame;
- δ_{offset} is the ratio between the asynchrony offset time and the TS duration;

- N_2 is the number of interfering MTs from cell 2.

While, in DL, one has [QiWD00a]:

$$I_{Total_{DL}} = I_{Inter_{DL}} + I_{Intra_{DL}} \tag{3.26}$$

$$I_{Inter_{DL}} = \left(1 - \delta_{offset}\right) \cdot I_{BS_2 \to MT_1} + \delta_{offset} \cdot I_{MTs_2 \to MT_1} \tag{3.27}$$

$$I_{Intra_{DL}}^{BS_1 \to MTs_1} = \alpha \sum_{i=1}^{N_1 - 1} P_{Tx_i} \tag{3.28}$$

The lack of synchronism represents the relation between the offset time and the duration of the TS. Thus, the asynchronism factor δ_{offset}, is the ratio between the time offset and the TS duration:

$$\delta_{offset} = \frac{t_{offset}}{t_{timeslot}} \tag{3.29}$$

These equations allow calculating the total interference in both modes. As it can be seen, the intra-cell interference does not depend on the timing displacements between adjacent cells, according to the interference model by [QiWD00a] that is the basis to the developed interference model.

Taking the existence of served, blocked and delayed MTs into account, the referred indicators can be calculated using:

$$P_b = N_b / N_{cov} \tag{3.30}$$

$$P_d = N_d / N_{cov} \tag{3.31}$$

$$P_s = N_s / N_{cov} \tag{3.32}$$

where,

- N_{cov} Number of covered MTs;
- N_b Number of blocked MTs;
- N_d Number of delayed MTs;
- N_s Number of served MTs.

In addition, the probability of having a non-covered MT, $P_{n\mathrm{cov}}$, is given by:

$$P_{n\mathrm{cov}} = N_{n\mathrm{cov}} / N_U \tag{3.33}$$

where,

- $N_{n\text{cov}}$ Number of non-covered MTs.
- N_U Number of system MTs.

For all MTs with dropped connections due to destructive interference, a forced termination probability, P_{ft}, is introduced:

$$P_{ft} = N_{ft} / \ N_{\text{cov}} \tag{3.34}$$

where,

- N_{ft} Number of destructively interfered MTs.

For all those MTs that become reduced due to interference effects, in a non-destructive way, and that see its service bit rate reduced, a low quality access probability P_{low} is introduced:

$$P_{low} = N_{low} / \ N_{\text{cov}} \tag{3.35}$$

where,

- N_{low} Number of bit rate reduced MTs due to interference (non destructively).

A numerical interference model was developed in this section. Its implementation is addressed in the next chapter.

Chapter 4

Simulator Description

This chapter provides a functional description of the simulator platform developed within the scope of this thesis. The chapter starts by pointing some aspects of the existing FDD simulator, and proceeds with the presentation of the developed TDD simulator.

4.1 Description of the Existing FDD Simulator

The current work consists on developing a network simulator for TDD. For the FDD, an existing simulator [SeCa04] is used as the basis to develop a new simulator for the latter. Most of the assumptions made in [SeCa04] are also used in this thesis, e.g., MTs are not distributed uniformly over the cell, and PC is assumed to be perfect. The existing simulator structure is depicted in Figure 4.1. Three major blocks compose it: User generation, network dimensioning, and network optimisation.

User Generation has the task of creating MTs based on input parameters that characterise them. After having MTs on the network, dimensioning starts based on fed network data, and cell coverage with network loads being calculated. After having a fully characterised network, the optimisation process begins when the existing network is found to be non optimal, and BSs are added in specific regions determined by positioning algorithms, also developed in that work.

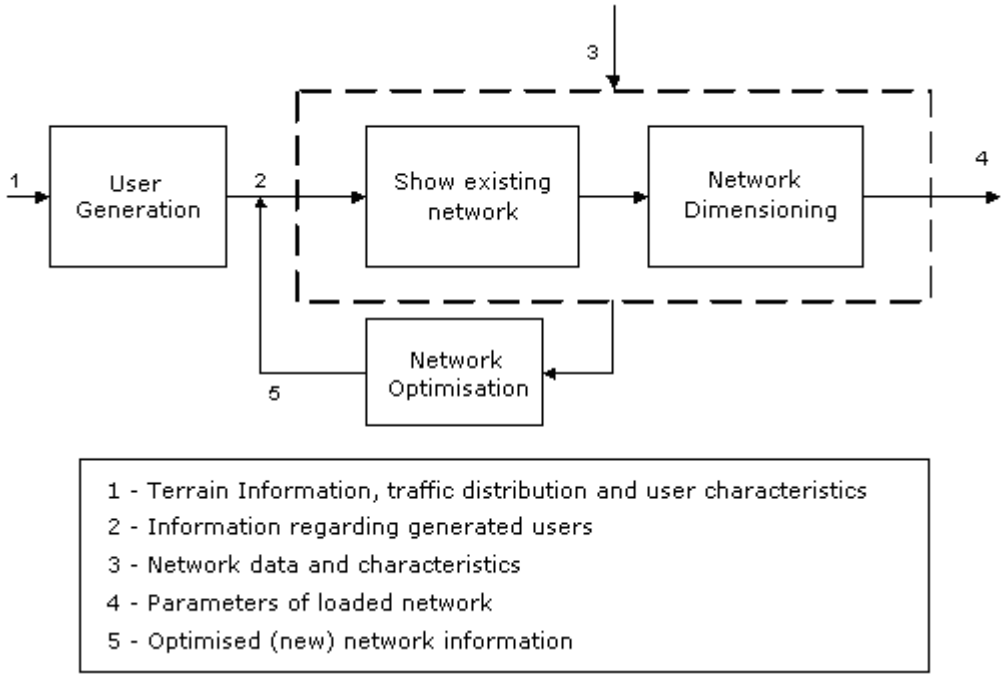

Figure 4.1 – Block diagram of the existing FDD simulator.

In order to obtain realistic data for evaluation, the simulator [SeCa04] takes several inputs based on actual scenarios, namely, non-uniform traffic distributions. The generation of an MT consists on the specification of two characteristics: mobility type and service generated by the MT.

Busy Hour Call Attempt (BHCA) grids specify the service usage for each pixel of the scenario. The number of MTs to be generated is described by a Poisson arrival process for the specific

BHCA, using data from MOMENTUM [MOME04]. A software tool, called *SIM*, was developed to handle all MTs generation, according to the traffic distribution in the city. MTs are generated based on known parameters, as the scenario type and the associated amount of traffic.

After having all of them completely characterised, with additional network data, MTs are linked to the respective BSs, and load and other network-related parameters calculations are made. The MTs generation algorithm can be found in Figure C.1, Annex C. MT generation stops after exporting all MT's characteristics to a data file, which is the common point between the application that generates MTs and the application that plans the network, called *Net*_Opt.

The Network Dimensioning block has several input parameters: BSs antenna radiation pattern, E_b/N_o values for every service and existing scenario, geometry of the region where the network is deployed, containing, among others, street information and exact BS location of the network. As output, this block produces the parameters of the existing network after dimensioning: cell radii taking into account the existing load, number of MTs per cell, UL and DL load factors, number of used frequencies, and transmitted power. This block also provides statistical data concerning the number of outage, blocked, delayed and served MTs. The *Net_Opt* application calculates all necessary data for network planning like BS transmit power, load factors, coverage and uncovered probabilities as well as soft and softer handover probabilities, based on data from a Geographic Information System (GIS) and *SIM* application. The flowchart for the *Net_Opt* application can be found in Figure C.3, Annex C. This application imports data files created by the GIS application, based on which a list of BSs is created with each one of the corresponding sectors. Each sector contains the number of MTs connected to it and other statistical data, e.g., the number of blocked, delayed and HHO MTs.

An active set of three BSs was included in the simulator. This number is configurable within the GIS application, and fed to the *Net_Opt*. The MT is associated to a BS with the minimum path loss. All MTs with distances to BSs greater than the maximum service radius are excluded from the network planning process, and marked as delayed MTs.

The third block, Network Optimisation, receives a list of BSs and starts by distributing frequencies (from a total of four) to the cell sectors. The algorithm assigns the first frequency to all BSs and, when load requirements or maximum BS transmit power demand more capacity, a new frequency is assigned. This block has as output parameters statistical data for the optimised network as well as the number of blocked, outaged and delayed MTs and also a list with all served MTs, number of used carriers, load factors, cell radii and number of MTs per service is

created. In an initial phase of the simulation, MTs are generated, fed to the dimensioning block and network performance is evaluated. The network dimensioning stops as soon as the blocking and delay probabilities drop below 1 %, or when there are no more carriers to be assigned. If the number of outaged MTs is higher than 1 %, network optimisation is executed, adding news BSs, after which the optimisation cycle restarts; otherwise, if the number of outaged MTs is below 1%, simulation stops and the network is considered to be optimised.

Four carriers/frequencies are allocated to sectors. A new carrier/frequency is allocated when the previous one does not meet load requirements in UL/DL. If all carriers are used and still load limits are not respected, MTs suffer bit rate reductions. Still if requirements are not met, sector radius is reduced, thus, reducing the number of covered MTs. This procedure reduces load factors to values below the target thresholds.

To enable visual display of results, the program creates two output files: *Users.out* and *Data.out.* The first file has all statistical data about MTs: blocked, delayed, uncovered, total number of MTs, and the number of MTs in CS and PS modes. The second file has all the data about the sectors, the number of used carriers, load factors, the maximum, minimum and average sector radius and the number of MTs per service.

The visual representation of the planning and optimisation results on the GIS, a third application was developed in *MAPBASIC*, called *UMTS_Simul*. This program calls *Net_Opt* to plan and optimise the network. The GIS application must be fed several information, in order to correctly display all desired data. That information is contained in several data files, divided by tables:

- *R_pattern.dat* – radiation pattern of the antennas for every angle;
- *Eb_No.dat* – bit energy over noise power spectral density ratio for every existing bit rate and scenario;
- *Dados.dat* – geographical information about the city;
- *Zonas.dat* – information about the areas of the city, ranging from streets to open areas;
- *Network.dat* – exact location of all BSs of the existing network;
- *Users.txt* – output file.

The application begins by visually presenting the cellular network and area where it is deployed. Afterwards, a list of MTs is created and displayed on the city map. Then, BS data is imported into the simulator and the BSs are displayed on the map.

The simulator stops its operation after generating two different data files: *Definitions.dat* and *Data.dat.* The first one has all the information on sectors, their corresponding BSs and the number of MTs connected to them. It generates a list of all covered and serviced MTs, following the algorithm of Figure C.2, Annex C. The second file contains the values of the network parameters selected in the GIS, e.g., propagation model parameters. After this, the simulator calls *Net_opt* and suspends itself until this application ends. *Net_opt* creates output files containing new sector radii with real loading accounted, and other important parameters for network planning, like the number of MTs on the sector, number of used frequencies, load factors in DL/UL, and transmitted power. When the application exits, the GIS continues its execution and shows new network data.

4.2 TDD Simulator Description

This section presents the description of the developed TDD simulator that enables studying TDD and its interference scenarios. It begins with general simulator aspects, followed by input and output parameters, finishing on developed RRM algorithms.

4.2.1 General Aspects

The objective of the simulator developed in this thesis is to simulate UMTS TDD. It also feeds the TDD network to the interference calculation model developed in the current thesis. Several changes had to be done to the existing FDD simulator, as shown in Figure 4.2, the first one consisting of allowing the simulator user to choose which mode to simulate. The possibility of choosing TDD or dual-mode TDD and FDD was added in the form of a new mode selection window, as it can be seen in Figure H.5 from Annex H.

The simulator user is also given the possibility of choosing TS asymmetry. Default asymmetry is 9D3U, so that, at least, one 1920 kbps MT can be served. Channel asymmetry also accounts for the existence of Control and Signaling (C&S) channels. The number of C&S channels can range from one to three.

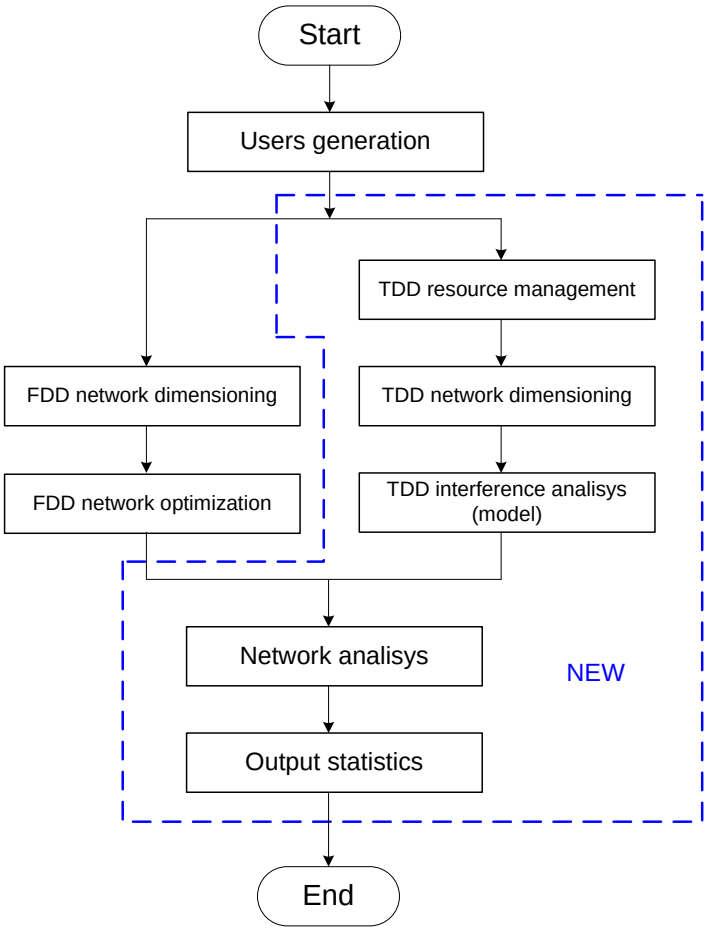

Figure 4.2 – Main TDD/FDD simulator workflow.

The network dimensioning process had to be adapted to TDD. The major novelty is allowing a simulation based on TSs, as well as having code, bit rate and MT allocation per TS. The simulator adapts itself to different TDD frame asymmetries, and also takes reserved TSs for C&S into account. An important aspect of the TDD simulator is the way that codes per service are calculated. According to [HoTo01], TDD MT bit rate for a single code in one TS and half-rate channel coding with a spreading factor of 16 is 13.8 kbps.

Taking into consideration that, for each code, the bit rate is 13.8 kbps, the number of codes for the several bit rates must be calculated using the following equation:

$$Number\ of\ Codes = RoundUp\ (\ Service\ Bit\ Rate\ /\ One\ Code\ Bit\ Rate\ ) \quad (4.1)$$

The results of applying this formula to all services bit rate is shown in Table 4.1. In TDD, each TS has a maximum of 16 codes, which leads to a maximum bit rate of 220.8 kbps per TS. One of the major modifications that were made to the existing simulator is the way network dimensioning is done. The main difference is that for TDD there is only one frequency in the network - and not four, as it happens in the FDD simulator – leading to different network

dimensioning processes represented by the flowchart of Figure C.4.

Table 4.1 – Number of codes per service.

Service bit rate [kbps]	One code bit rate [kbps]	Number of codes	TS per service	MaxCodes per TS
16	13.8	2	1	16
64		5	1	
128		10	1	
384		28	2	
1920		140	9	

For all these MTs, UL and DL load calculations are made and tested against the maximum values of 50 % and 70 % respectively, per TS. The calculations of TS load in UL/DL are presented in Figure C.5 and Figure C.6, respectively.

Code allocation has different processes for UL and DL. It is assumed that UL bit rate can not be higher than 64 kbps. The non-symmetrical bit rate extreme case appears when an MT is servicing at 1920 kbps in DL and 64 kbps in UL. The algorithm is depicted in Figures C.7 and C.8. Based on the MT's service, the number of needed codes is calculated.

There are other processes important in TDD which allows generating statistical data. The flowcharts of Figure C.9 and Figure C.10 show the process used in TDD simulator to attach an MT to a TS in UL and DL, respectively.

Other components and algorithms can be found in greater detail in Annex C.

4.2.2 Input and Output Parameters

This sub-section lists all input and output parameters for both FDD and TDD simulators. As input parameters one has:

- Demographic data of the city (files: *Dados.dat* and *Zonas.dat*);
- Scenarios: vehicular, pedestrian and indoor (file: *Users.txt*);
- BS location data (file: *Network.dat*);
- BS antenna gain (file: *R_pattern.dat*);
- Users spatial traffic distribution, from the *SIM* application (file: *Users.txt*);
- Service configuration (configured by tool);

- E_b/N_o for each service and scenario (file: *Eb_No.dat*);
- Propagation model parameters (configured by tool);
- Link budget parameters (configured by tool);
- MT and BS configuration (configured by tool);
- Slot symmetry (UL/DL), configured by tool (default: 9/3);
- Number of control slots in a TDD frame, configured by tool (default: 3);
- TDD frequency, configured by tool (default: 1900 MHz);
- Operation mode (FDD or TDD), configured by tool (default: TDD);
- BS maximum throughput, configured by tool (default: 1920 kbps).

The outputs are the following:

- N_{cov}, N_U and $N_{n\text{cov}}$;
- P_b, P_d and P_s, evaluated from (3.30), (3.31) and (3.32), respectively;
- N_b, N_d and N_s;
- η_{DL}^{FDD} and η_{UL}^{FDD} evaluated from (3.5) and (3.1), respectively;
- Free codes per TS and per BS in both links for TDD;
- Bit Rate reduction due to initial RRM algorithm activation per MT/BS;

Regarding interference, as this is not a single algorithm that works within the simulator, it does not have specific input parameters other than the ones referred before. Nevertheless, there are important input parameters that need to be listed and that are used in interference calculations, which are:

- Global Network's Frame asymmetry;
- BS synchronisation offset time;
- Maximum allowed load per TS UL/DL (same as the one for the BSs).

Specific output parameters and indicators considering the presence of interference and asynchronism are:

- η_{DL}^{TDD}, η_{UL}^{TDD} (compared with the values without interference) evaluated from (3.6) and (3.2), respectively;
- $I_{Intra_{UL}}$, $I_{Inter_{UL}}$ evaluated from (3.23) and (3.24), respectively, per BS;
- $I_{Intra_{DL}}$, $I_{Inter_{DL}}$ evaluated from (3.28) and (3.27), respectively, per BS;
- P_{ft} and P_{low}, evaluated from (3.34) and (3.35), respectively;

- N_{low} and N_{ft};
- Amount of reduced bit rate per service;
- Codes per TS/BS in UL/DL (compared with the values without interference);

4.2.3 Radio Resource Management

In order to simulate reality as close as possible, two RRM algorithms were developed: one that checks if there are enough codes on each BS to serve the requesting MTs, and another that reduces MTs service bit rate. The macroscopic flowcharts of each RRM algorithm are described in more detail in Annex C.

In order to model code reductions, it is assumed that:

- Services at 1920 kbps and 384 kbps suffer a maximum of two reductions;
- Services at 128 kbps are reduced only once.

One should take into consideration that in order not to have a code bit rate reduction from 1920 kbps to 384 kbps, consisting of 112 codes, an intermediate bit rate had to be added to the existing five. Therefore, due to the need of code reduction schemes, a service bit rate of 512 kbps using 40 codes was defined. Still, it is necessary to know how many codes are reduced each time. Table 4.2 to Table 4.4 show the different reduction steps defined for each service.

Table 4.2 – Reduction Steps for 1920 kbps.

	Reduction steps for service with bit rate of 1920 kbps			
	Reference bit rate	Codes	Reduced bit rate	Reduced codes
	1920	140	-	-
Red1	512	40	1408	100
Red2	384	28	128	12

In conclusion, MTs requiring to service at 1920 kbps may be reduced to a minimum of 384kbps, while MTs wanting to service at 384bkps and 128 kbps may be reduced to a minimum of 64 kbps. Table 4.5 shows the minimum bit rates after maximum reduction.

Table 4.3 – Reduction Steps for 384 kbps.

	Reduction steps for service with bit rate of 384 kbps			
	Reference bit rate	Codes	Reduced bit rate	Reduced codes
	384	28	-	-
Red1	128	10	256	18
Red2	64	5	64	5

Table 4.4 – Reduction Steps for 128 kbps.

	Reduction steps for service with bit rate of 128 kbps			
	Reference bit rate	Codes	Reduced bit rate	Reduced codes
	128	10	-	-
Red1	64	5	64	5

Table 4.5 – Minimum servicing bit rates after reduction.

Reduction Summary			
Before reduction		After reduction	
Reference bit rate [kbps]	Codes	Reference bit rate [kbps]	Codes
1920	140	384	28
384	28	64	5
128	10	64	5

There are two different concepts that may be mistaken with each other: there are MTs that have been totally reduced (e.g., a 1920 kbps MT that is servicing at 384 kbps after being reduced two times) and are able to service at LBR, and MTs that have become outaged because even after being totally reduced there were still not enough codes to accommodate them.

The high level flowchart of the initial RRM algorithm is presented in Figure 4.3. The algorithm is applied to all existing BSs in the network, and is executed right before an MT enters the network analysis of the simulator. This way, it is ensured that the network has enough resources for all MTs “loaded” onto it. After this algorithm is executed, the normal operation begins with code and TS allocation to MTs, after which, interference is calculated and its effects are analysed. A detailed explanation of MT reduction and outage algorithms is present in Annex C.

Figure 4.4 shows the high-level interference RRM algorithm, applied to all BS in the network, also.Again, more details on the overall functioning of the algorithm can be found in Annex C.

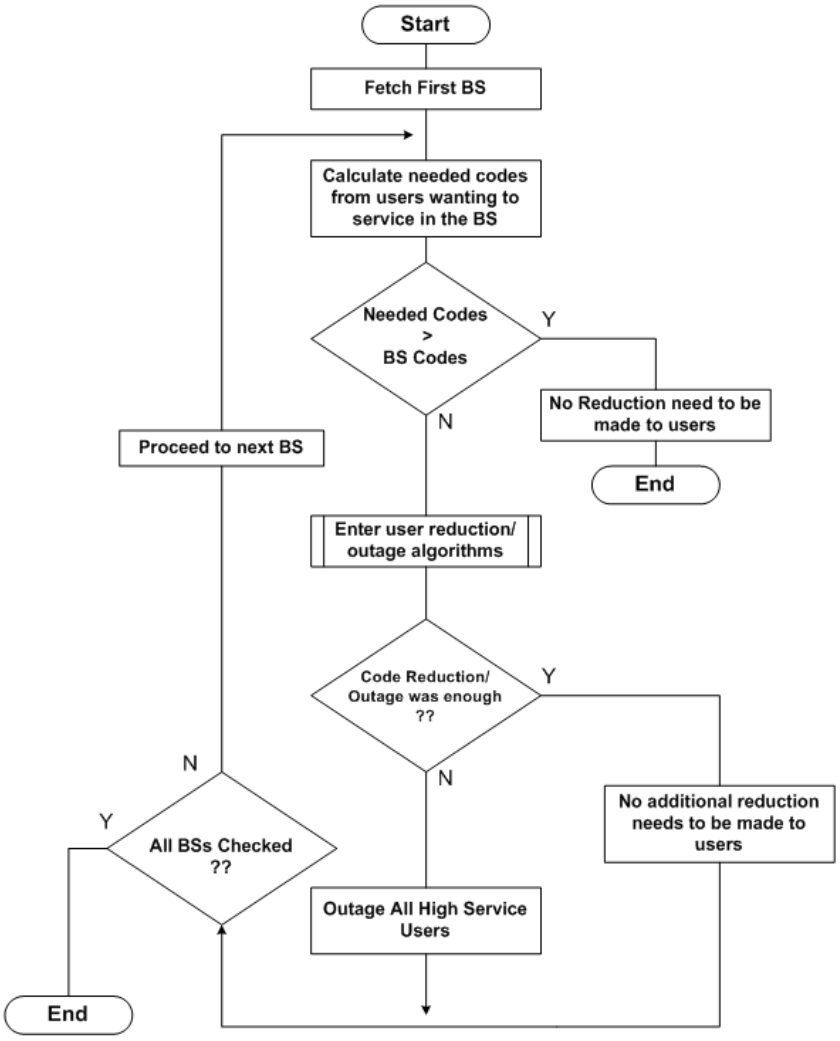

Figure 4.3 – Radio Resource Management Algorithm.

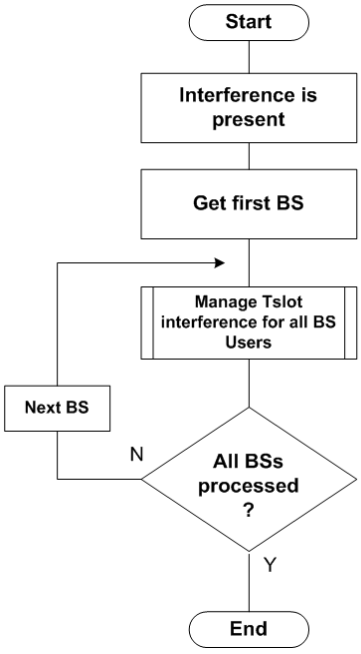

Figure 4.4 – TS interference management algorithm.

4.3 Simulator Assessment

This section addresses the assessments made to validate the simulator results, which allow simulations with a certain degree of confidence. The more important parameters are analysed here others being referred in greater detail in Annex D. All assessments regarding the existing FDD simulator were already done in [SeCa04].

The assessment on the number of codes and TSs, has the objective of testing codes generation and finding out if the correspondence between services bit rate and codes is correct. As seen in Table 4.1, for each bit rate there are different number of needed codes. Taking into account that a single code has a bit rate of 13.8 kbps, as seen before, the number of codes needed per service is drawn by dividing the service bit rate by this one-code bit rate. As expected, the results of this division were not integer values, hence, there was the need to make an excessive round-up. The result is the number of codes show in Table 4.1. It was proved by calculations that the simulator was able to calculate the needed codes per service based on its bit rate. Figure D.1 shows the difference between the theoretical number of codes and the results of the simulator, which leads to the conclusion that the codes generation was working as expected.

Regarding the number of TSs, after knowing the number of needed codes per service it is possible to find the number of TSs needed per each service. The theoretical values state that for each service the number of needed TSs is given by dividing the service bit rate per the bit rate of a single code – thus, finding the needed codes – and dividing the result by the number of codes per each TS. That correspondence is shown in Table 4.1. The practical results of the simulator can be seen in Figure D.3, confirming the correct behavior of the simulator concerning the calculation of the maximum number of MTs per TS as a function of their service bit rate.

Next on the assessment study, service and TS bit rates were focused. A bit rate assessment is done in order to find out if after being generated, MTs are given the correct bit rate according to the service. As previously referred, the number of codes that each service is granted is rounded up accordingly to the service bit rate. This round-up creates excessive bit rate for each service. As an example, a 16 kbps service would only need 1.16 codes, but taking into consideration that a code is an integer concept, it was chosen to round-up the number of codes and, in this case, 2 would be the number of codes allocated. The only downside of this approach is that a service that normally needs a bit rate of 16 kbps is, in practice, using 2 codes, hence, 27.6 kbps. This

leads to what is called a bit rate leakage and, in this case, leakage is roughly 11 kbps, thus, two concepts were created: network and target bit rates. The target bit rate is the one that the service is supposed to need, and the network bit rate is the effective bit rate that the service has after the round-up process in the number of codes. The comparison between these two concepts can be found in Figure D.6. This figure also shows that the simulator is correctly calculating the service bit rate.

Next on the assessment studies the number of MTs per TS and BS were studied. The objective is to check the maximum number of MTs that the simulator allows per each TS and BS. Theoretically, based on the number of codes per service depicted in Table 4.1, the maximum number of MTs per TS is as presented in Table 4.6.

Table 4.6 – Maximum number of MTs per TS.

Service bit rate [kbps]	Codes needed	MaxCodes per TS	Max. MTs per TS
16	2	16	8
64	5		3
128	10		1
384	28		0
1920	140		0

The results of the simulator are shown in Figure D.2. The next MT related study that required assessment is the maximum number of MTs supported on a single BS according to its TDD frame asymmetry. As previously referred, frame asymmetry is a global input parameter and all BSs share the same asymmetry throughout the network. In order to assess the simulator only four asymmetries were tested: 9D3U, 8U4D, 7D5U and 6D6U. Theoretically, the number of supported MTs is as depicted in Table 4.7.

Table 4.7 – Maximum number of MTs for different frame asymmetries in DL/UL.

			Number of MTs per frame asymmetry							
Frame asymmetry			9D3U		8D4U		7D5U		6D6U	
Number of codes DL/UL			144	48	128	64	112	80	96	96
Bit Rate [kbps] / Codes needed	16	2	72	24	64	32	56	40	48	48
	64	5	28	9	25	12	22	16	19	19
	128	10	14	4	12	6	11	8	9	9
	384	28	5	1	4	2	4	2	3	3
	1920	140	1	0	0	0	0	0	0	0

These theoretical values are confirmed by simulation results, as seen in Figures D.4 and D.5.

Load assessment is also necessary. The load that an MT creates on single TS is directly

dependent on its service bit rate. The load assessment process is simple: theoretically calculate the load that a single MT with different bit rates causes over a single TS, and compare it with the value from the simulator. This way, several calculations were made being proved, as shown in Figure D.8, that the simulator results are practically the same as the theoretical ones.

It is also shown that a single MT with service bit rate of 16 kbps causes a minimum TS load of 3.42 %, whilst 384 kbps or 1920 kbps MTs create a maximum load of 30.6 %, all in DL. Taking into account that the maximum load allowed in DL is 70 %, the maximum is smaller than half the acceptable limit. Regarding the opposite link, it is seen that the 16 kbps MT causes a minimum TS load of 2.4 %, whilst the maximum is 18.3 %, roughly. Refer to Annex D for more details.

As this work focuses mainly on interference, these are the most important set of validations and assessments that have to be made. It is never too much to recall that interference is seen from a power level perspective. Thus, a single MT receives interference in DL as the sum of the power of all the signals (other than its own) that arrive in the same TS the MT is using. On the other hand, in the opposite link, at the BS it is the sum of all interference power signals that arrive from MTs.

The first test focused on interaction between a single MT and its BSs in both links. Intra-cell interference is the focus. Simulator results were as expected: as MTs travel further from their BSs, the received power decreases, and suffered interference increases. This is observed in Figures D.15 and D.16. For the UL, as MTs are farther away from their BS less interference is caused, as assessed. It is also shown that more servicing MTs exist when no interference is considered.

The second set of tests consisted of deploying two BSs. This way, not only intra-cell interference but also inter-cell one could be evaluated and validated. Theoretically, an MT located closer to its cell edge suffers more interference from adjacent BS as the received interference power is higher. This was proven and can be seen on Figure D.18.

Another test was made: how much interference would the several services create? Theoretically, HBR services create higher levels of interference. The results can be seen in Figure D.20 and D.21, for the own and adjacent BSs, respectively, and are clear: HBR MTs cause more interference than LBR ones. Also, with these same conditions and tests another theoretical aspect is proved: MTs closer to adjacent BS contribute more to the global inter-cell interference

and MTs away from the adjacent BS do not generate as much interference, thus, contributing less to inter-cell interference. As seen in Figure D.21, an MT moving away from its BS is getting closer to the adjacent BS, increasing UL interference power levels on that BS. Once again, simulator results are as expected.

One last test consisted of evaluating interference between two MTs as they get closer or farther apart. As shown in Figure D.22, simulator results confirm theory, showing that as the distance between MTs increases, interference caused on each other decreases, and vice-versa. The global results allow concluding that the simulator is behaving correctly and that the algorithms developed – especially interference related ones – are behaving as expected. Once again, it is important to refer to Annex D in order to further read about the tests and validations made to the simulator.

In order to be able to find how many simulations must be made per each indicator, a simulator sensitivity study was made, being compared among them for 5, 10 and 15 simulations. The chosen parameters to simulate were the network load in both UL and DL and the delay probability with and without considering interference. The results can be seen in Figure 4.5, for both the average and the standard deviation.

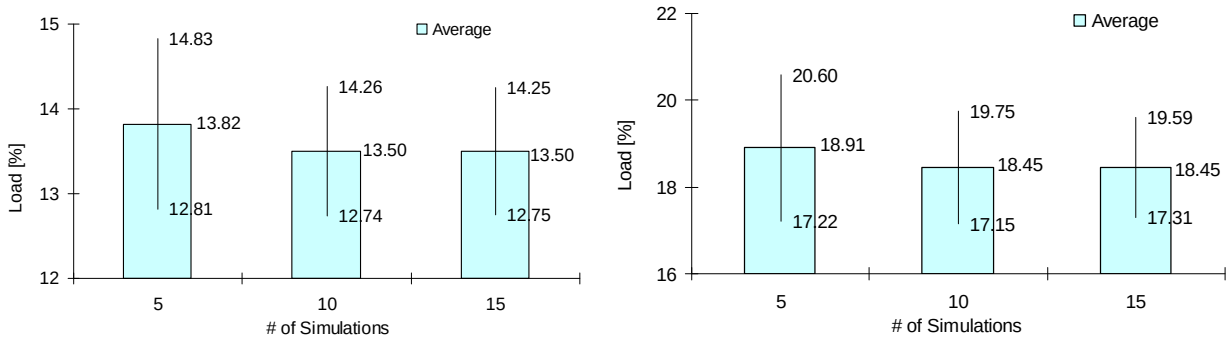

(a) Without interference. (b) With interference.

Figure 4.5 – Network load.

Both 10 and 15 simulations produce more accurate results than only 5 simulations. Results become stable after 10 simulations. As a result of this study, 10 was chosen as number of simulations to be done for all parameters.

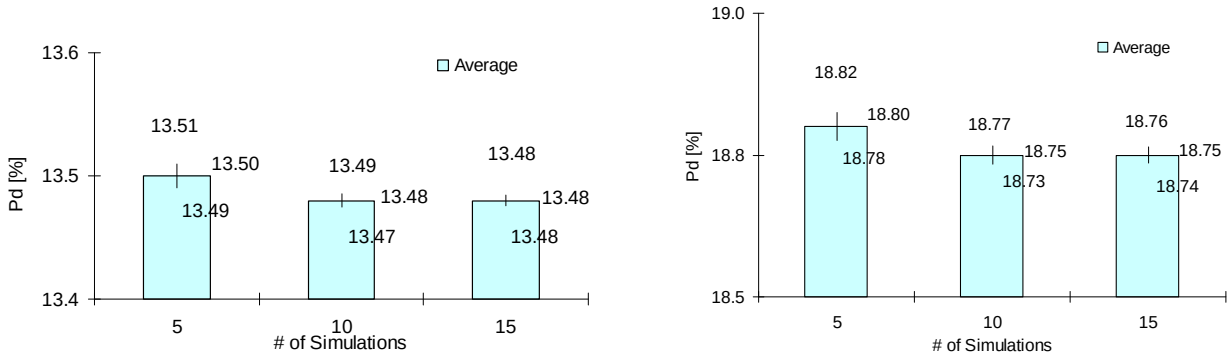

(a) Without interference. (b) With interference.

Figure 4.6 – Delay probability.

Chapter 5

Analysis of Results

This chapter provides simulation analysis of all scenarios. After introducing the scenarios (demographics, geography, MT profiles, bit rate and services penetration), and choosing an area of study, the second section presents the steps taken towards the choice of a reference scenario and network configuration. Finally, several simulations are presented with the corresponding results and conclusions are drawn.

5.1 Scenarios Description

This section focuses firstly on the scenario inherited from the existing simulator and after on the evolution to the final scenario used in the simulations of this work. The existence of a previous scenario must be taken into account, because a scenario fit to FDD may not be appropriate to TDD. Hence, there is the need to characterise that scenario prior to any study, in order to discover if it fits the objectives of the current work.

The existing scenario covers the geographic area of Lisbon. It is an area with high density urban zones and also open green ones. It is a scenario with mixed environments, thus, mixed propagation situations, Figure 5.1.

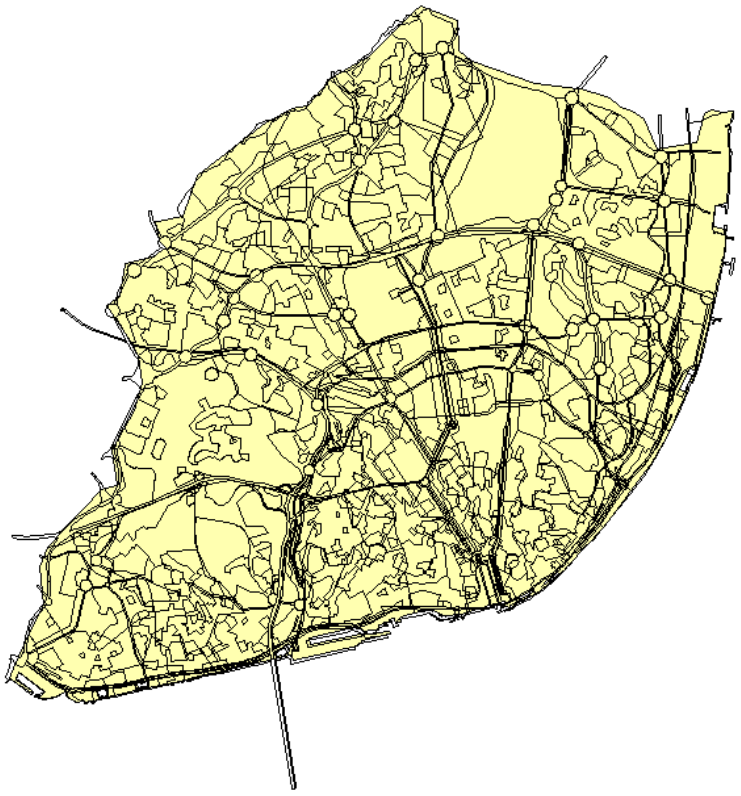

Figure 5.1 – Lisbon Metropolitan Area.

As the existing simulator referred to FDD, HBR services have low penetration rates. Voice and CS based services have larger penetration rates, and the higher bit rate is 384 kbps. These service characteristics do not fit TDD, as seen previously. The existing scenario has a GSM network [SeCa04] associated, comprised of 194 BSs, mapped according to terrain/MTs characteristics and densities. Figure 5.2 shows the cellular deployment and corresponding

coverage in FDD.

Having characterised the network and area of interest from the initial scenario, it is still necessary to analyse how many MTs were considered in that scenario. The work presented in [SeCa04] concluded that, for the whole metropolitan area of Lisbon, the existing network was capable of servicing a total of 9000 MTs. However, it was necessary to check if the area used for FDD was also suitable for TDD.

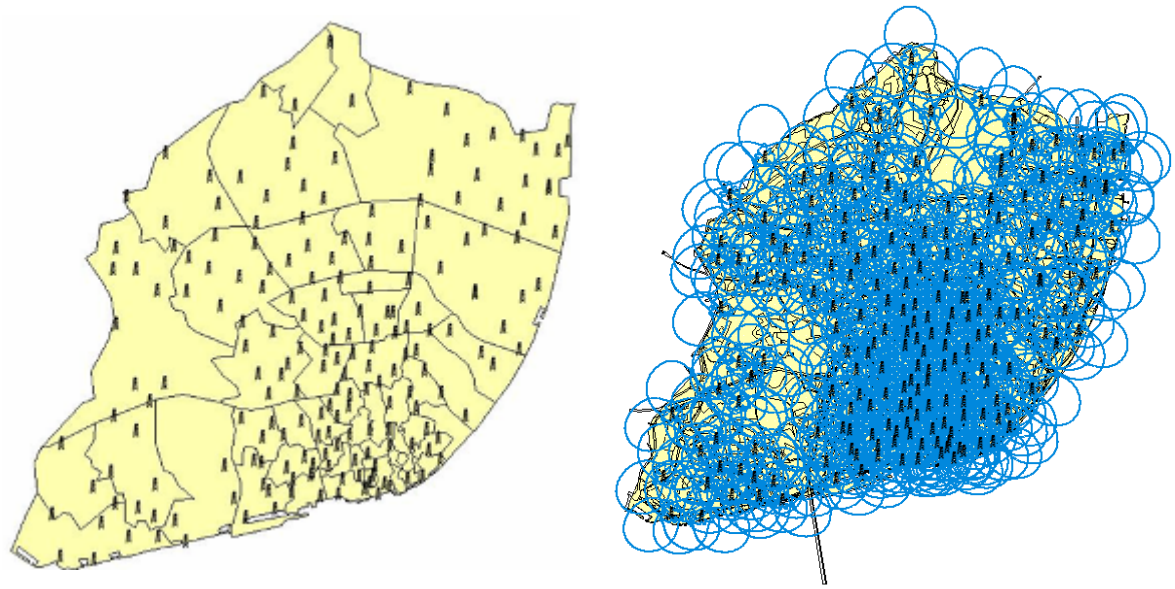

(a) BS Location. (b) FDD cellular coverage.

Figure 5.2 – Cellular deployment.

By simply taking the existing cellular deployment as TDD, the obtained cellular coverage is sparser, due to the fact that the radius of a single TDD BS is smaller than an FDD one, Figure 5.3. Figure 5.4 shows the population density per square kilometre. It can be seen that downtown Lisbon has a mean value higher than 10 000 inhabitants per km^2, whether suburbs have lower than that.

In order to obtain HBR MTs and high values of network load in TDD, the area of interest was reduced to the area where inhabitant densities are higher.

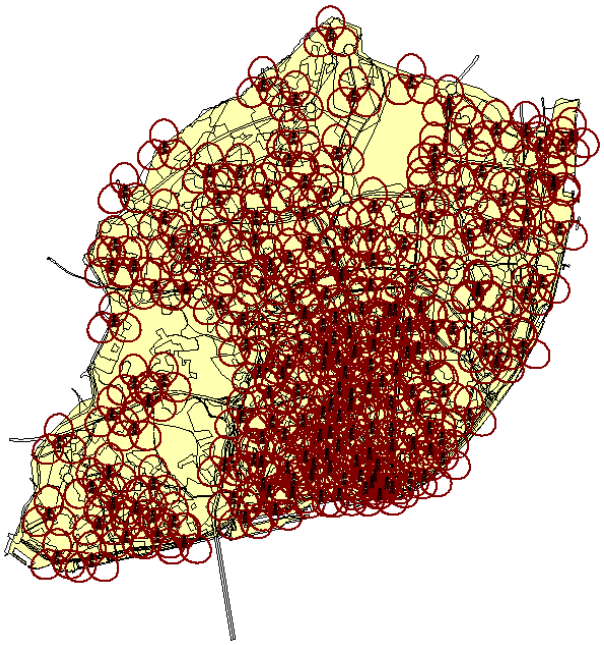

Figure 5.3 – Cellular coverage for TDD in the whole area of Lisbon.

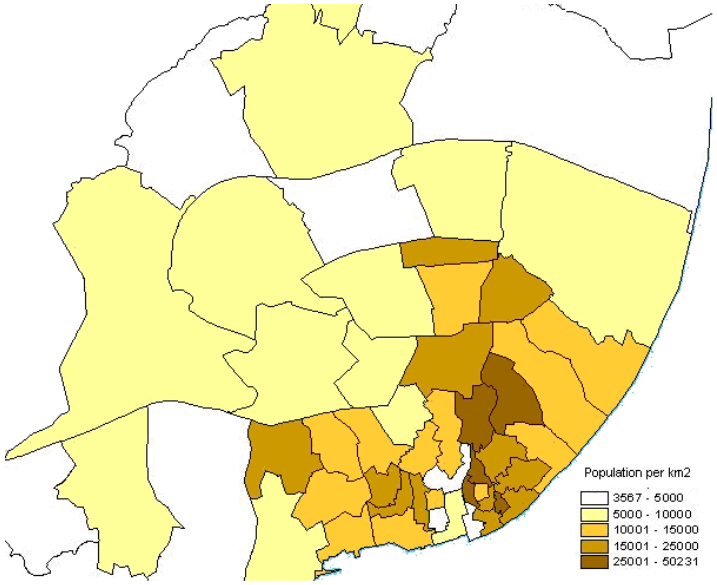

Figure 5.4 – Population density on the area of interest (adapted from [CMLi06]).

Figure 5.5 shows the new service area, downtown Lisbon. The scenario is comprised of 29 districts, four of which are the most populated ones of the whole metropolitan area. A total of 94 FDD BS exist in the area of interest. Figure 5.6 shows the cell coverage in the area of interest for both modes. It can be seen that in FDD the area is almost completely covered, while in TDD, there are still some coverage holes. Coverage considerations are made later in this document.

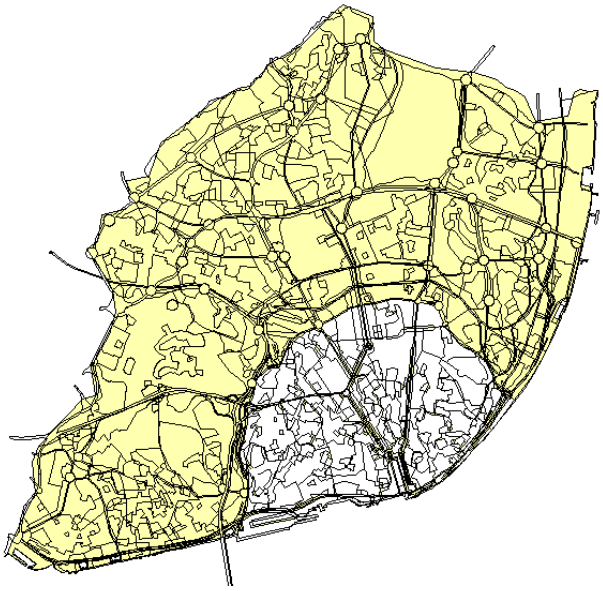

Figure 5.5 – New area of interest for TDD (in white).

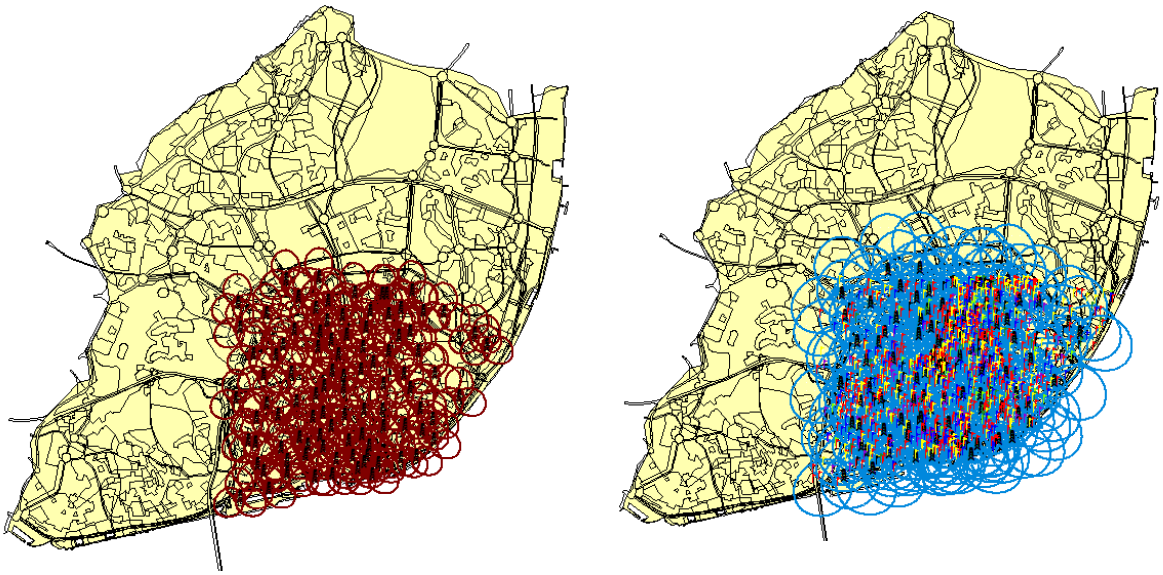

(a) TDD mode. (b) FDD mode.

Figure 5.6 – Cellular coverage in the area of interest.

Before starting the simulations, it was necessary to define the services penetration rates for this scenario, but taking into account that this was a new scenario; some tests had to be done prior to defining it as final. Several different scenarios were created and evaluated in order to find the one that would better fit the simulation needs. Six scenarios were defined, Table 5.1, ranging from a voice centric scenario (where more than 50 % MTs have LBR services) to a data mostly one (where more than 50 % MTs have HBR services), and network performance indicators were analysed in both UMTS modes. The services characteristics are according to the ones presented in Chapter 2.

Table 5.1 – Different test scenarios and corresponding services penetration rates.

Service	Bit rate [kbps]	CS/PS	Scenario penetration rates [%]					
			1	2	3	4	5	6
Speech telephony	12.2	CS	70	50	30	30	30	30
VoIP	16	PS						
Video telephony	64	CS	4	5	7	5	4	2
Location based	64	PS	3	5	6	5	3	1
MMS	64	PS	3	5	7	5	3	2
Email	128	PS	10	15	20	15	10	5
Video streaming	384	PS	2	5	7	10	12	15
File download	384	PS	3	5	8	10	13	15
Web browsing	1920	PS	5	10	15	20	25	30

Figure 5.7 and Figure 5.8 present the service and radio bearer distributions respectively for the six scenarios. The first two scenarios are clearly CS centred, with LBR services being predominant, while the last two are mainly PS centred, with HBR services.

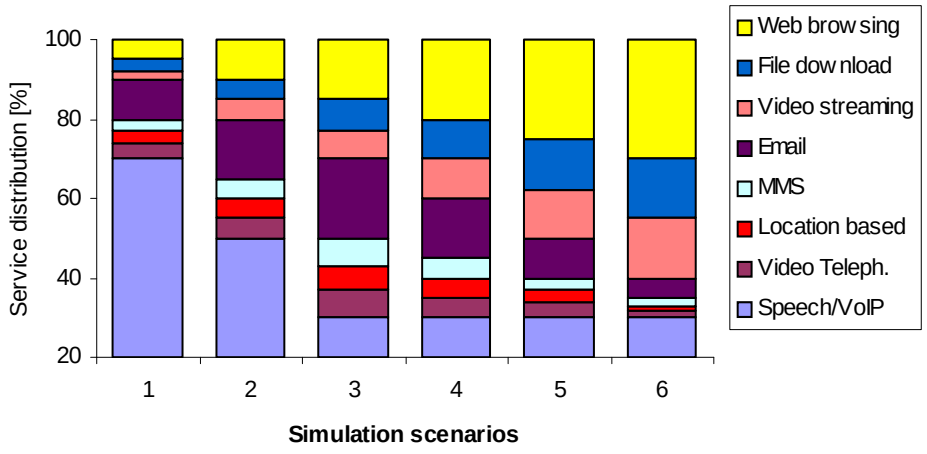

Figure 5.7 – Services distributions across the different scenarios.

The simulator requires several input parameters, as described in Chapters 3 and 4. The majority have default values as presented in Tables 5.2 and 5.3.

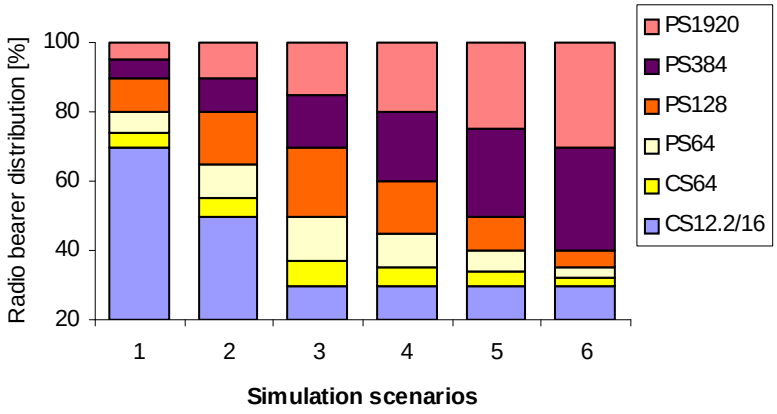

Figure 5.8 – Radio bearer rates per scenario.

Table 5.2 – Network specific default input parameters.

Input parameter	Value
Maximum DL load factor [%]	70
Maximum UL load factor [%]	50
BS Maximum power [dBm]	38
Active set for FDD	3
Scenario	Pedestrian
Frequencies	4 to FDD and 1 to TDD

Table 5.3 – Propagation model specific default input parameters.

Input parameter	Value
Building height [m]	24
BS height	Building height + 1
Street width [m]	24
Width between buildings centres [m]	48
Departing angle from the closest building [º]	90
MT height [m]	1.8

5.2 Reference Scenario

This section addresses the choice of the most adequate scenario. The scenario with 9000 MTs presented in [SeCa04] and applied to the downtown of the city (nearly 1/3 of map) is the departure point with a mean value of 3200 MTs in the area of interest. The choice of the reference scenario is based on blocking and delay probabilities for FDD, which are expected to be less than 2 %. All performance parameters are presented in Annex F.

Figure 5.9 presents load variation in DL when the scenario changes. It can be verified that the most resource-demanding scenario is Scenario 6, and that its corresponding load is small compared to the maximum allowed of 70 %.

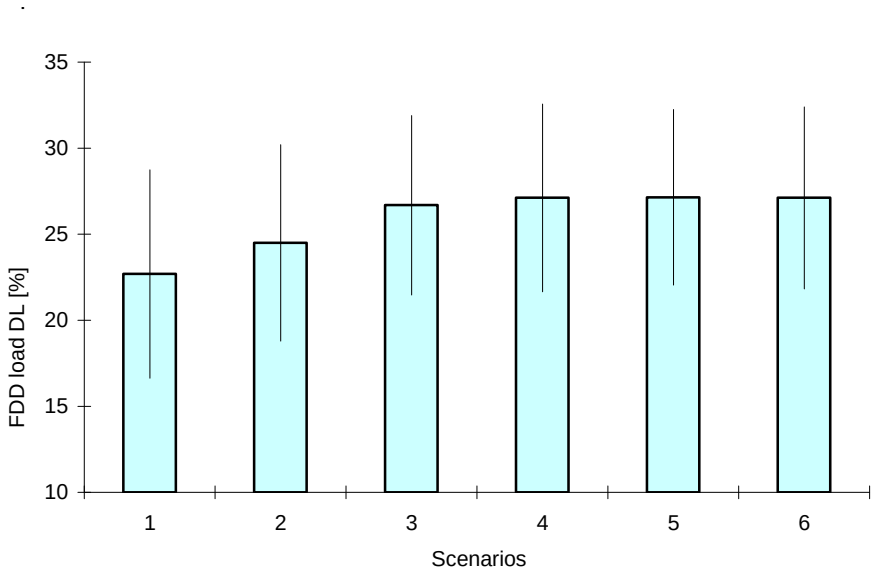

Figure 5.9 – DL FDD load for the six scenarios.

Figure 5.10 presents blocking and delay probabilities, respectively, which increase when the scenarios tend to HBR traffic. Scenario 5 and 6 have unacceptable probability values, while Scenarios 3 and 4 are the most balanced ones.

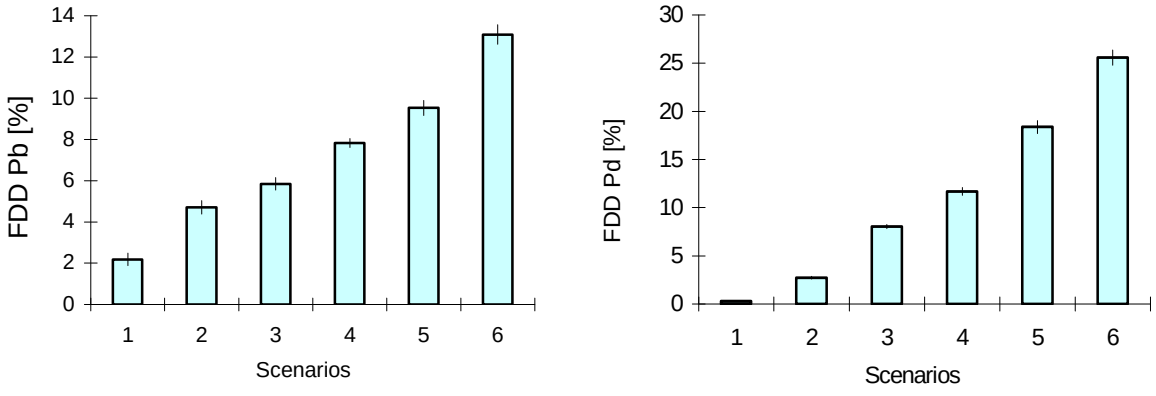

(a) Blocking. (b) Delay.

Figure 5.10 – FDD block and delay probability for the six scenarios.

For all scenarios, 10 simulations were performed leading to a simulation period of around 120h (roughly 10 days), and generating approximately 2 GB of data.

Concerning FDD, Scenario 2 fits best as reference scenario considering the decision parameter. The same parameter was analysed for TDD, for which each cell radius is smaller,

therefore, global uncoverage and delay probabilities rise. Also, as more HBR services are available, MT's maximum allowed distance per service decreases, thus, more uncovered MTs exist.

The next step was the evaluation of this network topology on TDD, network load being the major parameter to focus in these conditions. Figure 5.11 shows DL network load results.

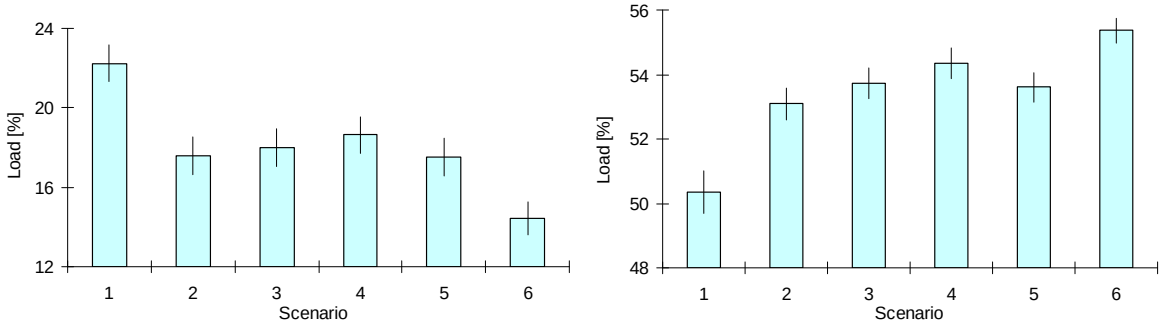

(a) Without interference. (b) With interference.

Figure 5.11 – Mean network load DL per scenario.

In order to lower network load to values similar to the ones of FDD, there were two alternatives: either reduce services throughputs maintaining the network topology, or change it in a way that would allow more MTs to be covered, and globally more HBR services to exist. Taking into consideration that the desired operation mode is TDD with HBR services, the choice was to change the network topology, by adding more BSs. This way, shadowing is reduced and more MTs service. The process was done manually with new BSs being placed into areas where MT densities are higher and more shadow zones exist. For each set of two BSs, a new one was added. The resulting cellular topology has a total of 185 BSs. Figure 5.12 shows the new TDD coverage, which is now larger, with almost no uncovered areas.

All tested scenarios must again be simulated in the new cellular network. DL load with interference remains the decision parameter. The global results can be found in Annex E. Results regarding decision parameters, i.e., the ones that define the reference scenario, are presented here.

(a) Original coverage. (b) New coverage.

Figure 5.12 - TDD network.

It can be seen in Figure 5.13 that with the new network the load in the first two scenarios is almost similar, due to the scenarios characteristics, which are very close to each other. Also, in these scenarios, interference exists, but its effect is not as destructive as it happens in the other ones. Figure 5.14 shows the load rise when interference is considered. As the scenarios evolve, HBR services penetration rates rise, interference is higher, therefore, load increases globally. It is interesting to look at Scenario 6, with the highest penetration rates of HBR services, where the load without interference is the lowest – mainly due to fewer HBR MTs servicing, excessive distance to the BS and RRM algorithm effects. When interference is considered, this scenario presents the higher load value, due to the fact that the majority of MTs servicing are HBR ones, as it can be seen in Figure 5.14. Refer also to Annex E for further details.

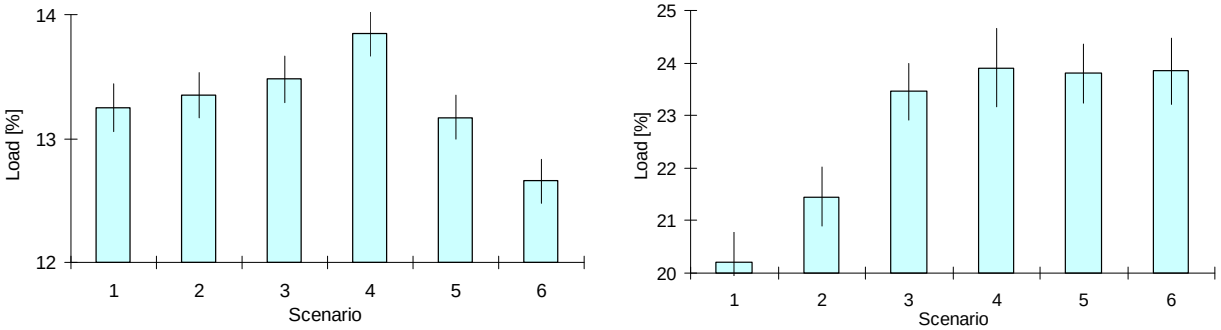

(a) Without interference. (b) With interference.

Figure 5.13 – DL load for the new network topology.

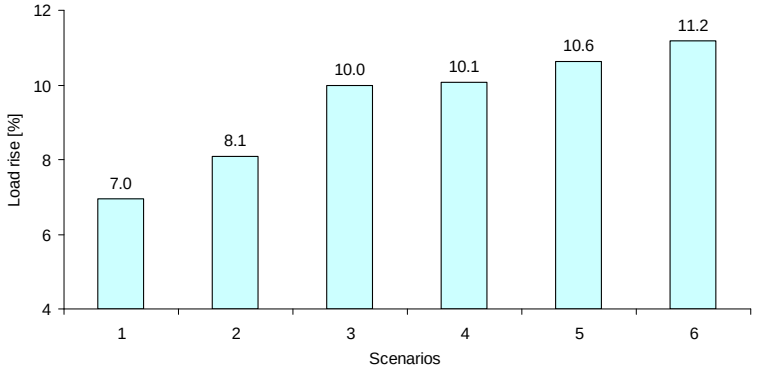

Figure 5.14 – Load rise in DL due to interference.

Scenarios 3 and 4 are very similar, the former being chosen as reference. Several simulations were made on that scenario to characterise it as much as possible. For each parameter, 10 simulations were made, leading to a simulation period of around 200h (roughly 12 days), and generating approximately 4.5 GB of data. There are several performance metrics that can be extracted from Table 5.4, and that can be used for quantifying performance.

Table 5.4 – Reference sceario characterisation.

Scenario 3 characterisation					
Parameter (185 BSs)	Av.	Max	Min	Std dev	Obs.
Network load DL without interference [%]	13.48	21.20	6.74	0.11	Network
Network load DL with interference [%]	23.46	65.96	12.56	3.89	Network
Network load UL without interference [%]	13.29	19.20	1.91	0.54	Network
Network load UL with interference [%]	13.29	19.20	1.91	0.54	Network
Network users	3379	3540	2899	216	Network
Outaged MTs due to initial RRM algorithm [%]	17.89	18.11	17.46	0.2	Network
MTs servicing without interference [%]	82.1	82.5	81.9	0.2	Network
Forced termination probability P_{ft} [%]	27.1	27.6	26.9	0.3	Network
MTs servicing with interference [%]	72.9	73.1	72.4	3.4	Network
Reduced MTs due to E_b/N_o <target and more than 1 TS DL [%]	26.6	27.3	25.3	0.7	Network
Reduced MTs due to E_b/N_o <target and more than 1 TS UL [%]	5.0	5.8	3.6	0.8	Network
Probability of low quality access P_{low} [%]	53.8	63.9	44.2	7.2	Network
Bit rate and code usage DL [%]	55.9	58.3	54.8	1.3	Network
Bit rate and code usage UL [%]	51.2	52.7	49.7	1.1	Network
Free codes DL [%]	44.1	45.2	41.7	1.3	Network
Free codes UL [%]	48.8	50.3	47.3	1.1	Network
TS usage DL [%]	60.3	62.9	59.0	1.5	Network
TS usage UL [%]	67.6	69.2	66.7	1.1	Network
Free TS DL [%]	39.7	41.0	37.1	1.5	Network
Free TS UL [%]	32.4	33.3	30.8	1.1	Network
Active MTs per BS UL/DL	11	13	10	1	BS
Intra-Cell interference power [mW] DL	36.5	46.7	23.7	7.5	Network
Intra-Cell interference power [mW] UL	34.4	67.2	19.9	16.8	Network
Inter-Cell interference power [mW] DL	0.114	0.118	0.108	0.004	Network
Inter-Cell interference power [mW] UL	0.180	0.185	0.177	0.003	Network

Regarding DL network load without considering interference, the scenario presents around 13.5 %, and, when interference is added, this value rises to 23.5 %. A parallel can be made now: the value of network load without interference indicates that in general terms the great majority of MTs are servicing at 64 kbps, roughly. As interference is accounted for, the 10% load rise indicates that the same MTs are now servicing at a mean of around 128 kbps. This is also supported by the value of mean bit rate per TS in the network.

When interference is considered, P_{ft} becomes 27 % and P_{low} 53 %. Service priorisation schemes (where, for instance, a HBR MT would see its needed resources allocated before a LBR MT) were not developed and subject of analysis in this work. This aspect is very important also because one of the premises was that only the three HBR services would suffer reduction, thus, meaning that these are the ones that suffer the most due to the existence of limited resources in the network. Services 1 to 3 are reduced, hence, without any kind of resource allocation priorisation scheme, LBR services are served first, leaving the remaining resources for HBR services. This, in fact, leads to high outage rates and delay of HBR services when the RRM algorithm applies. Results presented in Annex E support these statements.

Scenario 3 is the departure point. Scenario 4 would also be an interesting reference one, but it is more sensitive to the RRM algorithm.

5.3 Frame Asymmetry

The first set of tests on the TDD reference scenario is frame asymmetry. At this point, it is considered that frames are synchronised in the whole network. Several parameters are analysed, as a function of frame asymmetry:

- The network's codes and bit rate with and without interference;
- P_{low} and P_{ft};
- The number of partial reductions due to interference effects;
- The system's intra-cell, inter-cell and total interferences.

Figure 5.15 and Figure 5.16 show the effects of interference on the number of codes and bit rate for different asymmetries, respectively. Code reduction percentage tends to rise as more TS are available in the DL, as a direct consequence of more HBR MTs being reduced due to interference. After 5D7U asymmetry, the bit rate or code reduction becomes stable around

45% when it would be expected to rise due to interference rise. As seen before, interference tends to level, due to the effects of the RRM algorithm, to the bit rate reduction when insufficient E_b/N_o exists, and also to the fact that MTs become outaged in the UL due to lack of codes. P_{ft} tends to rise as more DL TSs are available, but, after the 9D3U case, it begins to drop mainly due to the shortage of the number of codes in the UL, thus, forcing less HBR MTs to service in the network, Figure 5.17.

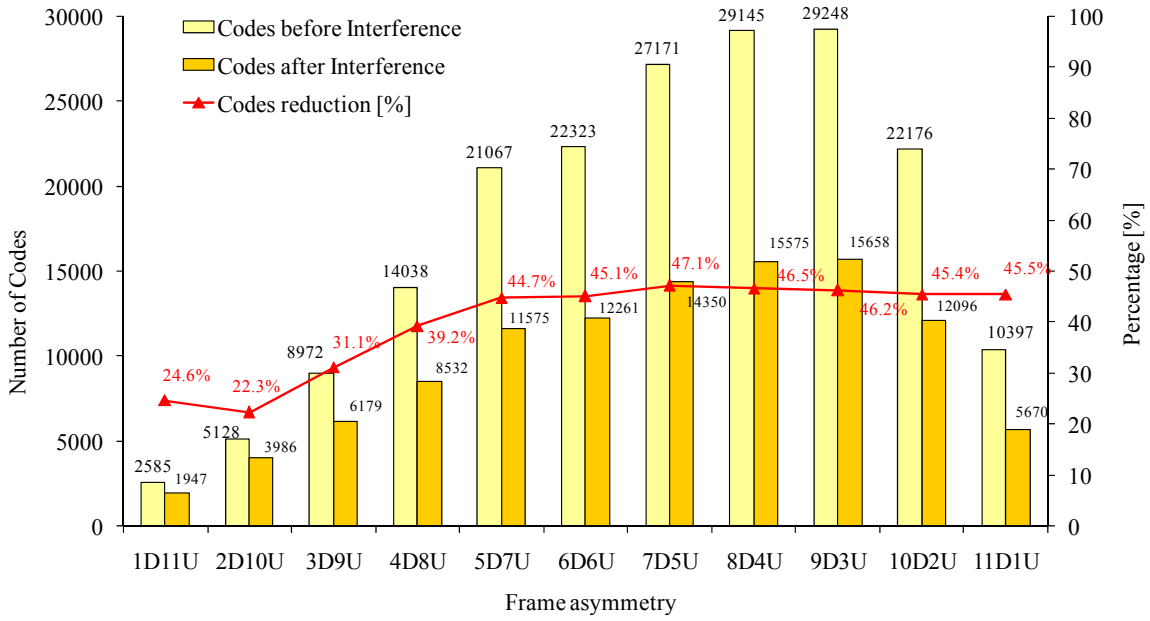

Figure 5.15 – Interference effects on codes as a function of the frame asymmetry.

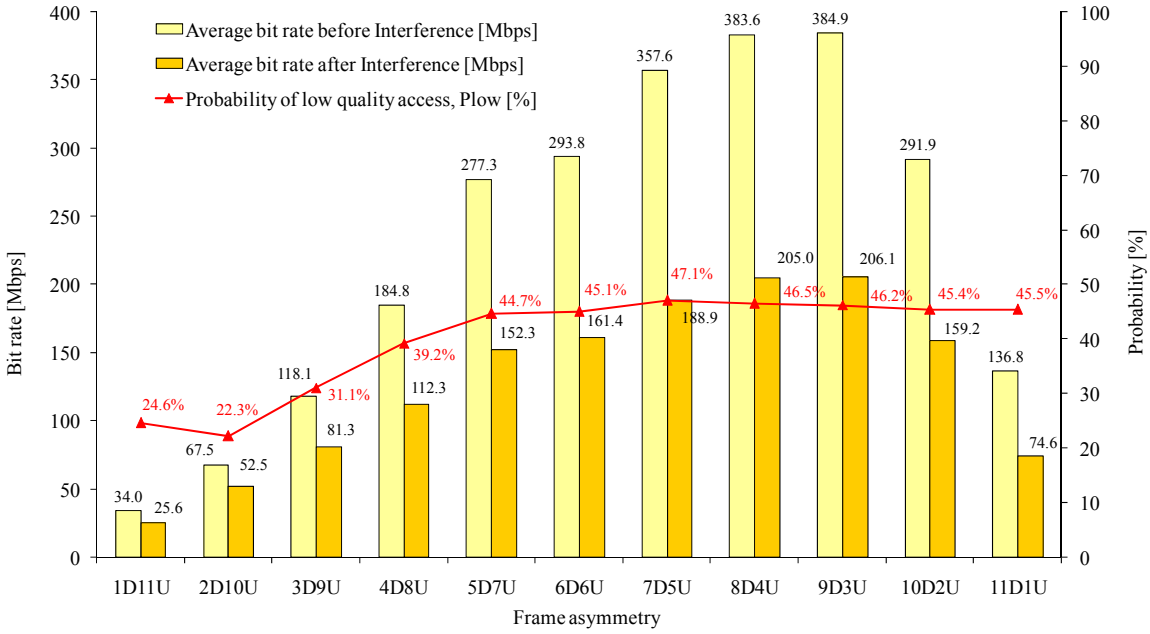

Figure 5.16 – Effects over the network bit rate as a function of the frame asymmetry.

Figure 5.18 shows the percentage of partial bit rate reductions due to interference effects for MTs using more than one TS. The extreme cases exist when only one TS is available for each link, and no partial reductions exist as there are no MTs using more than one TSs. As more DL/UL TS become available and more HBR MTs serve, it is expectable to have a higher number of MTs servicing on several TSs, therefore, higher levels of bit rate reduction.

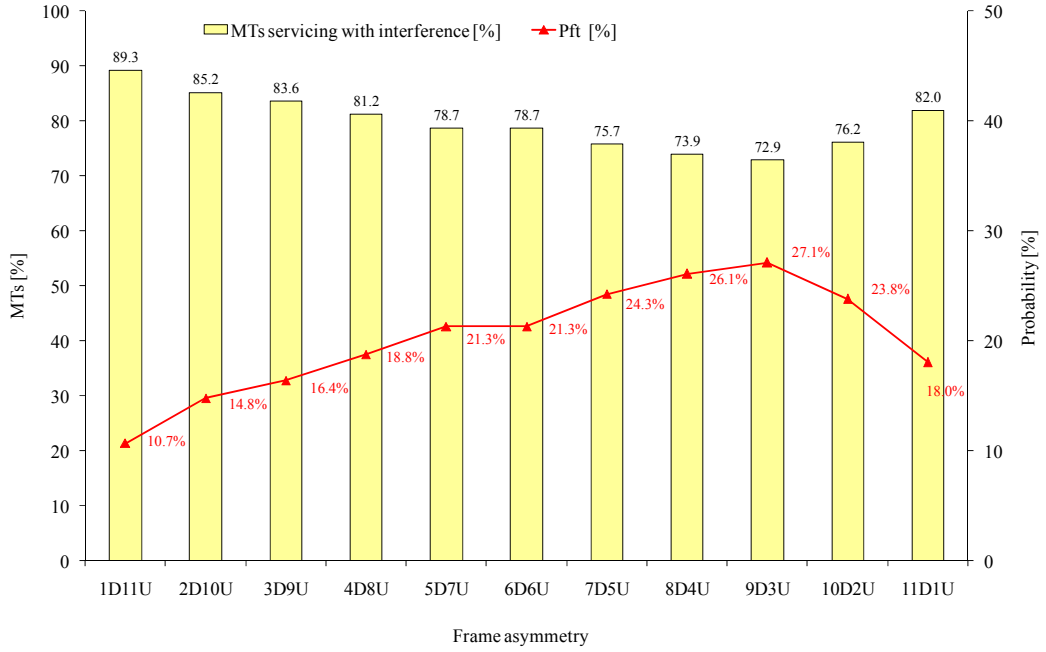

Figure 5.17 – Probability of forced termination as a function of the frame asymmetry.

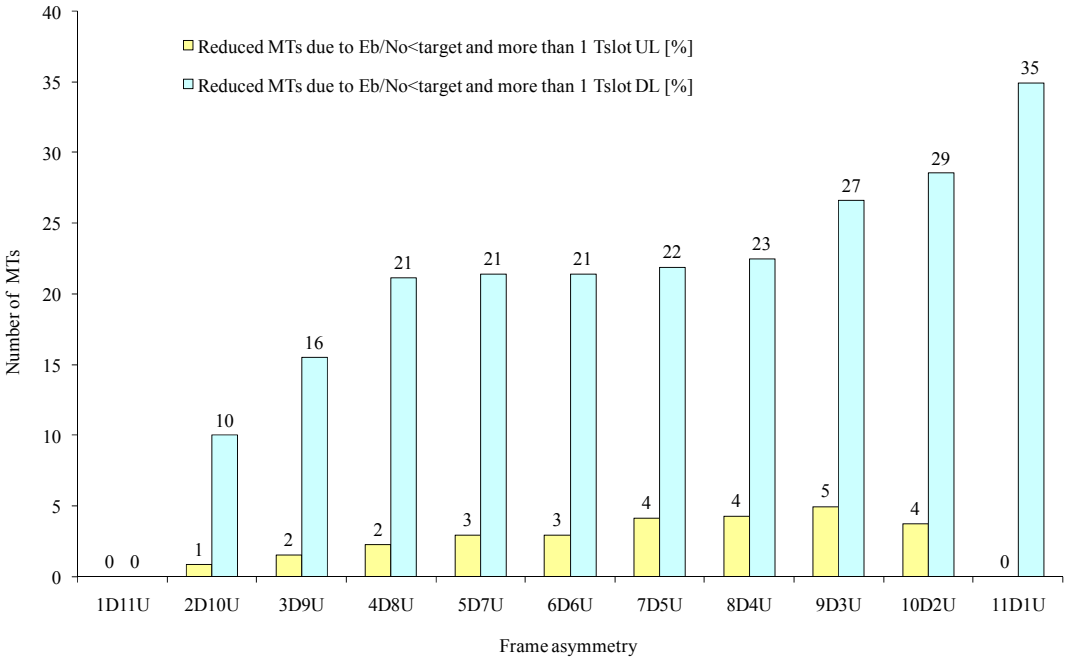

Figure 5.18 – Reduction due to non-destructive interference as a function of the frame asymmetry.

Figure 5.19 shows the effects of different frame asymmetries on interference. DL intra-cell interference is higher than UL one, as expected. Also, intra-cell interference rises as the number of servicing MTs per BS rises. The 9D3U asymmetry is the most appropriate one when load is concerned, however, when considering interference, it can be seen that this asymmetry has fewer MTs servicing compared to 7D5U and 8D4U, but on the other hand, less interference is precisely due to the fact that without one additional UL TS, several MTs are delayed and interference reduced. The cost for this interference reduction is only two less MTs servicing, in mean values, which is assumed to be an acceptable trade-off.

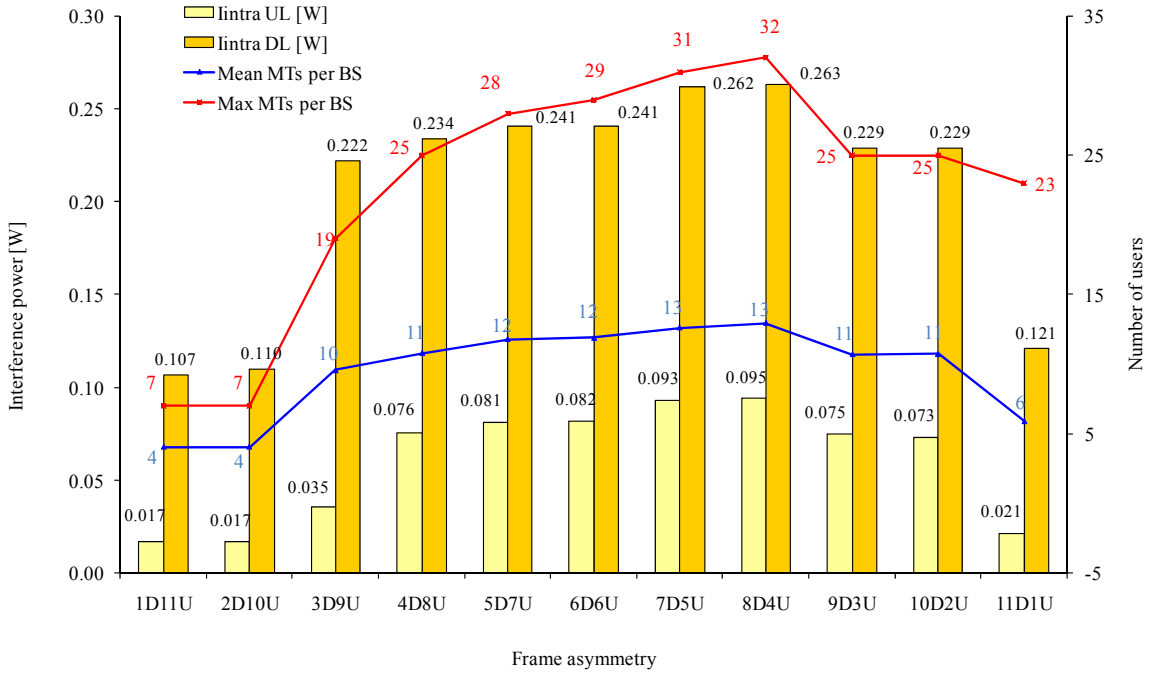

Figure 5.19 – Intra-cell interference and mean MTs servicing per BS.

Regarding inter-cell interference, it is lower than intra-cell one as expected, Figure 5.20. In some asymmetries, UL inter-cell interference is higher than in DL, but the opposite happens in others. Taking 11D1U asymmetry as a reference, it can be seen that inter-cell interference in UL is smaller than in DL. This happens because there is only an UL TS in the whole network, and the number of MTs that are mainly concentrating in the first available UL TS are not enough to create a level of interference higher than in DL. However, for smaller asymmetries where more UL TSs are available, MT concentration per UL TS is higher than in DL TSs and it is natural to have a higher inter-cell interference per TS, per BS and, as a whole, per network. In DL, MTs are spread among existing TSs, which means that per TS in DL, inter-cell interference is smaller, thus, smaller BS mean inter-cell interference and, finally, global network inter-cell interference.

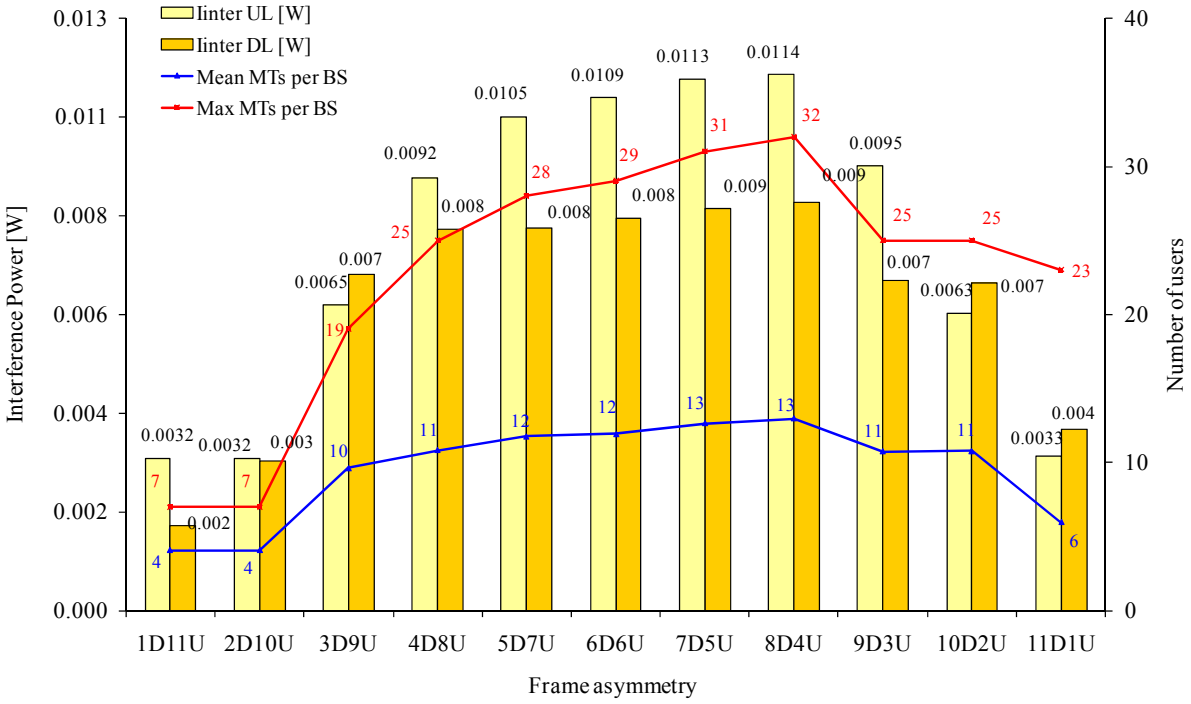

Figure 5.20 – Inter-cell interference and mean MTs in the network.

9D3U presents the best inter-cell values for HBR scenarios. Since the total inference is the sum of inter- and intra-cell components, higher values exist in DL than in UL, as confirmed by the results shown in Figure 5.21. 7D5U, 8D4U, 9D3U and 10D2U are acceptable asymmetries from an interference point of view, if seen as trade-off. As more MTs are servicing, higher values of interference exist in UL and DL. However, RRM algorithms play an important role, because they level the number of MTs in all these asymmetries, leaving them with very similar results when interference is considered.

So, a choice for an asymmetry must be made on another level: the MT and service levels. TDD is aimed to allow services up to a maximum of 1920 kbps. 7D5U and 8D4U asymmetries would never support 1920 kbps services. Therefore, the choice is now narrowed down to the remaining two asymmetries, 9D3U and 10D2U, which are the ones from the four that have lowest interference on both links.

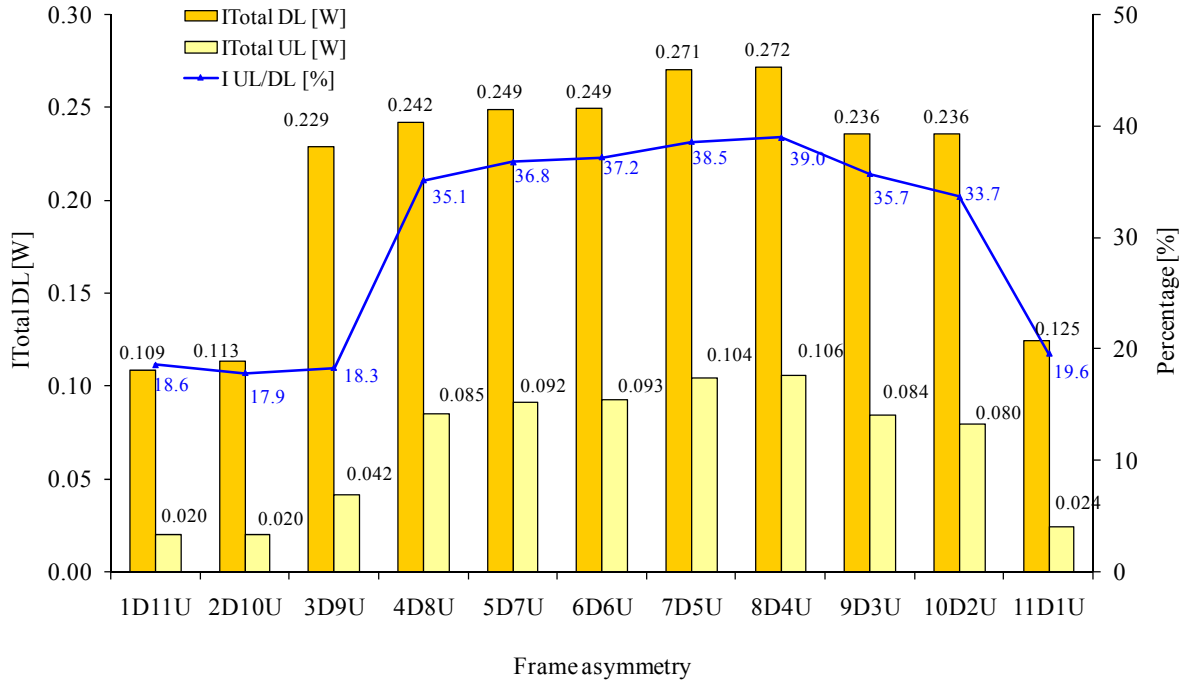

Figure 5.21 – Total interference in the UL and DL.

10D2U asymmetry allows 1920 kbps and more MTs in the DL than 9D3U. In UL, having one less TS may lead to less MTs servicing on DL due to lack of UL codes. From the results, there is not an obvious advantage of both scenarios on each other. One could say, by looking at Figure 5.18, that 10U2D has higher levels of MTs with reduced bit rate due to interference; however, even if reduced, the global network capacity is similar because there are more MTs servicing, scenario 10D2U also has lower P_{ft}. The great majority of the literature assumes that 9D3U symmetry is the most balanced one. This work results do not contradict that. From a global network interference point of view, there are no clear advantages of 10D2U asymmetry over 9D3U. Also, the mean number of MTs per BS is equal in both cases. This is an effect of the RRM algorithm that handles resources, in such a way that these two scenarios become levelled between each other. For additional statistics, refer to Annex F, Table F.1. 9D3U asymmetry is chosen and considered on the following tests.

5.4 Network Asyncronism

UMTS TDD is a hybrid TDMA/CDMA MAT, thus, time must be considered and some sort of synchronism must exist in the whole network. The last subsection presented interference calculations considering that the entire BS in the network shared a common time source and were synchronised. As seen in Chapter 3, by considering no time offset between adjacent

BSs, interference scenarios are fewer. Effects of network asynchronisation are noticed only in the inter-cell interference.

The synchronisation factor was incremented in 5 % steps, resulting on a total of twenty interference scenarios, performing a total of 300 hours of simulations and close to 6GB of data. By inspecting (3.24) and (3.27), as δ_{offset} becomes progressively higher, MT to MT and BS to BS interference powers in UL rise, whereas MT to BS in UL and BS to MT in DL interference powers drop. The numerical model is used at this point to generate all interference calculations and results.

It is important to note that the following results of interference rise and dropage are calculated by having as reference inter-cell interference power when synchronism exists. The results of rising the value of δ_{offset} in UL are presented in Figure 5.22. When synchronism exists (δ_{offset} = 0) there is no interference among BSs.

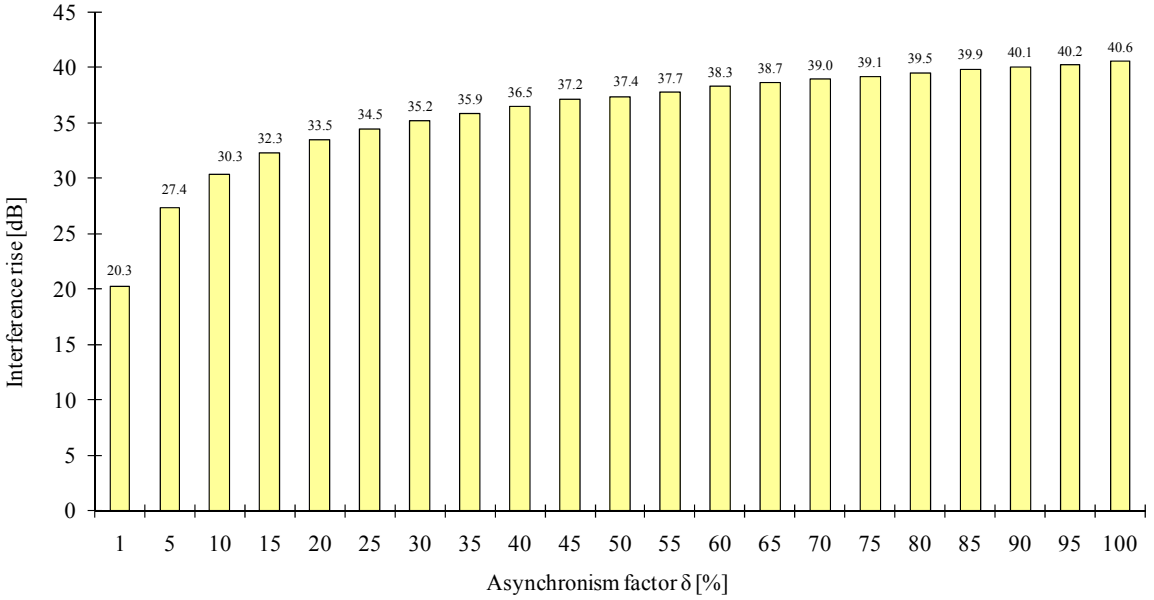

Figure 5.22 – Effects of δ_{offset} on the interference between BSs in UL.

The worst scenario where BSs are completely misaligned, with the highest time offset, represents an increase of 40 dB of interference power. δ_{offset} equal to 1 % represents an inter-cell interference rise of 20 dB relative to interference levels when δ_{offset} equals 0 %.

Conversely, interference among MTs and BSs drops as the offset factor becomes higher. As shown in Figure 5.23, when synchronism exists interference dropage is zero, and δ_{offset} rises the interference power among BSs and MTs actually drops, leading to a total interference dropage of 13 dB.

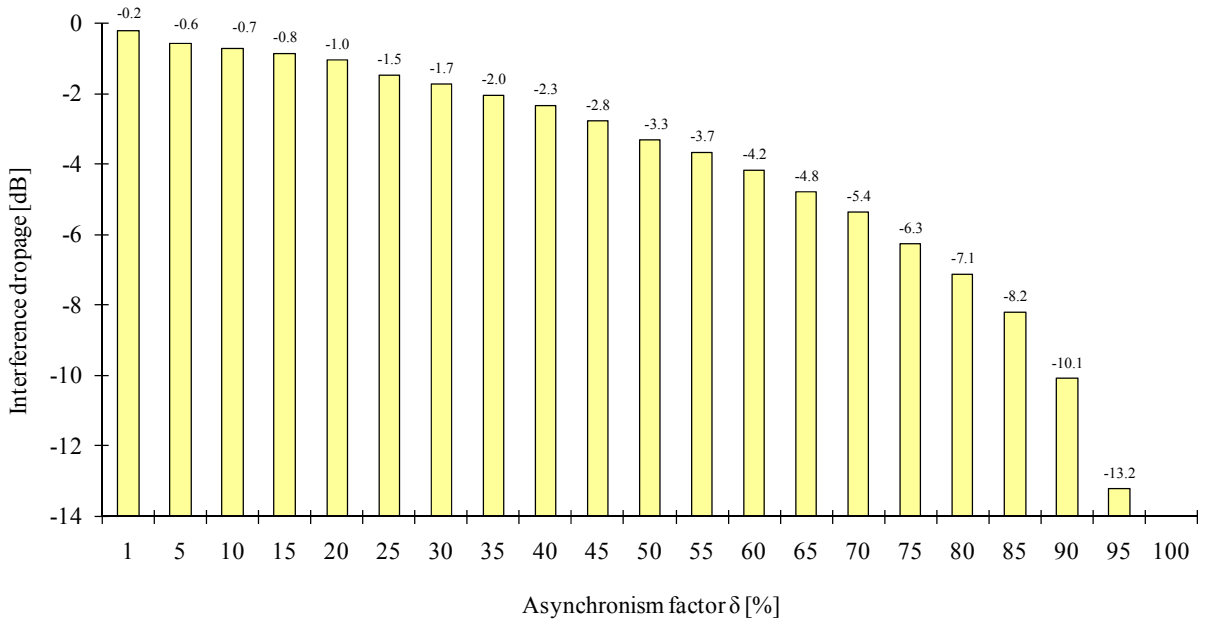

Figure 5.23 – Effects of δ_{offset} on the interference between the BSs and MTs in UL.

When comparing both interference types, Figure 5.24, it is clear that interference among BSs tends to rise and that among MTs and BSs drops, both as a direct dependence on the value of δ_{offset}. When cells are completely misaligned in time, an interference increase of 40 dB appears in UL, whilst in DL the total inter-cell interference drops 13 dB, leading to a capacity increase in DL, but very large decrease in UL.

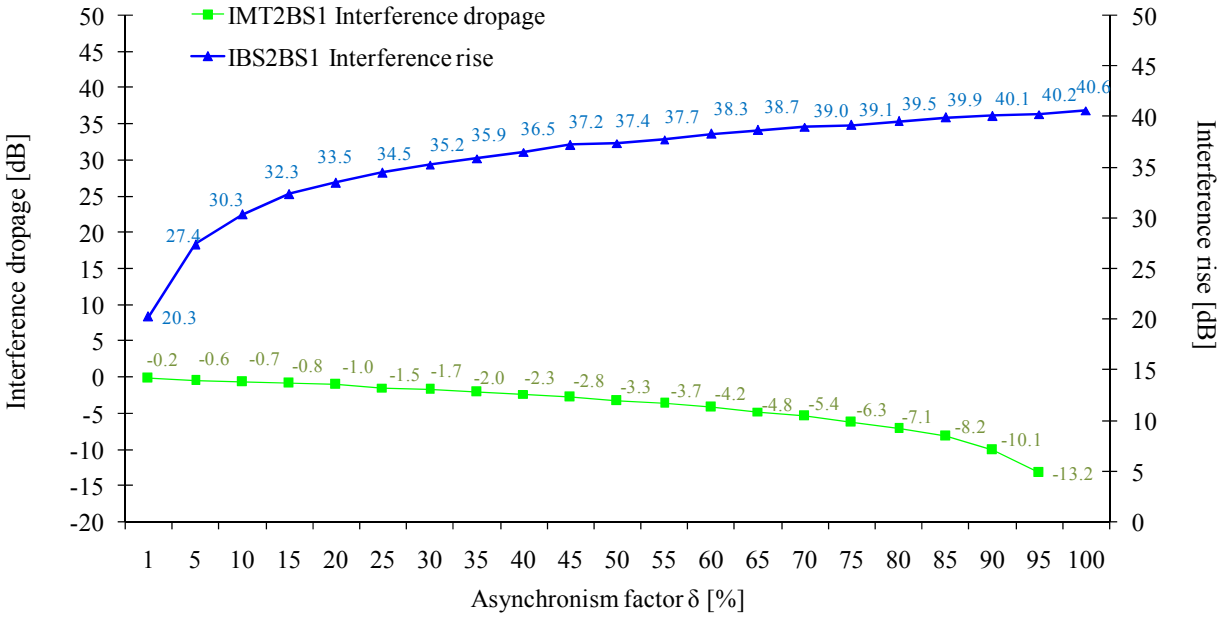

Figure 5.24 – Effects of δ_{offset} in the two inter-cell interference components in UL.

These results are consistent to the theoretical model, where the two inter-cell components are inversely affected by δ_{offset} between each other.

Figure 5.25 shows that the whole system's inter-cell interference follows the behavior of BS to BS interference, due to the fact that this type of interference depends greatly on the path loss among both BSs and - taking into consideration that in the cellular deployment they are very close to each other – that it is the result of summing MT to BS interferences. More details can be found in Annex G. In the current cellular network, inter-cell interference rises to a maximum of 40 dB when asynchronism is maximum. This interference rise in the UL clearly affects the network's capacity in that link. In DL, there are two interference components: interference among MTs and BSs and among MTs, which appears as a result of asynchronism. As the value of δ_{offset} rises, interference among MTs also does, to a total of 34dB higher than when synchronism exists.

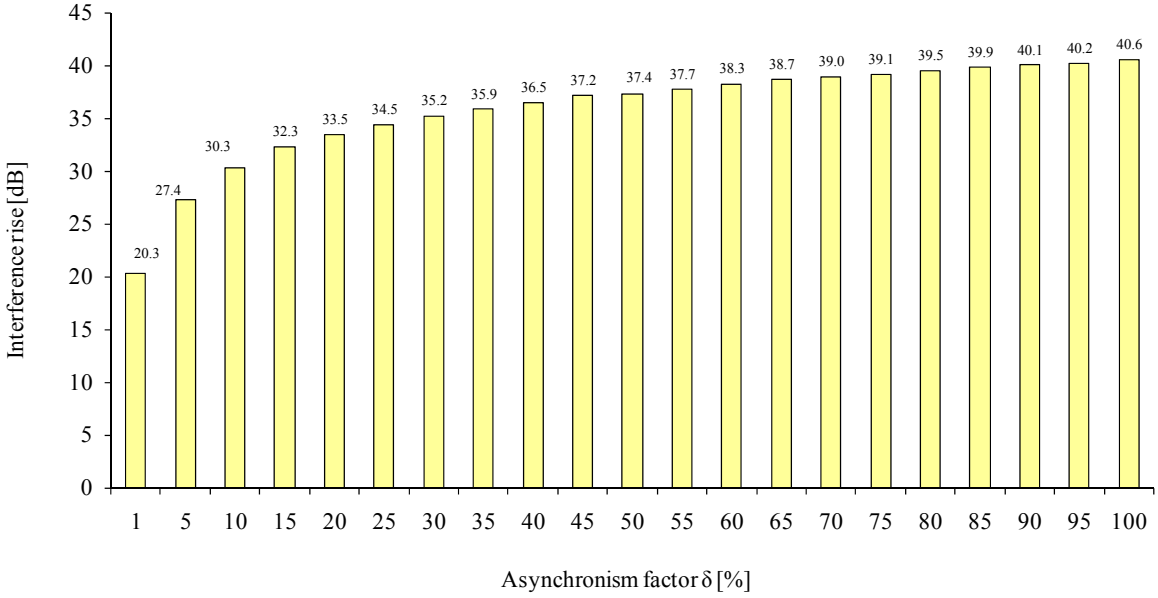

Figure 5.25 – Influence of δ_{offset} on the whole network inter-cell interference in UL.

These results are consistent with the theoretical interference model. Figure 5.26 shows the dependency of the MT-to-MT interference with δ_{offset}. Interference among MTs increases because it depends directly on the increase of δ_{offset}. This result is expected, because interference among MTs only exists when synchronism does not exist between adjacent cells. Nevertheless, this is only one of the two components that form the inter-cell interference. In UL, interference due to asynchronism is higher than MT to BS interference experienced when synchronism exists. So, the global inter-cell interference in UL follows the behaviour of BS to BS interference.

A similar study was conducted for DL. The second component of the inter-cell interference in DL is interference between BSs and MTs. Figure 5.27 shows the results of the reference

model, after applying it to the existing reference scenario and network topology.

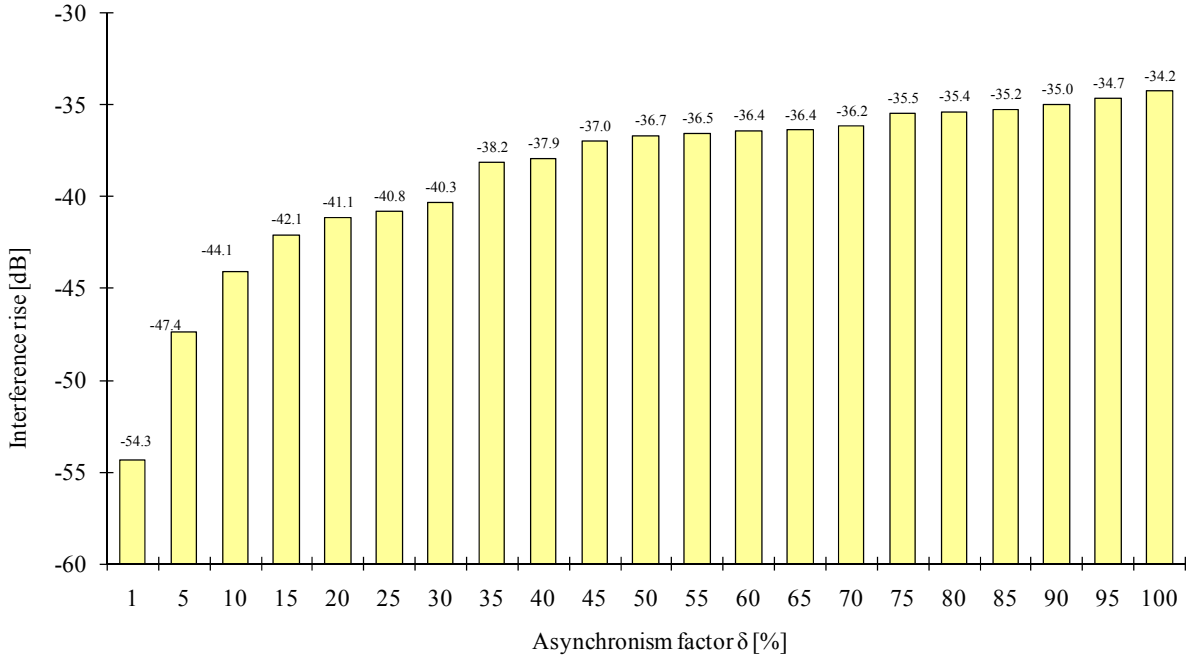

Figure 5.26 – Influence of δ_{offset} on the MT-to-MT inter-cell interference in DL.

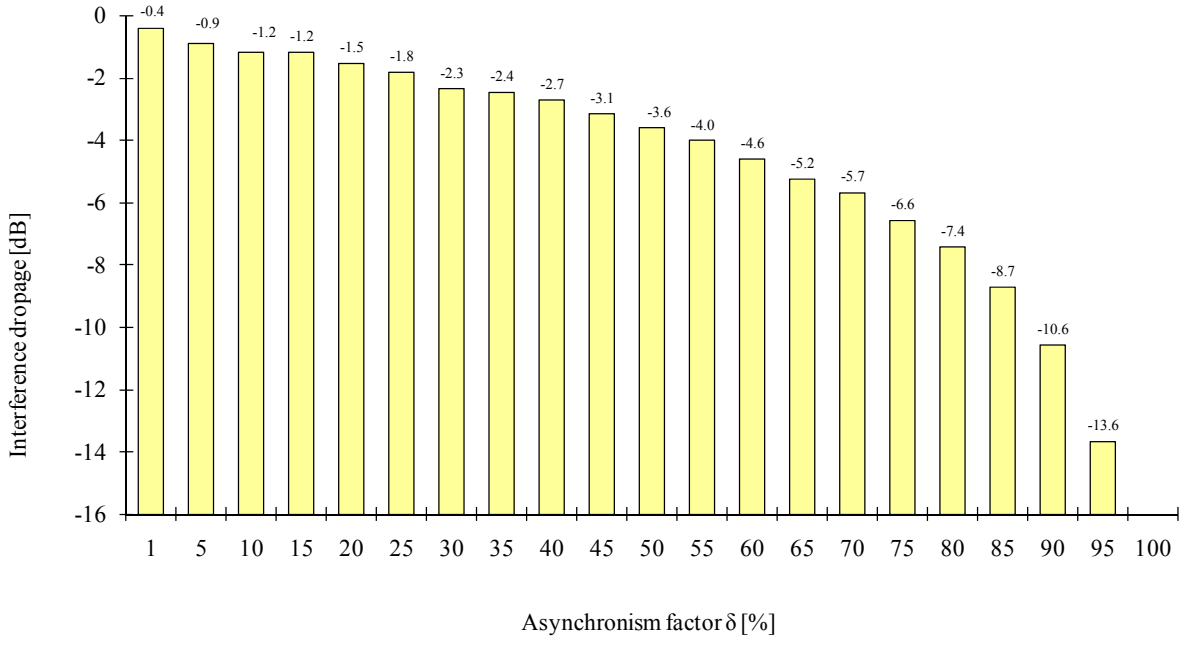

Figure 5.27 – Influence of δ_{offset} on the BS-to-MT inter-cell interference in DL.

Figure 5.28 shows the overall inter-cell interference in DL. It can be seen that the global inter-cell interference follows the component that already exists when synchronism is considered. This has to do with the values of interference power, as referred before.

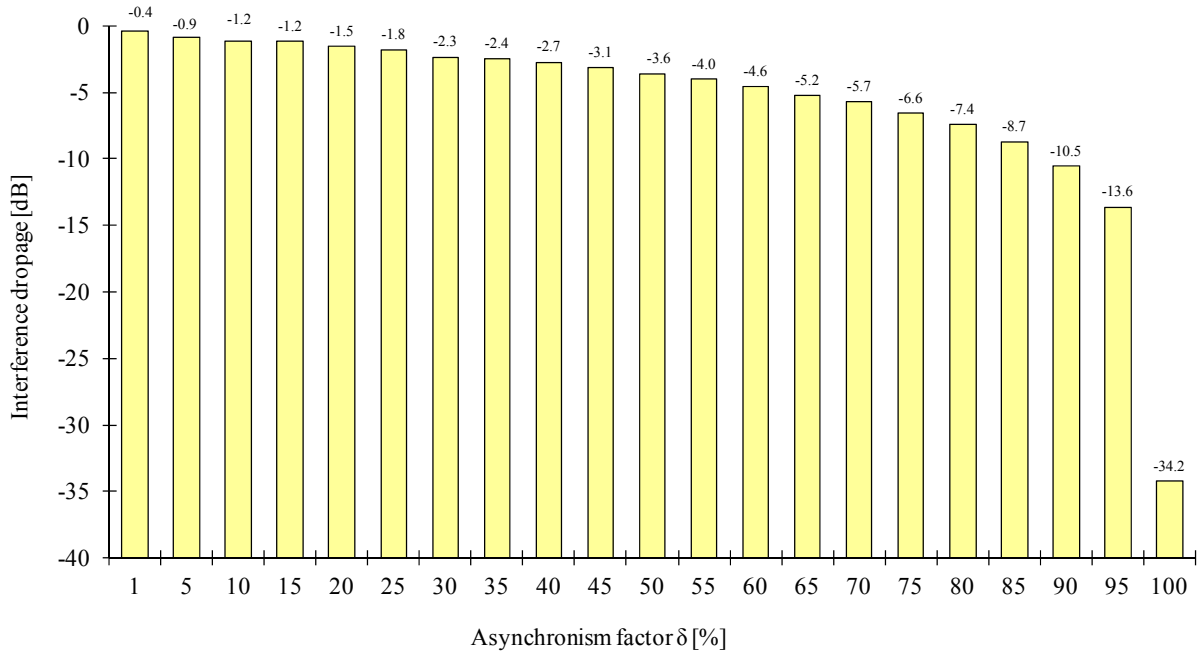

Figure 5.28 – Influence of δ_{offset} on the global network inter-cell interference in DL.

It can be seen from Figure 5.29 that the inter-cell interference among MT and BS maintains its behaviour, decreasing to a maximum of 13 dB less interference.

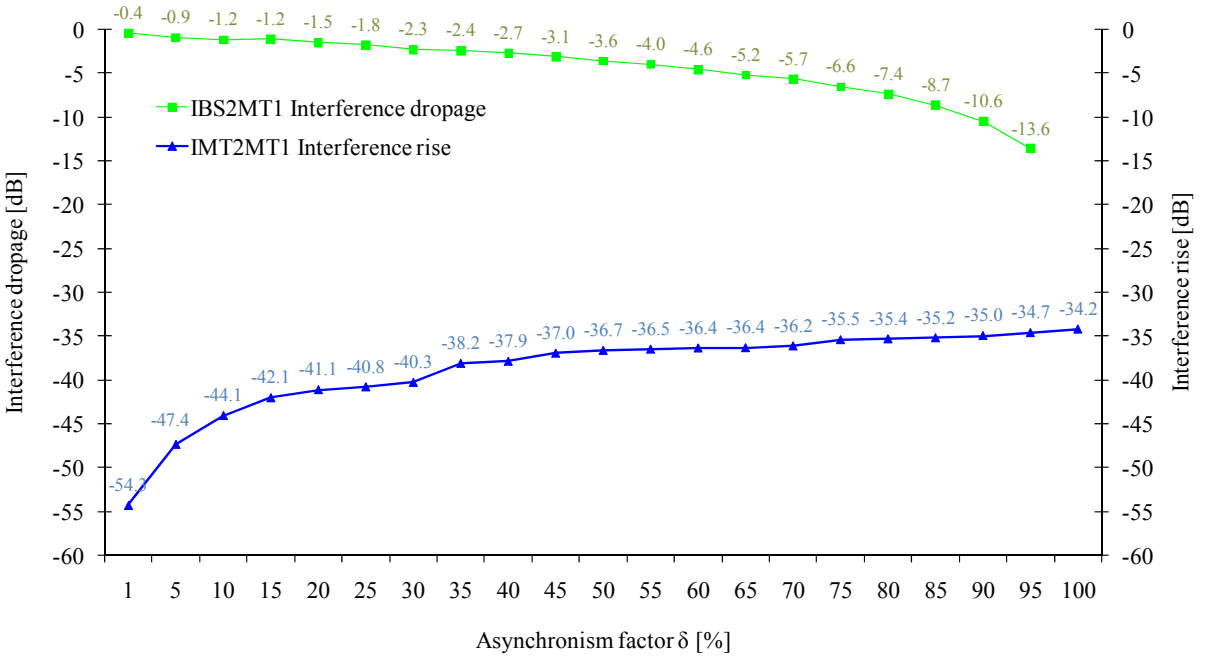

Figure 5.29 – Effects of δ_{offset} in the two inter-cell interference components in DL.

Conversely, as expected, interference among MTs increases, but its power is neglectable when added to interference power of the MT to BS link, thus, leading to a total inter-cell interference in DL following the behaviour of interference among MT and BS.

The results show that for DL a different behaviour exists, and that DL does not suffer as much as UL, neither does the capacity drop as dramatically as it does in UL. In fact, a capacity increase is noticed in DL, as it is referred in the following paragraphs. As it happens for UL, in DL intra-cell interference does not depend on network synchronisation, thus, its behaviour is considered only when the interference model analysis focuses on the global network interference.

It is interesting to see that inter-cell interference gets as low as 34 dB less in interference power when the total asynchronism exists, Figure 5.28. This happens because at that point there is no BS to MT interference power but only MT to MT one, which is very low.

The results this far show that inter-cell interference rise in UL is very high in the current scenario with the current network topology. It also shows that interference among MTs and BSs is smaller, and tends to drop when the synchronism offset rises, as it happens with MT to BS interference in DL. The other component of DL inter-cell interference rises as the asynchronism factor also rises, but with less expression in the global inter-cell interference power in DL due to its mean interference power, being one thousand times smaller than the interference experienced among MTs and BSs. The BS to BS interference depends greatly on the path loss between these two entities, which may lead to the conclusion that this cellular network topology is not the most adequate for the scenario, due to the high value of interference rise.

In order to have a global view of interference in the current network, the total interference power must be analysed. Figure 5.30 shows the total network's interference in both links. This figure allows stating that the inter-cell interference rise in the UL is almost dramatic, as it becomes higher than the intra-cell interference, thus, greatly reducing the overall network's capacity in the UL. It can be seen that for a small offset of 1 % the inter-cell interference in the UL rises about 20 dB, corresponding to the BS to BS interference rise and drops about 1dB corresponding to the BS to MT one. This is consistent with what was referred before, i.e., that DL is not as sensitive to network asynchronisation as UL is.

It is shown that the current network topology may not be the most appropriate and that the manual method used to deploy BSs is not the most desirable. In DL, the overall interference drops mainly due to dropage of the BS to MT interference. The MT to MT interference rises but taking into account that its interference power is 10^3 times smaller than the BS to MT one, its effects are not noticeable. In fact, when asynchronism exists, a capacity increase in DL

appears as fewer MTs suffer from interference effects, Annex G. This can also be seen on the forced termination probability compared to the same value without asynchronism. On the other hand, network becomes greatly limited in UL due to interference rise of the BS to BS interference, as the majority of the studies analysed conclude.

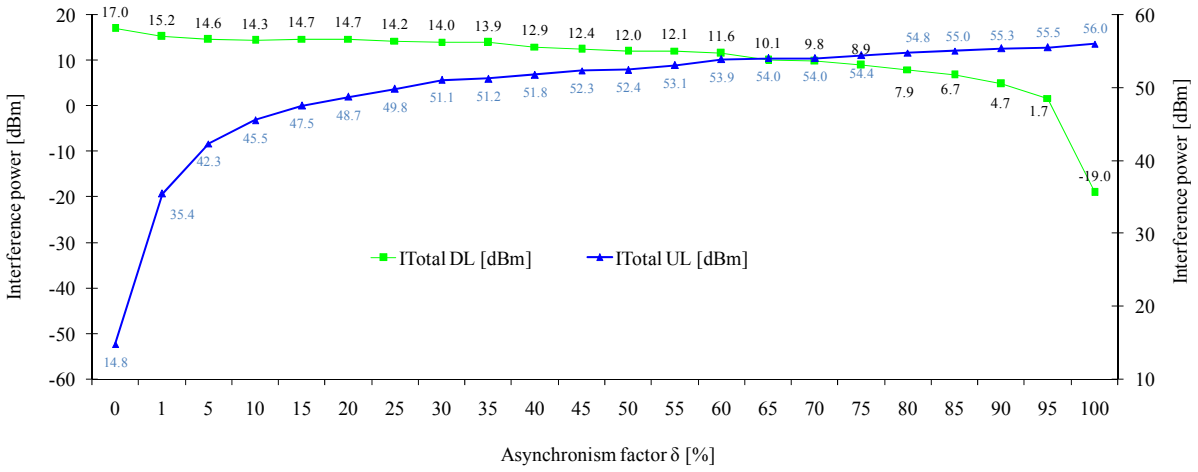

Figure 5.30 - Effects of δ_{offset} on the network's total interference in UL and DL.

If the interfering TDD cells are not synchronised additional interferences also occur. It is also shown that the worst case of interference in a TDD network often occurs among BSs. The MT to MT interference is also a problem, but most of this interference can be solved by using a dynamic resource allocation scheme, as referred before.

As for the BS to BS interference, as it depends greatly on the path loss among BSs, it may be resolved or reduced with a correct network planning. From the obained results one realises that mitigating this kind of interference is very important, thus, δ_{offset} should be kept small. However, for avoiding MT to BS interference, δ_{offset} should be kept high. In both cases, however, the control of this parameter implies a tighter control of inter-cell time and frame synchronisation, therefore, reducing TDD network flexibility.

Inter-operator interference is not considered on this work, although interference models allow studying it. Since all BSs are under control of the same operator, it is easier to apply interference mitigation techniques. In practice, in the current network topology, results show that UL capacity degrades almost linearly as BS to BS interference increases (δ_{offset} increases). DL performance is not as sensitive to frame synchronisation as UL due, mainly, to the fact that interference among MTs is small compared to the BS to MT interference. The results also show that the manual process used to deploy a new network is not the most appropriate as inter-BS interference increased greatly, indicating that a bad cellular deployment exists.

Chapter 6

Conclusions

This chapter presents conclusions and points aspects to be developed in future work.

The main objective of this work is the development of an interference model to allow the evaluation and calculation of interference effects over a TDD cellular network. The work is developed for UMTS TDD, although the interference model may be applied to other TDMA based networks. A simulator for TDD is developed, in order to support the developed interference model.

This work begins with an overview of the UMTS network on both FDD and TDD modes in Chapter 2. A description of the network architecture is provided. Radio interface aspects are presented, including spectrum allocation for both modes and the main WCDMA parameters. Afterwards, FDD and TDD are characterised and differentiated on major parameters. The TDD frame structure is also analysed. Chapter 2 ends by describing some of the RRM algorithms, and enumerating the services and applications available in UMTS.

Chapter 3 addresses the capacity aspects of FDD and TDD networks. The link budget is also referred and analysed. A description of the existing simulator for TDD is made. Several interference studies are presented and analysed, including the one that forms the basis for the interference model. This chapter finishes with interference modelling and model development.

The physical scenario considered is downtown Lisbon, where higher penetration rates of HBR services exist. Interference is evaluated as a function of frame asymmetry and network synchronism. The first allows finding the most desirable TDD frame asymmetry with lowest impact on network's interference; interference calculations were made and several performance indicators were derived as the frame asymmetry varied from 1D11U to 11D1U. The second allows studying asynchronism effects and its impact on the global network's interference; asynchronism offset ranged from 1 % to 100 % in 5 % steps.

Chapter 4 presents in greater detail the existing simulator and the newly developed TDD add ons. General aspects are presented, as long with the major input and output parameters. The developed RRM algorithms are also presented and discussed in greater depth, followed by the necessary assessment studies. Interference specific validations are presented, finishing with the sensitivity studies, in order to find the average number of simulations needed for each parameter to be analysed. Two RRM algorithm were developed. One manages existing network codes, evaluates code needs, and allocates them to MTs accordingly. This algorithm supports MT's service bit rate reduction to allow as many MTs as possible. The second RRM algorithm is a part of the interference model having the objective of analysing the number of

TS that each MT is using, and calculating the corresponding E_b/N_o with interference effects in each one of them, comparing with target values. This allows the introduction of two new concepts in this work: destructive and non-destructive interferences.

Chapter 5 is dedicated to the results. It begins with a description of possible adopted scenarios, from a total of six, and follows with the choice of a reference one. A manual cellular deployment was made, creating a new network topology with 185 BSs, allowing to simulate a HBR TDD environment.

Along the whole network analysis, evaluation and results, it is seen that the initial RRM algorithm has a strong influence on the whole network's behavior. It limits upfront HBR MTs, which leads to, when interference is not considered, the same levels of network load as LBR services. From the RRM algorithm, HBR services are reduced, thus, reducing network load. This is a positive aspect from one point of view, but on the other hand this is also a negative aspect when considering a TDD network that must have predominantly HBR MTs. Also, it is concluded that the initial RRM algorithm affects too much HBR MTs, because resources are allocated to MTs as they "appear", meaning that the majority of LBR services get served first, and the remaining resources (codes) are then distributed to HBR MTs. Clearly, this affects more HBR than LBR MTs, because they have its services more reduced, on the contrary of what should happen on a TDD network. The effects of the RRM algorithm on interference reduction are indirect. The RRM algorithm limits the number of HBR MTs in the network and also their service bit rate, thus, indirectly, limiting the amount of interference that these MTs generate.

Notice that service priorisation schemes (where, for instance, a HBR MT would see its resources allocated before a LBR MT) were not developed and subject of analysis in this work. This aspect is important, because one of the premises is that only the three HBR services would suffer reduction, thus, meaning that the HBR services are the ones that suffer the most due to the existence of limited resources in the network. This, in fact, leads to high rates of outaging and delay on HBR services when the RRM algorithm applies.

Results clearly illustrate that interference experienced within a TDD network is, in many aspects, more difficult to model when synchronisation and asymmetry issues are taken into account. Results also suggest that there are many benefits that can be gained by intelligently exploiting the interference properties within a TDD network, since different parts of each cell experience different levels of interference, depending on the geometry, asymmetry, and

synchronisation.

Intra-operator inter-cell interference can be handled more efficiently, since all BSs are part of the same network, therefore it can be easily time coordinated. Interference control can be achieved through a range of techniques, e.g., network synchronisation, and dynamic resource management. Synchronising TDD frames and even signal in links of all sectors reduces interference, but also flexibility and spectrum efficiency. A trade-off between flexibility and risk of harmful interference has to be made in each case, and full synchronisation should only be used in special situations where the risk of interference is very high.

It is demonstrated that the most important source of interference, when network synchronism does not exist, is between BSs. The interference rise is very noticeable – mainly due to the fact that the physical separation among BSs is very small and that cell overlapping exists in almost all cells - limiting network's capacity in UL. In the current network topology, the mutual interference among BSs is higher due mainly to the fact that it is a real network with overlapping cells, opposite to the majority of the existing studies where cells are considered not to be overlapped. Inter-cell interference becomes higher than intra-cell one in UL. Taking into consideration that BS to BS interference depends on the path loss among them, the conclusion is that the manual cellular deployment that was made is not the most correct, as it would be expected. In DL, a capacity increase is experienced mainly due to the fact that the BS to MT interference drops as the asynchronism factor increases. Nevertheless, interference between MTs rises and this is a difficult type of interference to mitigate. Dynamic channel allocation algorithms would help reducing this type of interference, while a correct network planning would reduce the inter-cell interference between BSs.

The work presents some simplifications and assumptions that create space for further developments. There is still work that can be done in the future, in order to improve the performance of the interference model. The following paragraphs focus on the future work and improvements that can be done to this work.

As referred before, interfering BSs are the ones from all tiers of adjacent BSs. It would be interesting to see from which tier on the lack of synchronism does no longer represent a problem (BS interference on a victim BS is neglectible), and synchronism is no longer needed. This study would allow finding the maximum distance at which BS to BS interference exists due to asynchronism. This, along with a careful planning, would allow the

reduction of the inter-cell interference among BSs. The simulator is prepared for this study, as the maximum radius of analysis is an input parameter of the simulator.

As for the allocation algorithm, a new scheme, with prioritisation among services, would greatly improve the interference model, as the HBR MTs would not be more penalised than LBR ones. The developed algorithm does not take into account the type of service and any kind of service priority among different MTs. Also, if this algorithm could take as input the information about the different asymmetries or time offsets in TDD frames, it would be possible to dynamically adapt itself to asynchronism conditions and correctly allocate MTs to TSs, in such a manner that would allow reducing overall inter-cell interference. This new dynamic resource allocation scheme would allow the reduction of the inter MT interference also.

To ideally reduce among between BSs, a careful planning should have been done. It would be a major improvement to be able to feed the whole network's interference information to a dynamic network planning algorithm as the one described in [Pires07]. This way, having interference calculations and identifying the most interfered zones as input parameters, the dynamic network planning algorithm would generate a certain network topology, which would then be evaluated as a new network by the interference model. The process would then be cyclic, converging to a cellular deployment with lower interference levels throughout the whole network.

Globally, looking at the results, one can conclude that probably the main reason why TDD did not see the light of day is surely related to synchronism. It may also be related to the fact that additional BSs would have to be deployed to maintain the same coverage and capacity, rising the whole network cost for the operator. Nevertheless, synchronism needs is the determining factor. In the case of a single operator in a certain region, it may be acceptable not to have synchronism on the whole network if a careful planning is performed, along with good dynamic resource allocation algorithms. However, in real scenarios, where several operators exist in the same region, the lack of synchronism can be devastating among their networks. In order to coexist in TDD, the following requirements would have to be fulfilled:

- At the intra-operator level, where it is simpler to have synchronism:
    - a very accurate clock at MTs should exist, in order to have a synchronised timing for UL;

  - to obtain full synchronisation between the BSs and MTs, a reference clock must be distributed via a separate channel (e.g., the BSs and MTs could derive a frequency reference from the GPS).

- At the inter-operator level, where it is very difficult to have synchronism among each other:
  - if TDD frames in different cells shall be synchronised, the BSs must be locked to the same time reference source;
  - the necessary timing information could be distributed via the backbone network or derived from an external source (e.g., GPS or synchronisation channel) and be shared by all network operators.

This implies that all operators should share the same timing reference and that, at the minimum offset, interference levels could rise greatly, causing high damages on each operator networks. Also, synchronising all TDD frames would imply the loss of flexibility of the whole TDD network. This factor may have well been the driver for operators searching for other network technologies instead of deploying TDD.

Annex A

Propagation Models

In the present annex, the Walfisch-Ikegami propagation model is presented and also additional propagation models for the several interference scenarios.

For a good estimation of the received average power, one may use the Walfisch-Ikegami propagation model adapted by COST 231 for micro-cell environment [DaCo99].

Figure A.1 presents the input parameters used in the COST-231 Walfish-Ikegami model.

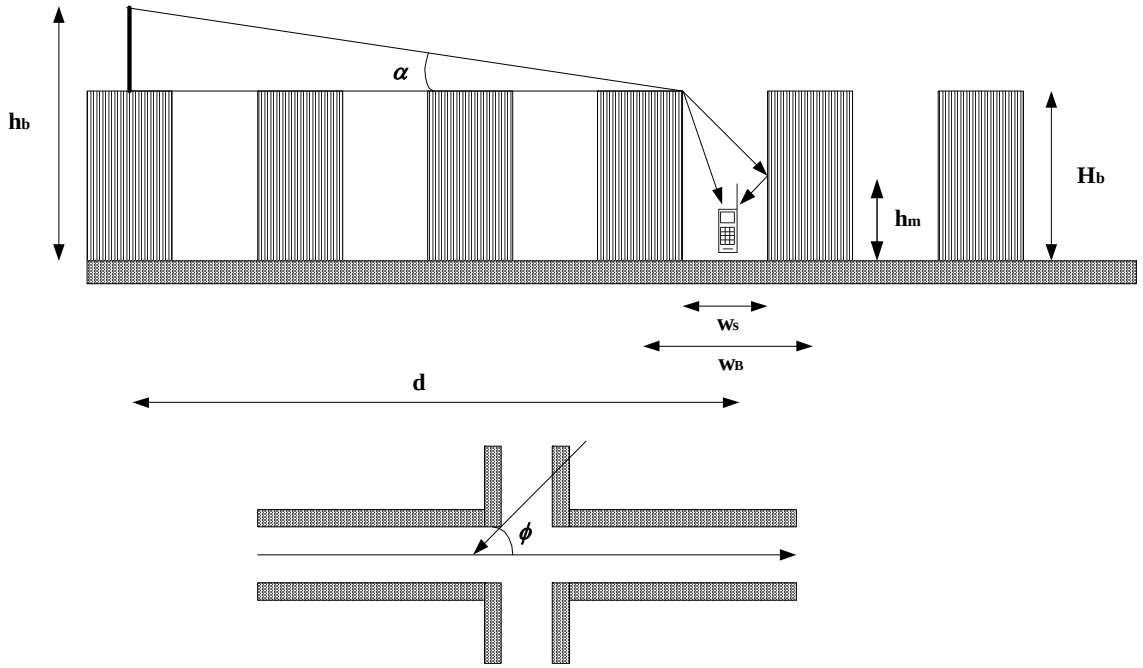

Figure A.1 - COST-231 Walfish-Ikegami model parameters (based on [Corr99]).

When line-of-sight exists between MT and BS, the propagation losses are obtained through:

$$L_{p[\mathrm{dB}]} = 42.6 + 26 \cdot \log\left(d_{[\mathrm{km}]}\right) + 20 \cdot \log\left(f_{[\mathrm{MHz}]}\right), \qquad \text{for } d \geq 0.02 \text{ km.} \tag{A.1}$$

If the line-of-sight is obstructed, the path loss estimation is given by the following equation:

$$L_{p[\mathrm{dB}]} = \begin{cases} L_{o[\mathrm{dB}]} + L_{rts[\mathrm{dB}]} + L_{msd[\mathrm{dB}]} \\ L_{o[\mathrm{dB}]} \end{cases}, \qquad \text{for } L_{rts} + L_{msd} \leq 0, \tag{A.2}$$

where each of these components reflects:

- L_o, free space loss;
- L_{rts}, roof-top-to-street diffraction and scatter loss;
- L_{msd}, multi-screen loss.

The free space loss is given by:

$$L_{o[\mathrm{dB}]} = 32.4 + 20 \cdot \log\left(d_{[\mathrm{km}]}\right) + 20 \cdot \log\left(f_{[\mathrm{MHz}]}\right). \tag{A.3}$$

The roof-top-to-street diffraction and scatter loss is obtained through:

$$L_{rts[\mathrm{dB}]} = -16.9 - 10 \cdot \log\left(w_{s[\mathrm{m}]}\right) + 10 \cdot \log\left(f_{[\mathrm{MHz}]}\right) + 20 \cdot \log\left(H_{B[\mathrm{m}]} - h_{m[\mathrm{m}]}\right) + L_{ori[\mathrm{dB}]}, \tag{A.4}$$

where:

$$L_{rts[\mathrm{dB}]} = \begin{cases} -10 + 0.354 \cdot \phi_{[^\circ]} & \text{for } 0^\circ \le \phi \le 35^\circ \\ 2.5 + 0.075 \cdot \left(\phi_{[^\circ]} - 35\right) & \text{for } 35^\circ \le \phi \le 55^\circ \\ 4.0 + 0.114 \cdot \left(\phi_{[^\circ]} - 55\right) & \text{for } 55^\circ \le \phi \le 90^\circ \end{cases}. \tag{A.5}$$

The multi-screen loss may be calculated via:

$$L_{msd[\mathrm{dB}]} = L_{bsh[\mathrm{dB}]} + k_a + k_d \cdot \log\left(d_{[\mathrm{km}]}\right) + k_f \cdot \log\left(f_{[\mathrm{MHz}]}\right) - 9 \cdot \log\left(w_{B[\mathrm{m}]}\right), \tag{A.6}$$

where:

$$L_{bsh[\mathrm{dB}]} = \begin{cases} -18 \cdot \log\left(1 + h_{b[\mathrm{m}]} - H_{B[\mathrm{m}]}\right) & h_b > H_B \\ 0 & h_b \le H_B \end{cases}, \tag{A.7}$$

$$k_a = \begin{cases} 54 & h_b \le H_B \\ 54 - 0.8 \cdot \left(h_{b[\mathrm{m}]} - H_{B[\mathrm{m}]}\right) & d \ge 0.5\ km \ \text{ and } \ h_b \le H_B \\ 54 - 1.6 \cdot \left(h_{b[\mathrm{m}]} - H_{B[\mathrm{m}]}\right) \cdot d_{[\mathrm{km}]} & d < 0.5\ km \ \text{ and } \ h_b \le H_B \end{cases}, \tag{A.8}$$

$$k_d = \begin{cases} 18 & h_b \le H_B \\ 18 - 15 \cdot \dfrac{h_{b[\mathrm{m}]} - H_{B[\mathrm{m}]}}{H_{B[\mathrm{m}]}} & h_b \le H_B \end{cases}, \tag{A.9}$$

$$k_f = \begin{cases} -4 + 0.7 \cdot \left(\dfrac{f_{[\mathrm{MHz}]}}{925} - 1 \right), & \text{for medium sized cities and suburban centres} \\ 5 \cdot \left(\dfrac{f_{[\mathrm{MHz}]}}{925} - 1 \right), & \text{for metropolitan centres} \end{cases} \tag{A.10}$$

In case the data on the structure of the buildings and roads is unknown, it is recommended to use the following values:

- Building separation (w_B) ϵ [20, 50] [m];
- Widths of roads (w_s), $w_s = 0.5 \times w_B$;
- Heights of buildings (H_B), $H_B = 3 \times \{\text{number of floors}\} + H_{roof}$;
- Roof height (H_{roof}), H_{roof};
- Road orientation with respect to the direct radio path (ϕ), $\phi = 90º$.

The validity ranges of the COST-231 Walfish-Ikegami model are the following:

- Frequency (f) ϵ [800, 2000] [MHz];
- BS height (h_b) ϵ [4, 50] [m];
- MT height (h_m) ϵ [1, 3] [m];
- Distance (d) ϵ [0.02, 5] [km].

Finally, the overall expression for the propagation losses between the MT and the BS is given by:

$$L_{MT-BS_{[\mathrm{dB}]}} = L_{o_{[\mathrm{dB}]}} + L_{rts_{[\mathrm{dB}]}} + L_{msd_{[\mathrm{dB}]}} \tag{A.11}$$

The COST-231 Walfish-Ikegami propagation model is the one used in the interference model to calculate the propagation losses between the MT and BS.

As seen before, in TDD there are two new interference scenarios: between MTs and between BSs. In order to cover these cases an outdoor micro model was used [QiWD00a]. In [Xia97] an MT-MT case is introduced. The model is based on path loss formula from H. Xia considering that the height of the BS antenna is below the average building height. This is seen as reasonable approximation of the considered scenario. The MT-to-MT path loss is given by:

$$L_{MT-MT_{[dB]}} = -10\log_{10}\left(\frac{\lambda}{4\pi R_{[m]}}\right) - 10\log_{10}\left[\frac{\lambda}{2\pi^2}\left(\frac{1}{\theta_{[°]}} - \frac{1}{2\pi+\theta_{[°]}}\right)^2\right] - 10\log_{10}\left[\left(\frac{d_{[m]}}{2\pi R_{[m]}}\right)^2 \frac{\lambda}{\sqrt{\left(\Delta h_{Mobile_{[m]}}\right)^2 + d_{[m]}{}^2}}\left(\frac{1}{\phi_{[°]}} - \frac{1}{2\pi+\phi_{[°]}}\right)^2\right] \quad \text{(A.12)}$$

When synchronisation between adjacent BSs does not exist, interference between the BSs appears in UL. The propagation model for the BS-to-BS interference scenario is:

$$L_{BS-BS_{[dB]}} = -10\log_{10}\left(\frac{\lambda}{4\pi R_{[m]}}\right) - 10\log_{10}\left(\frac{d_{[m]}}{R_{[m]}}\right)^2 \quad \text{(A.13)}$$

where,

- $\theta_{[°]} = \tan^{-1}\left(\frac{\left|\Delta h_{Mobile_{[m]}}\right|}{x_{[m]}}\right)$
- $\phi_{[°]} = \tan^{-1}\left(\frac{\left|\Delta h_{Base_{[m]}}\right|}{d_{[m]}}\right)$
- $\Delta h_{Mobile_{[m]}} = h_{Building_{[m]}} - h_{Mobile_{[m]}}$
- $\Delta h_{Base_{[m]}} = h_{Base_{[m]}} - h_{Building_{[m]}}$
- R Transmitter-receiver separation;
- λ Wavelength;
- x Horizontal distance between the MT and the diffracting edges;
- Δh_{Mobile} Difference between mean building height and MT height;
- Δh_{Base} Difference between the BS height and the mean building height;
- $d_{Building}$ Average separation between rows of buildings.

Annex B

TDD and FDD Link Budget

This annex presents the necessary equations to perform the correct link budget calculations, for both TDD and FDDs.

The three main factors of radio network planning in UMTS are coverage, capacity and quality of service. The main parameters for coverage planning are related to the coverage regions, the area type information and propagation conditions. For capacity planning is important to take into account the spectrum available, the subscriber growth forecast and the density of traffic.

In addition to the general parameters used in the link budget estimation, there are some WCDMA-specific parameters that have to be taken in account [HoTo01]:

Interference margin – interference margin is needed in the link budget because the loading of the cell affects coverage. The more loading that is allowed in the network, the larger is the needed interference margin in the UL, and smaller is the coverage area.

Fast fading margin (power control headroom) – some headroom is needed in the MT transmission power for maintaining adequate closed-loop power control. This applies especially to slow-moving pedestrian mobiles MTs. Fast power control is able to compensate fast fading.

Soft handover gain – Handovers (soft and hard) give a gain against slow fading by reducing the required log-normal fading margin. This is because the slow fading is partly uncorrelated between the BSs, and by making a handover, an MT can select a better BS. Soft handover gives an additional macro diversity gain against fast fading by reducing the required Signal-to-Interference Ratio (SIR).

Concerning coverage, order to obtain initial coverage estimation it is required to perform the link budget calculations, which derives the maximum allowed path loss between the MT and BS, leading to a first approach on the maximum cell radius that meets the quality objectives defined in advance. The steps to determine its value follows.

The allowed propagation loss for the cell is given by [HoTo01]:

$$L_{pmax[\mathrm{dB}]} = P_{t[\mathrm{dBm}]} + G_{t[\mathrm{dBi}]} + G_{r[\mathrm{dBi}]} + G_{SH[\mathrm{dB}]} - P_{Rx\min[\mathrm{dBm}]} - \sum L_{x[\mathrm{dB}]} - \sum F_{M\,[\mathrm{dB}]} \qquad \text{(B.1)}$$

where,

- P_t Transmission power (delivered to the antenna);
- G_t Maximum Transmitting antenna gain;
- G_r Maximum receiver antenna gain;
- G_{SH} Soft-handover gain;
- $P_{Rx\min}$ Receiver sensitivity for a given service bearer;

- L_x Additional attenuations in a link: MT body loss L_{Body}, cable losses L_c, and others (car or building penetration losses) L_{Other};
- F_M Fading margins, i.e., fast fading margin F_{FM}, and slow fading margin F_{SM}.

The estimation of the receiver power in UL is by:

$$P_{Rx[\mathrm{dBm}]} = P_{r[\mathrm{dBm}]} - L_{c[\mathrm{dB}]} \tag{B.2}$$

where,

- P_{Rx} receiver-input power;
- P_r power at the antenna terminals;
- L_c cable losses.

In the DL one has:

$$P_{Rx[\mathrm{dBm}]} = P_{r[\mathrm{dBm}]} - L_{Body[\mathrm{dB}]} \tag{B.3}$$

The receiver sensitivity depends on the service:

$$P_{Rx\,\min[\mathrm{dBm}]} = E_b / N_{0[\mathrm{dB}]} - G_{p[\mathrm{dB}]} + N_{T[\mathrm{dBm}]} \tag{B.4}$$

The total noise plus interference is given by:

$$N_{T[\mathrm{dBm}]} = N_{R[\mathrm{dBm}]} + M_{\mathrm{int}[\mathrm{dB}]} \tag{B.5}$$

where ,

$$N_{R[\mathrm{dBm}]} = -174 + 10 \cdot \log(R_c) + NF_{[\mathrm{dB}]} \tag{B.6}$$

and

- $\mathrm{M_{int}}$ Interference Margin

Regarding the BS, the noise figure, *NF*, has typical values of 5 to 9 dB. The interference margin is considered in order to account for interference increase within the cell due to other MTs. It introduces a way to take into consideration the loading of the cell in the link budget, as expressed in (B.7):

$$M_{int} = -10 \cdot \log\left(1 - \eta\right) \tag{B.7}$$

where

- η Cell load

Typical values for interference margin are 3 dB, corresponding to 50 % loading.

The processing gain G_p for the FDD mode is given by:

$$G_{P[\mathrm{dB}]} = 10\log\left(\frac{R_{c[\mathrm{chips/s}]}}{R_{b[\mathrm{bps}]}}\right) \tag{B.8}$$

For the TDD mode, the processing gain is calculated differently, since the slotted structure of the TDD mode must be taken into account. In TDD there are fifteen slots and the information is transmitted in one or several slots using one or more codes, leading to:

$$G_{P[\mathrm{dB}]} = 10\log\left(\frac{R_{c[\mathrm{chips/s}]}}{R_{b[\mathrm{bps}]}} \cdot \frac{N_{Slots}}{15} \cdot \frac{chips\,in\,slot - midamble - guard\ period}{chips\,in\,slot}\right) \tag{B.9}$$

where,

- N_{Slots} Number of slots used for the service considered

The service bit rate is obtained by:

$$R_{b[\mathrm{bps}]} = \frac{\log_2(M)\cdot R_c \cdot (T_S \cdot R_{code} - G_{Per})}{SF \cdot T_f} \tag{B.10}$$

where M is the size of the symbol set (QPSK, i.e., 4), T_S is the slot duration (666.7μs), T_f is the frame duration (10ms), R_{code} is the code rate (1/3), G_{Per} is the length of the guard period (96 chips) and SF is the spreading factor. Assuming that burst type 1 is used for 12.2 kbps voice and burst type 2 is used for 128 kbps data, then the parameters are as follows: chips in slot = 2560, midamble (burst type 1/2) = 512/256, guard period=96.

Penetration losses have typical values of 8 dB for in-car and 15 dB for indoor MTs.

The maximum cell radius depends directly on the service bit rate of each service. Theoretically LBR services imply higher radius and conversely, HBR ones lower radius. Table B.1 presents BS radius results for the different services bit rates. As expected, the maximum radius for a 16 kbps service is three times larger than for 1920 kbps.

Table B.1– BS radius for different services bit rates.

Service bit rate [kbps]	BS radius [km]			
	Maximum	Average	Minimum	Std. dev.
16	0.31	0.18	0.10	0.07
64	0.26	0.17	0.10	0.05
128	0.21	0.12	0.04	0.05
384	0.16	0.08	0.04	0.03
1920	0.11	0.06	0.03	0.03

Annex C

Simulator Flowcharts

This annex presents the flowcharts of the simulator and its two modes of operation. First the most important flowcharts of FDD, and secondly the ones of TDD.

In order to correctly understand the flowcharts presented in this annex, and also to clarify all the processes of the simulator, it is necessary to summary the variables used in the flowcharts.

Tabble C.1 shows the several variables and constants that are used in the flowcharts and their meaning.

Table C.1 – Description of the several flowcharts variables and constants.

Flowchart Variable/Constant	Description
LOAD_MAX_UL, LOAD_MAX_UL	Maximum allowed load in UL and DL.
Load DL , Load UL	Cumulative load in UL and DL.
MAX_POWER	Maximum allowed BS TX power.
Users(Sector), Users(TSlot)	Number of MTs per Sector and per TS.
Num_BSs	Number of BSs in the network.
Load(TSlot), Bit Rate(TSlot)	Cumulative values of load and bit rate per TS.
Load(UL), Load (DL)	Instantaneous load in UL and DL.
UL_TSLOTS, DL_TSLOTS, MAX_SLOTS, CONTROL_TSLOTS	Number of UL TSs, DL TSs, maximum available TSs and control and signaling TSs.
Bit Rate(UL), Bit Rate(DL)	Instantaneous bit rate in UL and DL.
RB_MAX	Maximum allowed bit rate per BS (throughput)
Pow(TSlot), Pow(User)	Cumulative BS TX power per TS and BS TX power for user.

Having these variables and their meaning in mind, next pages present all the flowcharts of the simulator, starting with the most important ones existing in FDD simulator, followed by all the flowcharts of the processes developed for TDD simulator.

C.1 TDD/FDD General Algorithms

This section presents the general algorithms that form the simulator. Figure C.1 shows the algorithm for MTs generation, adapted from [SeCa04].

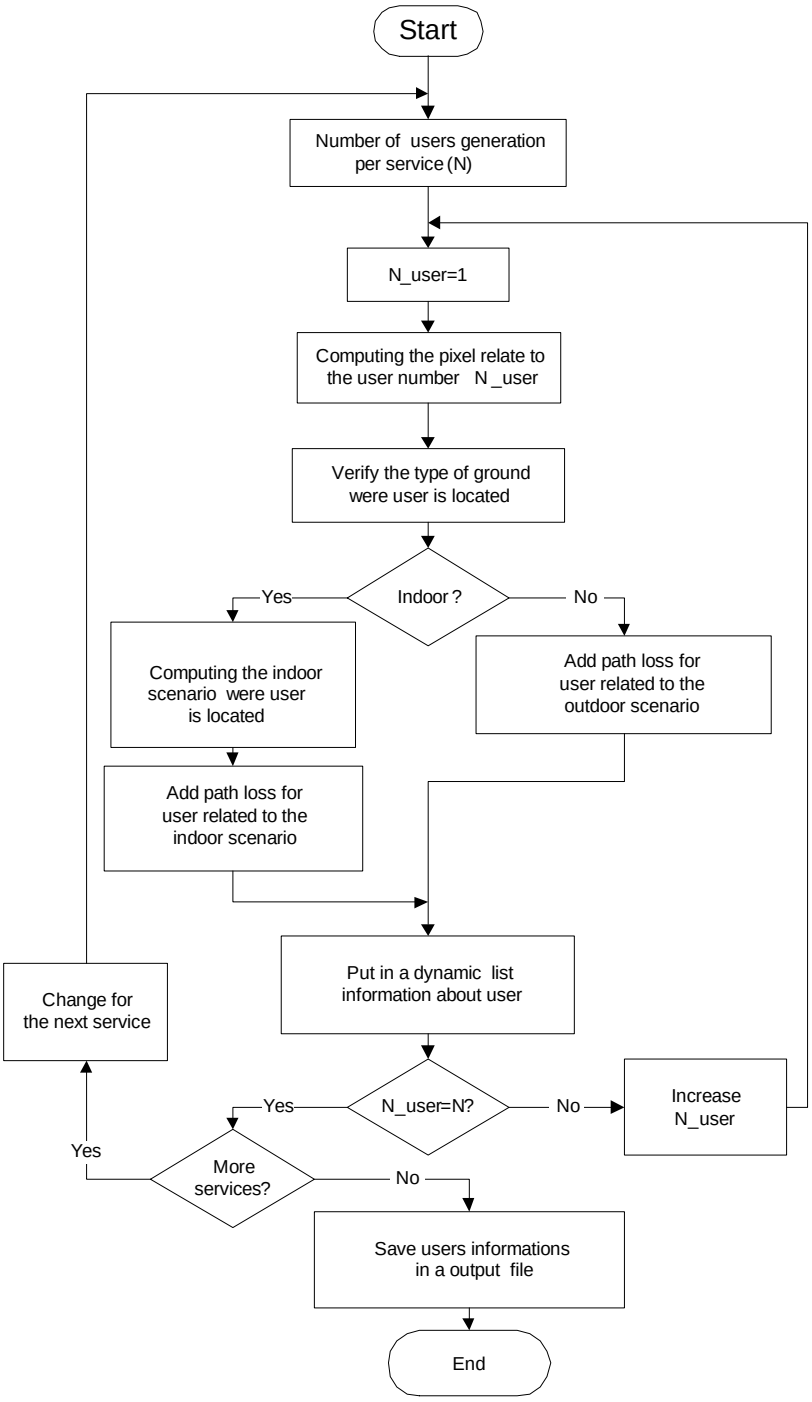

Figure C.1 – MTs generation algorithm (adapted from [SeCa04]).

After creating all the MTs with their respective characteristics, the users must be analysed and checked if they fulfill all requisites to service. Figure C.2 depicts the algorithm developed.

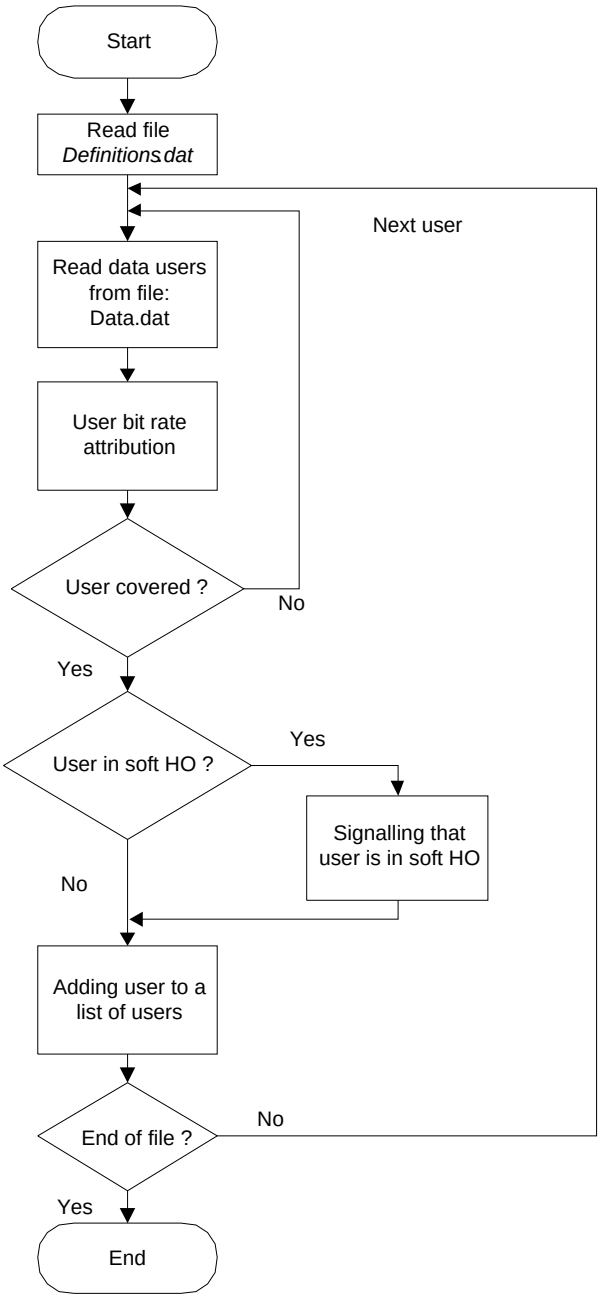

Figure C.2 – Flowchart for adding MTs in a list of MTs (adapted from [SeCa04]).

Figure C.3 shows the main flowchart of the application developed in C++ language.

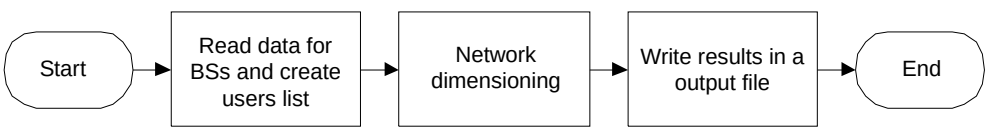

Figure C.3 – Flowchart *Net_opt* application (adapted from [SeCa04]).

C.2 TDD Specific Algorithms

Several TDD specific algorithms were developed or were the result of adapting existing FDD algorithms. This section focuses on them. Figure C.4 shows the network dimensioning process in TDD.

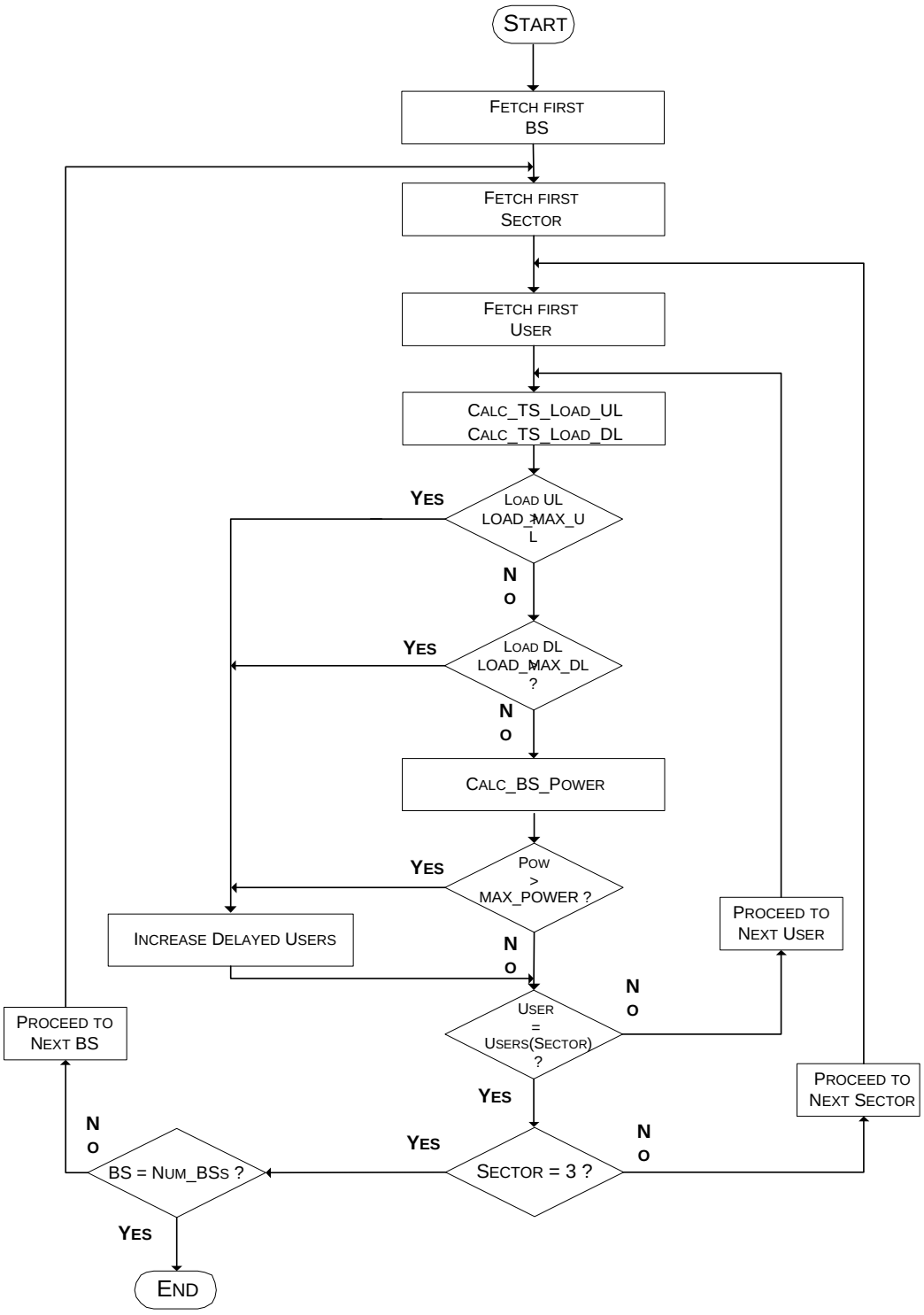

Figure C.4 – Network dimensioning in TDD.

The algorithm for load calculations in UL is depicted in Figure C.5.

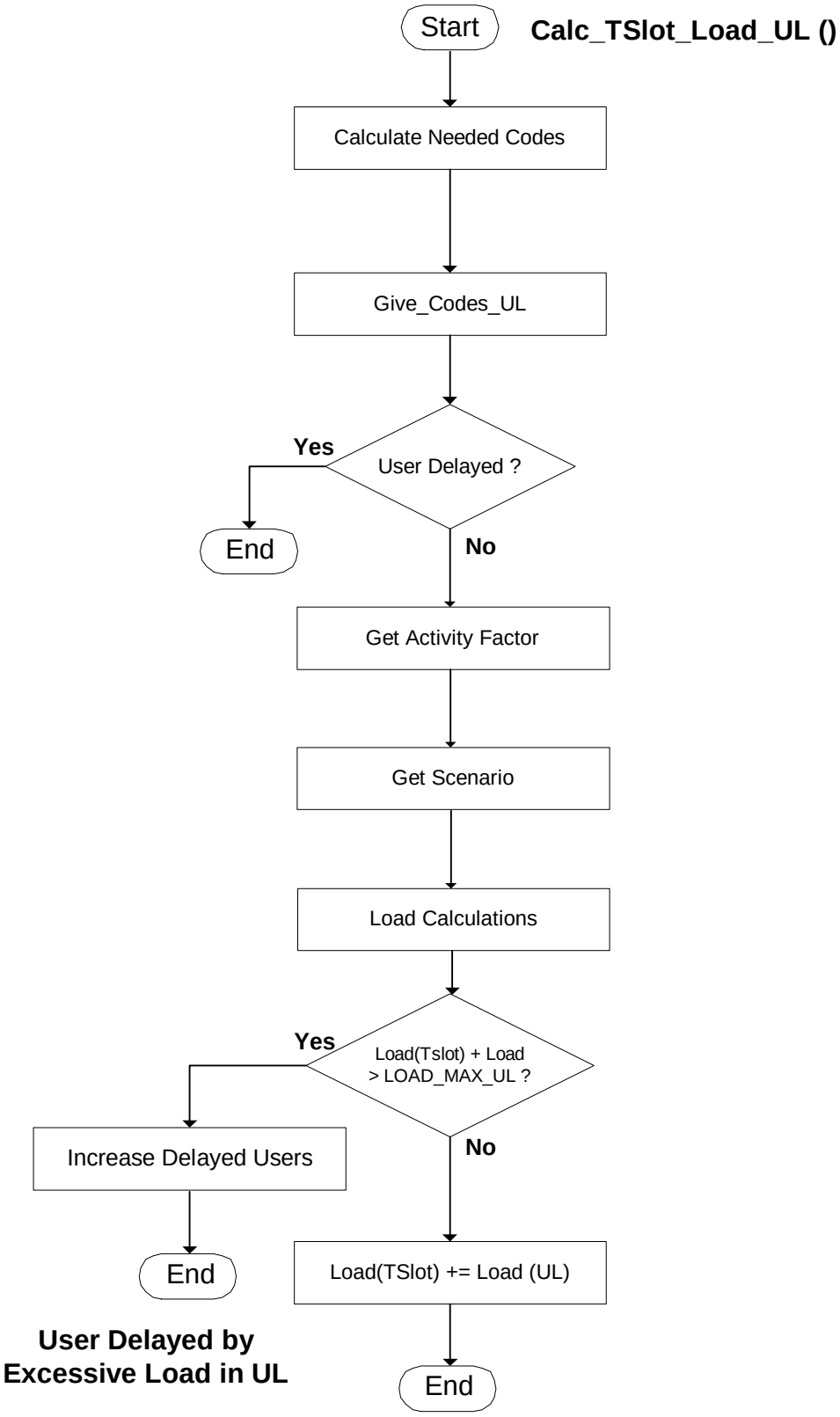

Figure C.5 – Load per TS in UL.

Figure C.6 shows the flowchart of load calculation in DL. The functioning is equal to the algorithm for the opposite link.

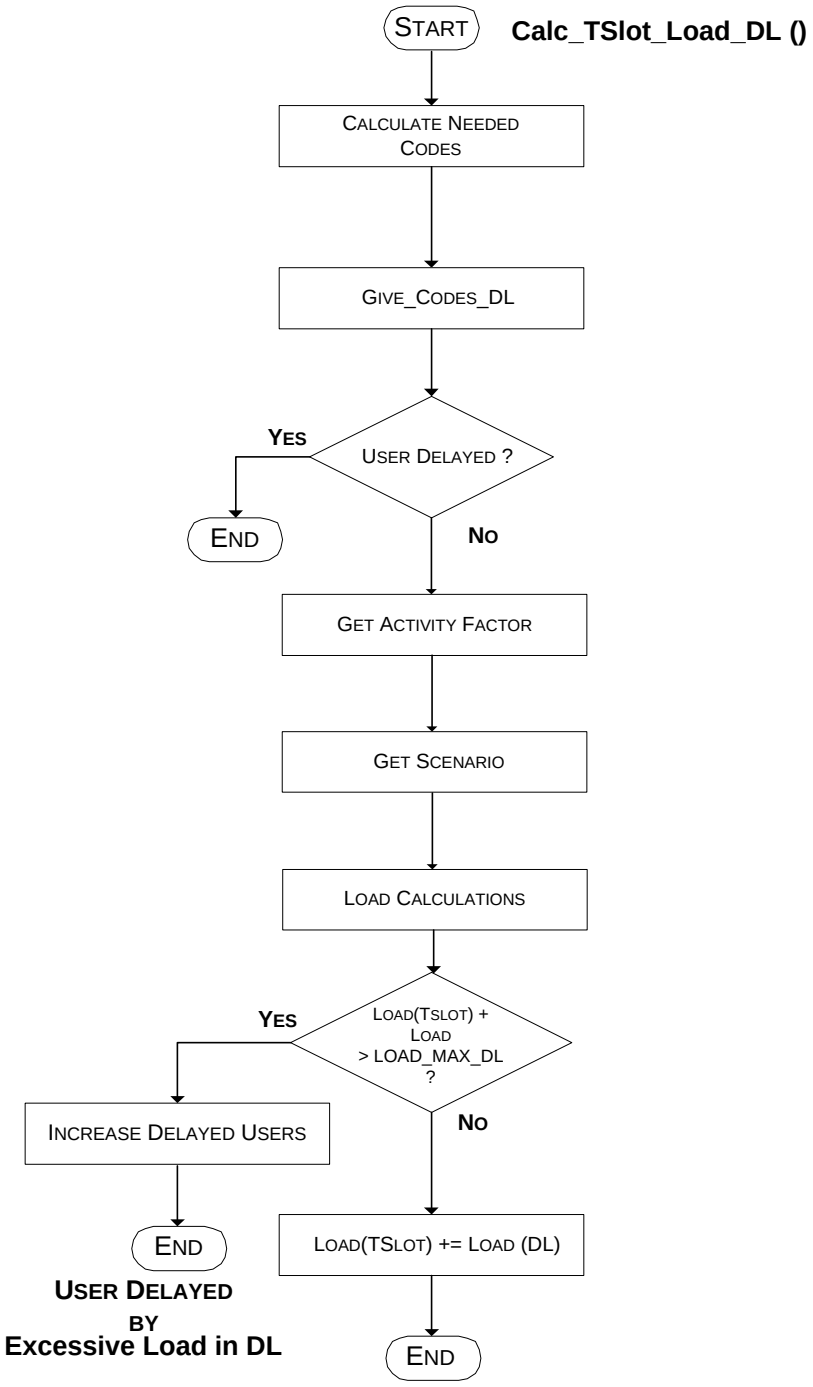

Figure C.6 – Load per TS in DL.

Figure C.7 and C.8 depict the algorithms to allocate codes in both DL and UL.

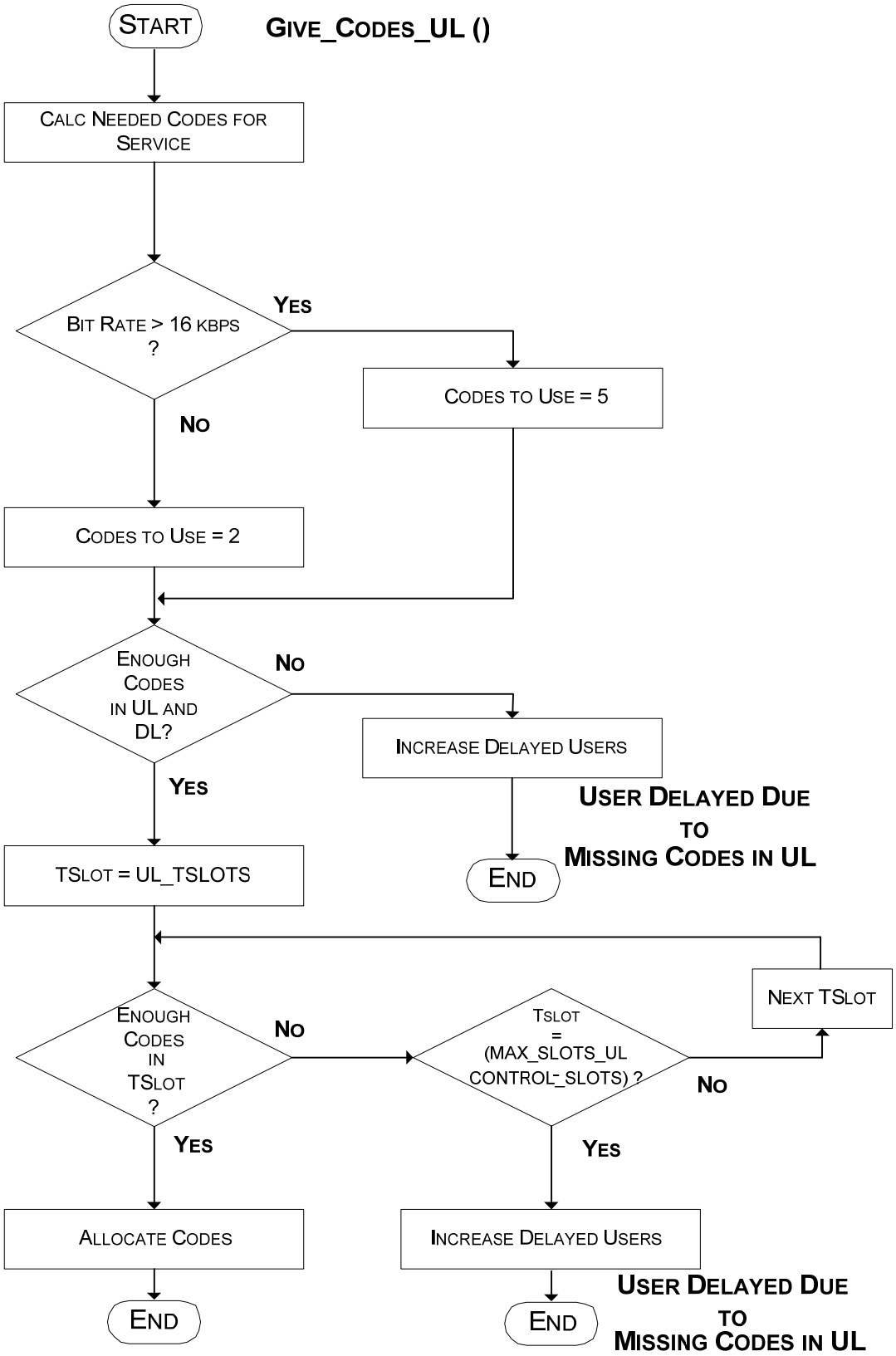

Figure C.7 – Codes allocation in UL.

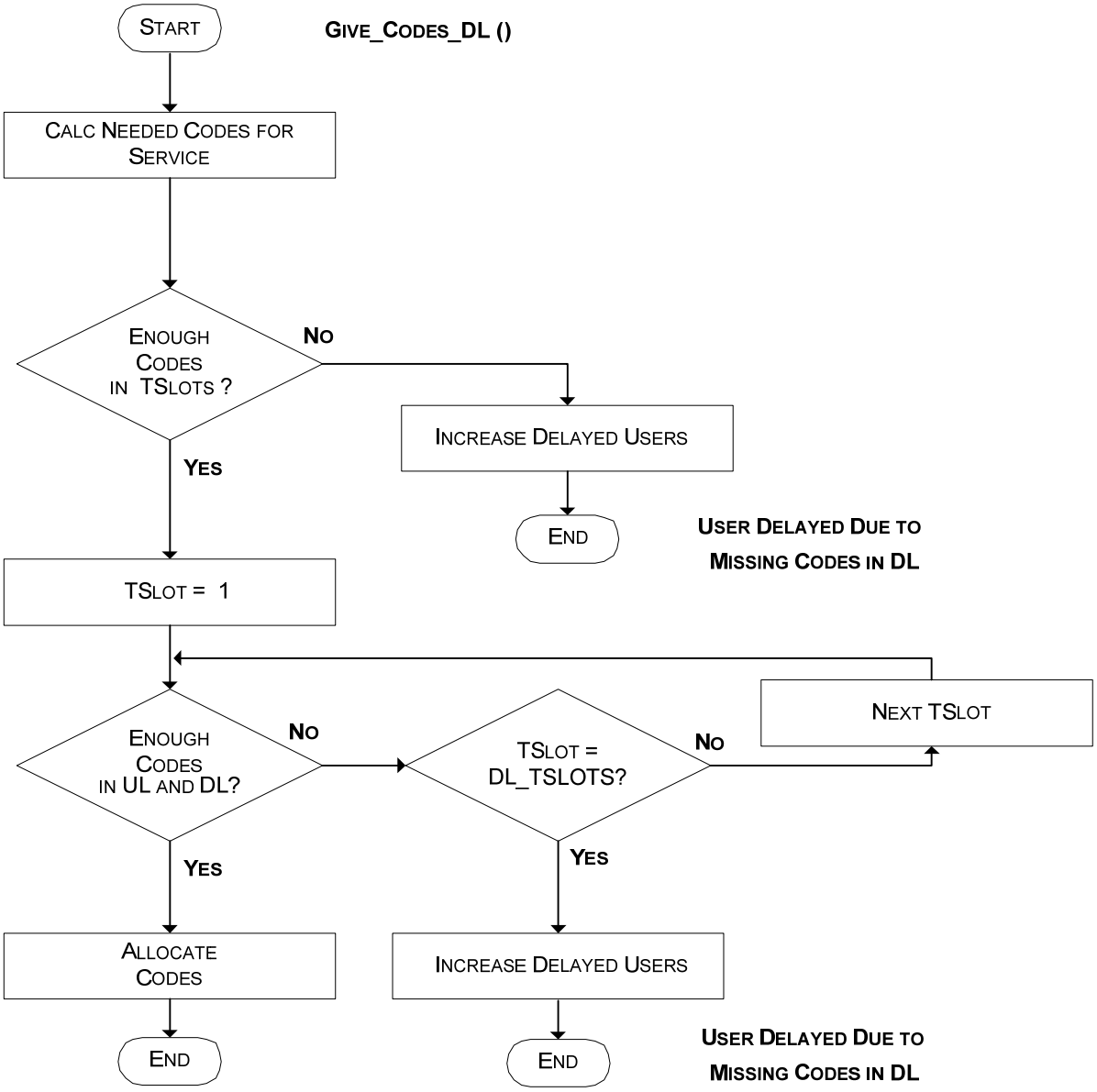

Figure C.8 – Codes allocation in DL.

Figures C.9 and C.10 show MT allocation algorithms for both links.

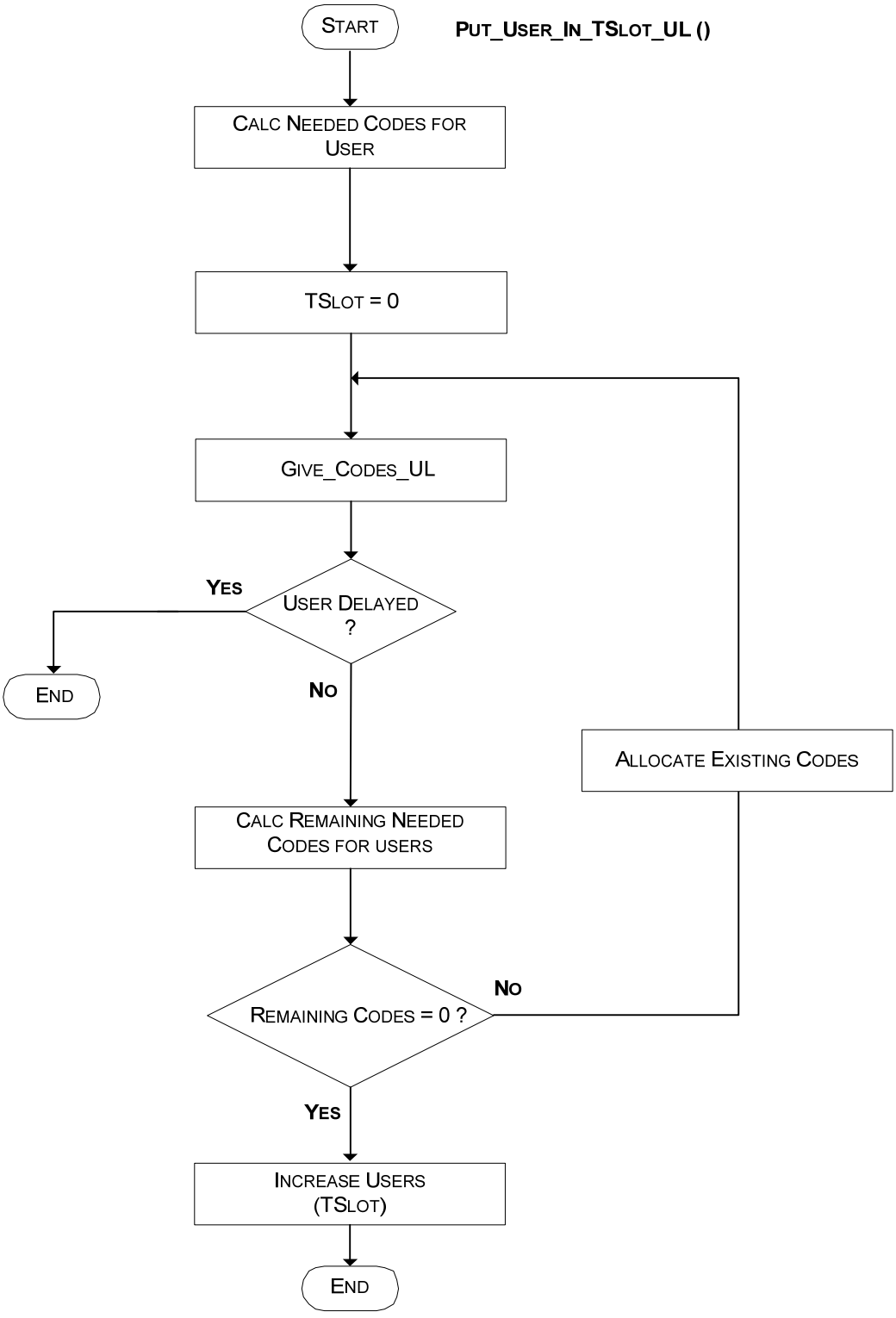

Figure C.9 – MT allocation per TS in UL.

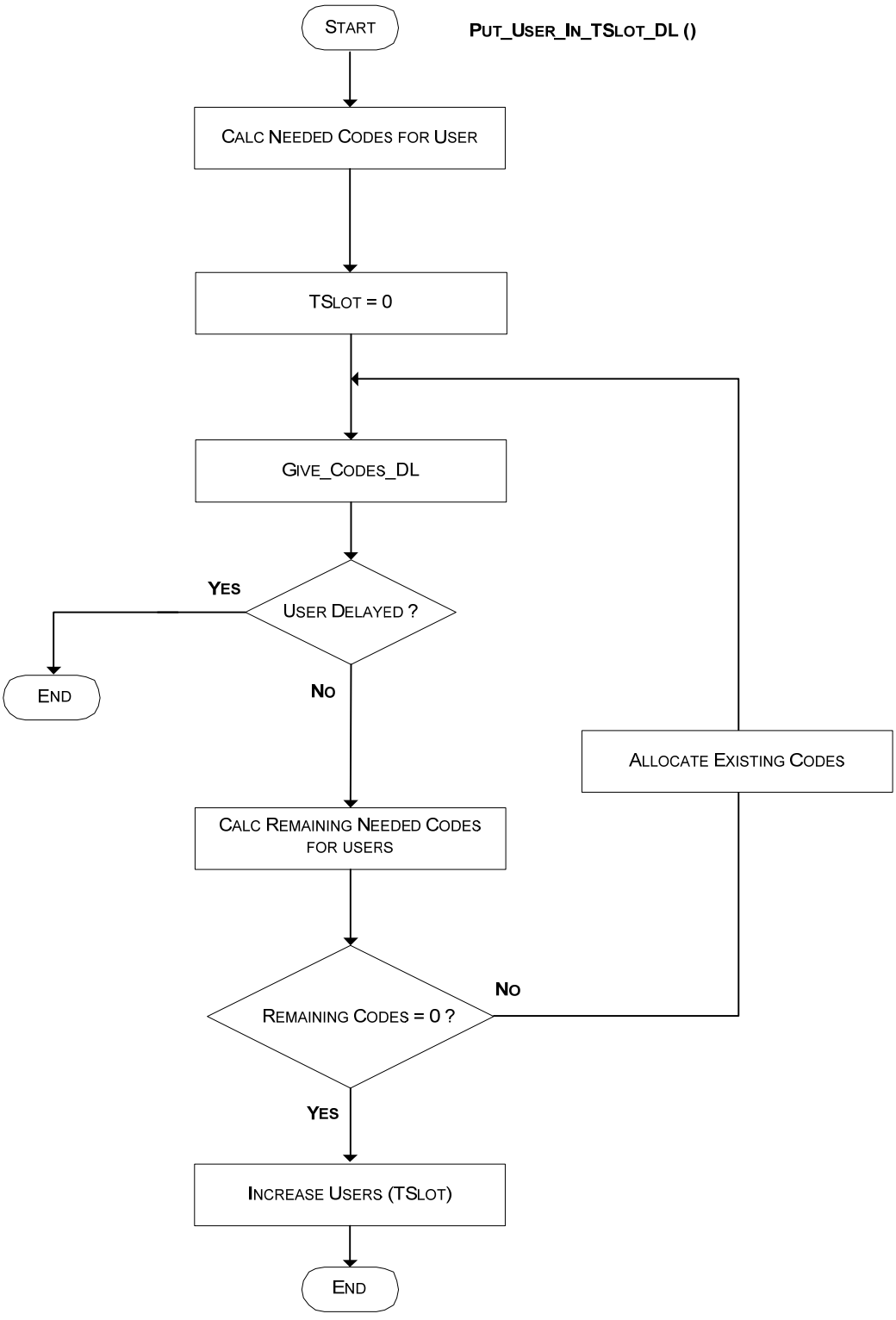

Figure C.10 – MT allocation per TS in DL.

Figures C.11 and C.12 show the bit rate allocation algorithms for both links.

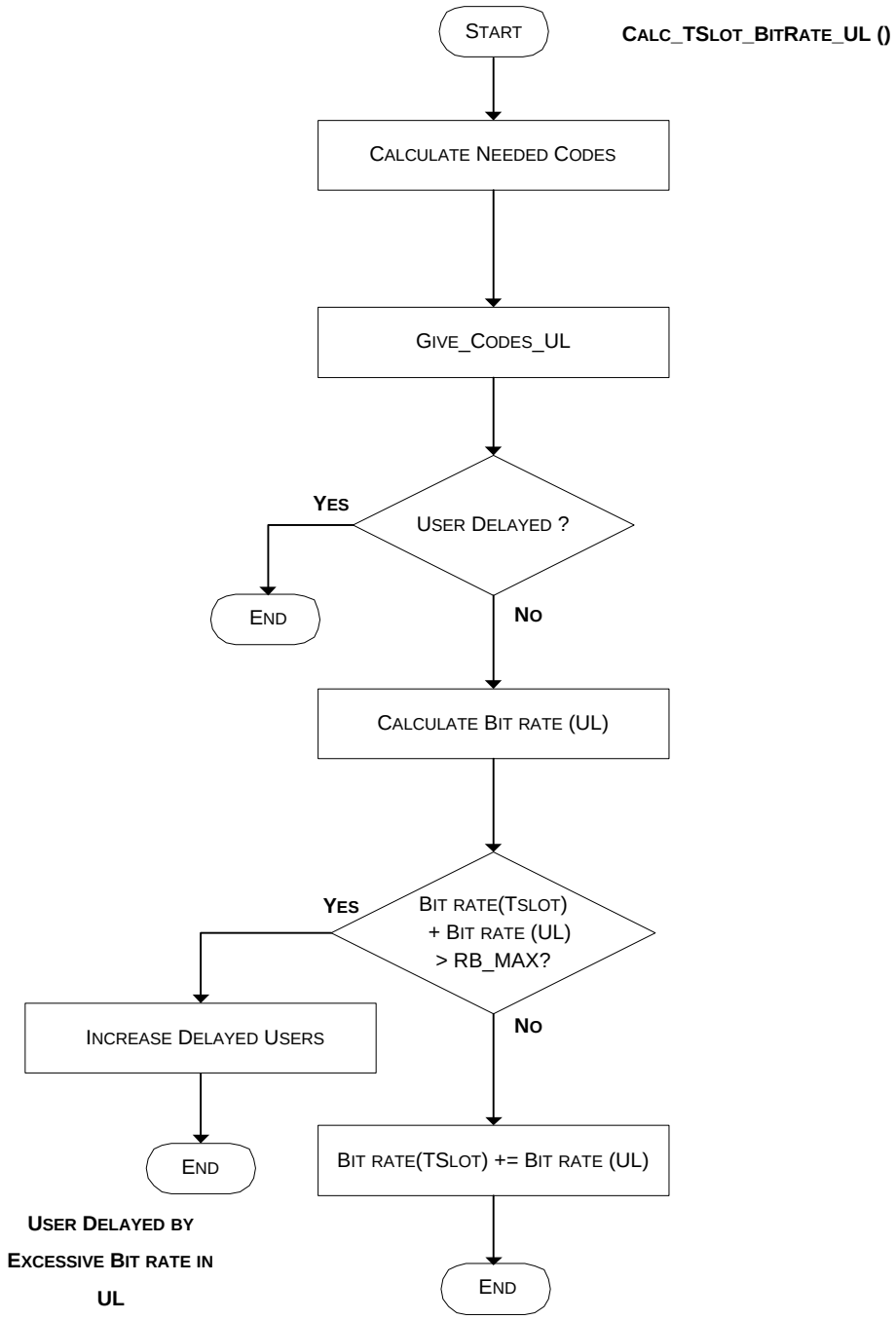

Figure C.11 – Bit rate allocation per TS in UL.

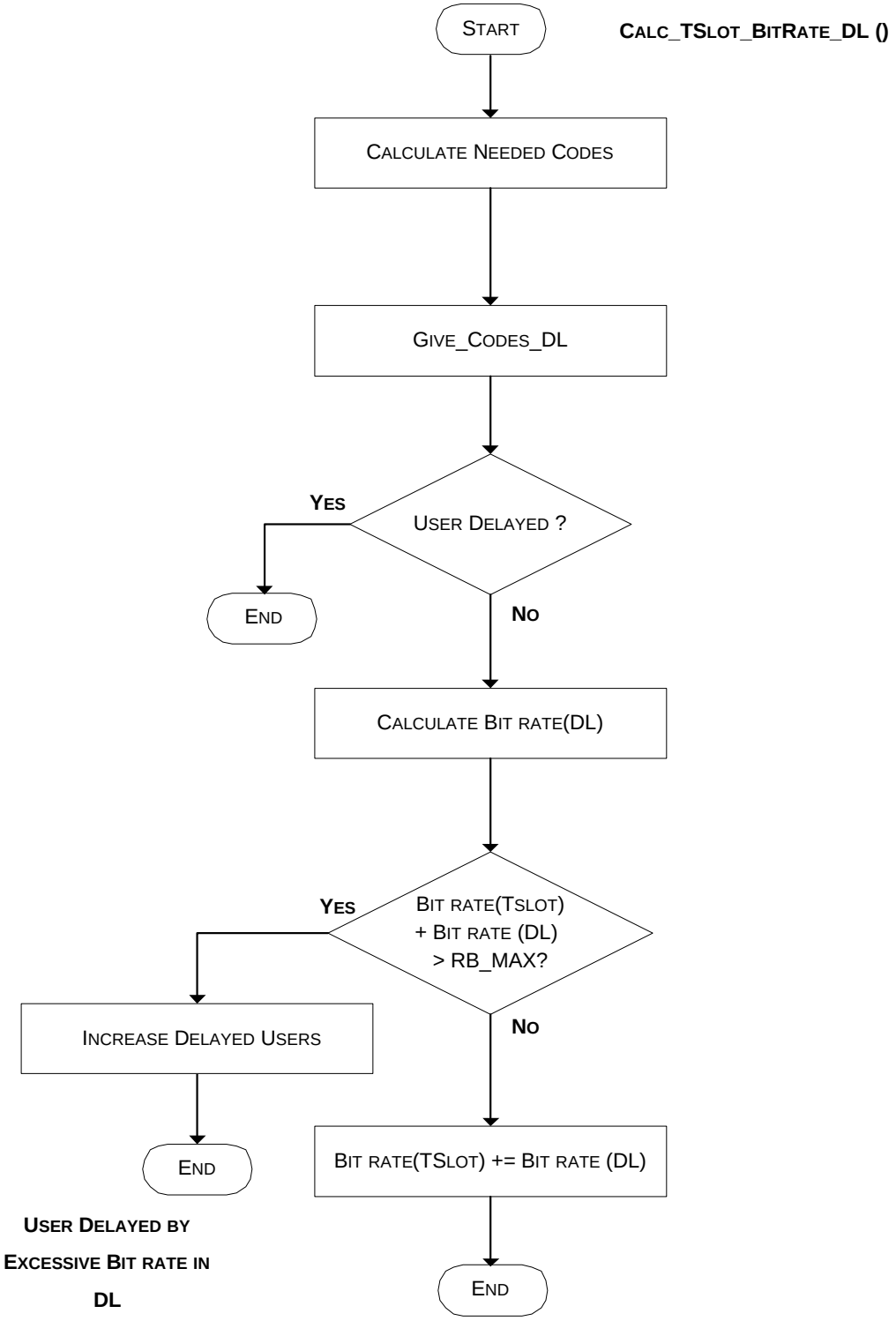

Figure C.12 – Bit rate allocation per TS in DL.

Figure C.13 shows the process to calculate the instantaneous power drain from a BS dependent on the number of MTs servicing.

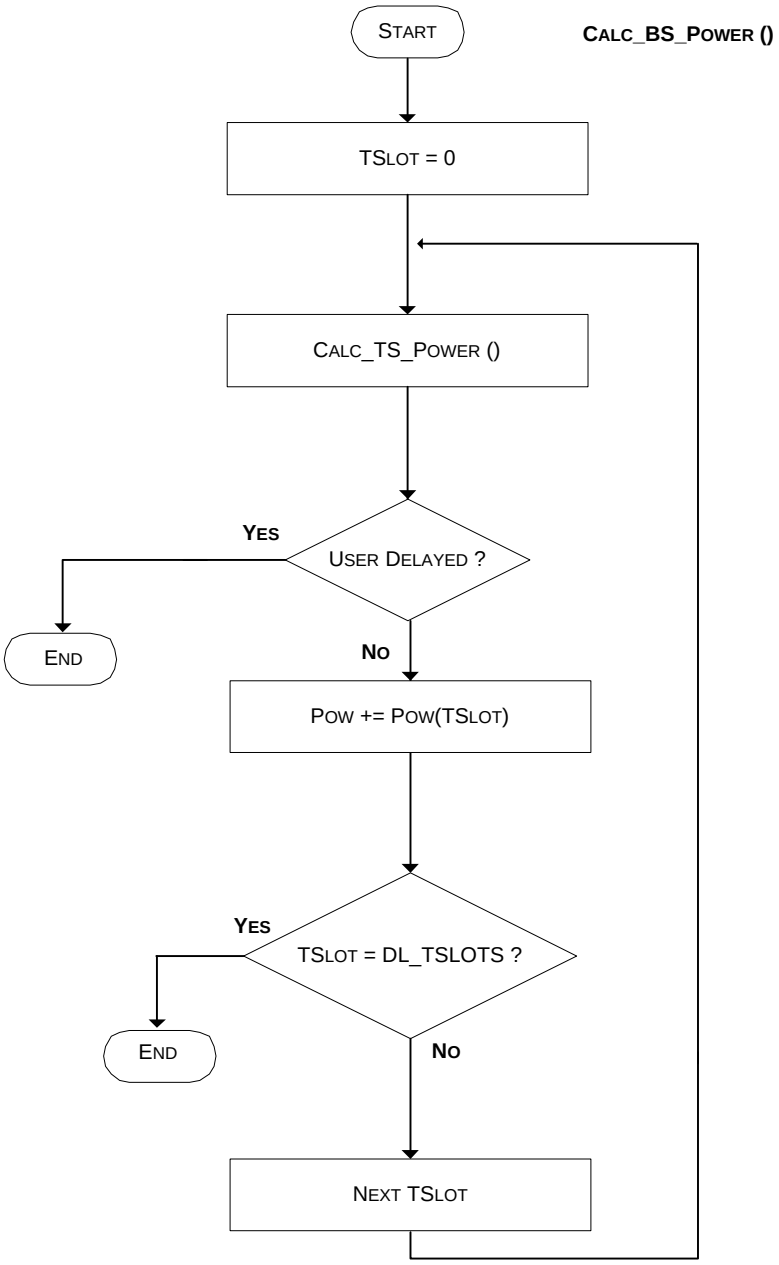

Figure C.13 – BS TX power calculation.

The transmitting power per TS in each BS is calculated in such a manner as depicted in Figure C.14.

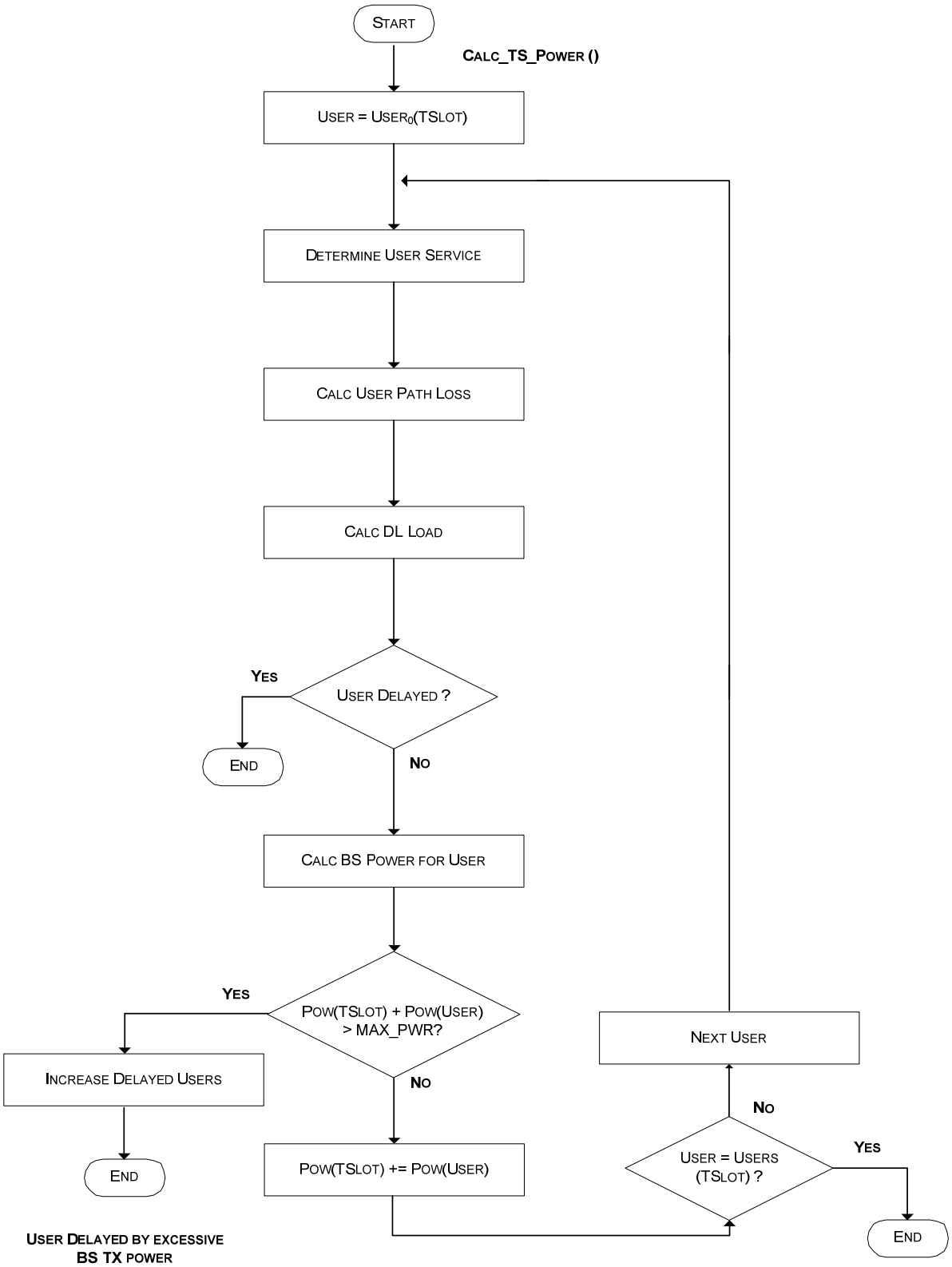

Figure C.14 – BS TX Power per TS allocation.

C.2 RRM Algorithms

This section presents the RRM algorithms that were developed in the simulator. As referred in Chapter 4, two RRM mechanisms were developed. The first one acts prior to the network dimensioning and checks if there are enough codes for all MTs that want to service, and the second one is in charge of reducing MT's service bit rate in all its TSs that do not have the minimum acceptable E_b/N_o. Figures C.15 and C.16 show these algorithms.

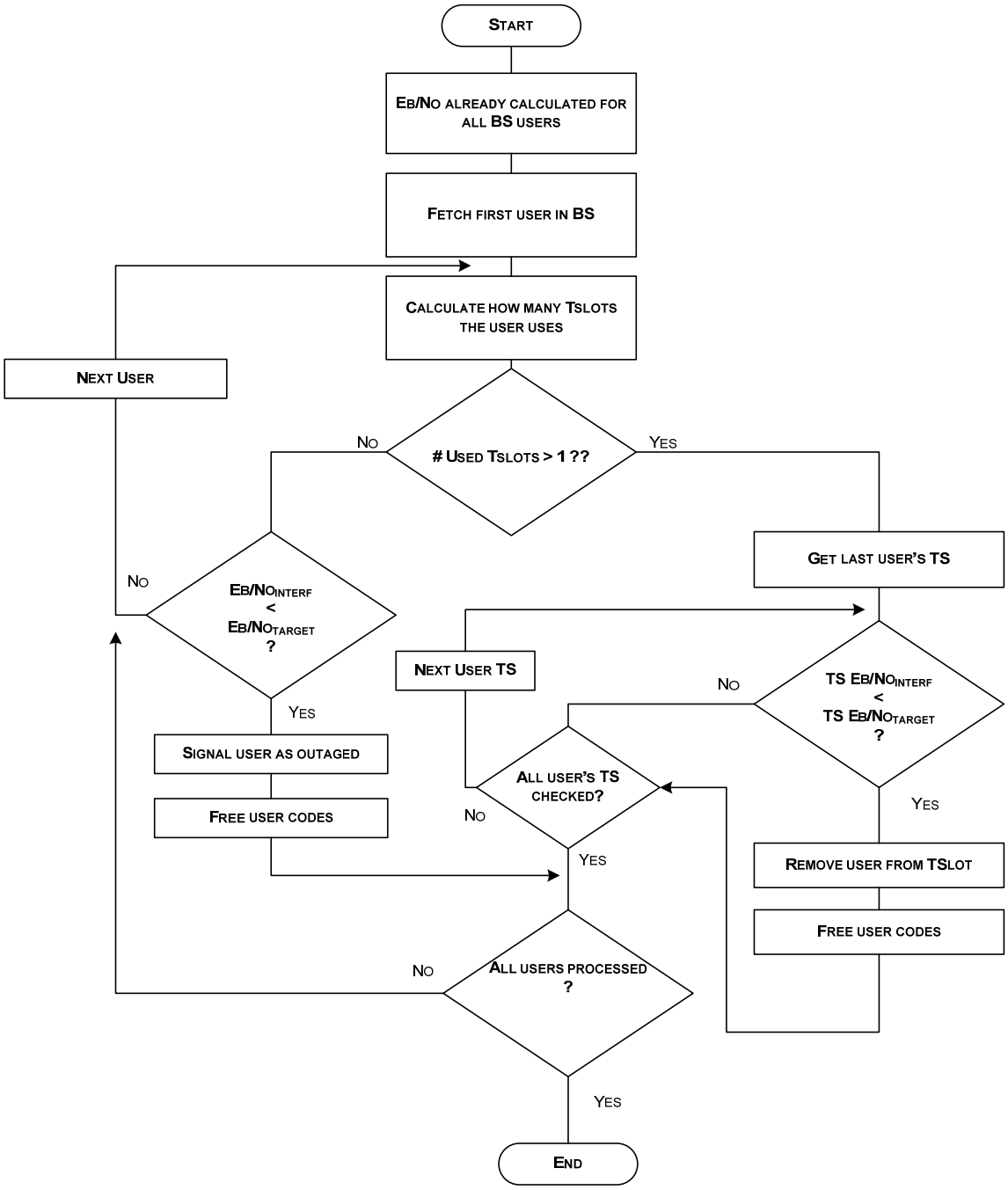

Figure C.15 – Manage TS Interference for all BS MTs.

From this point on until the end of this annex, for simplicity, consider that, when made reference to, the 1920 kbps, 384 kbps and 128 kbps services are referred as service 6, 5 and 4, respectively an globally as HBR services.

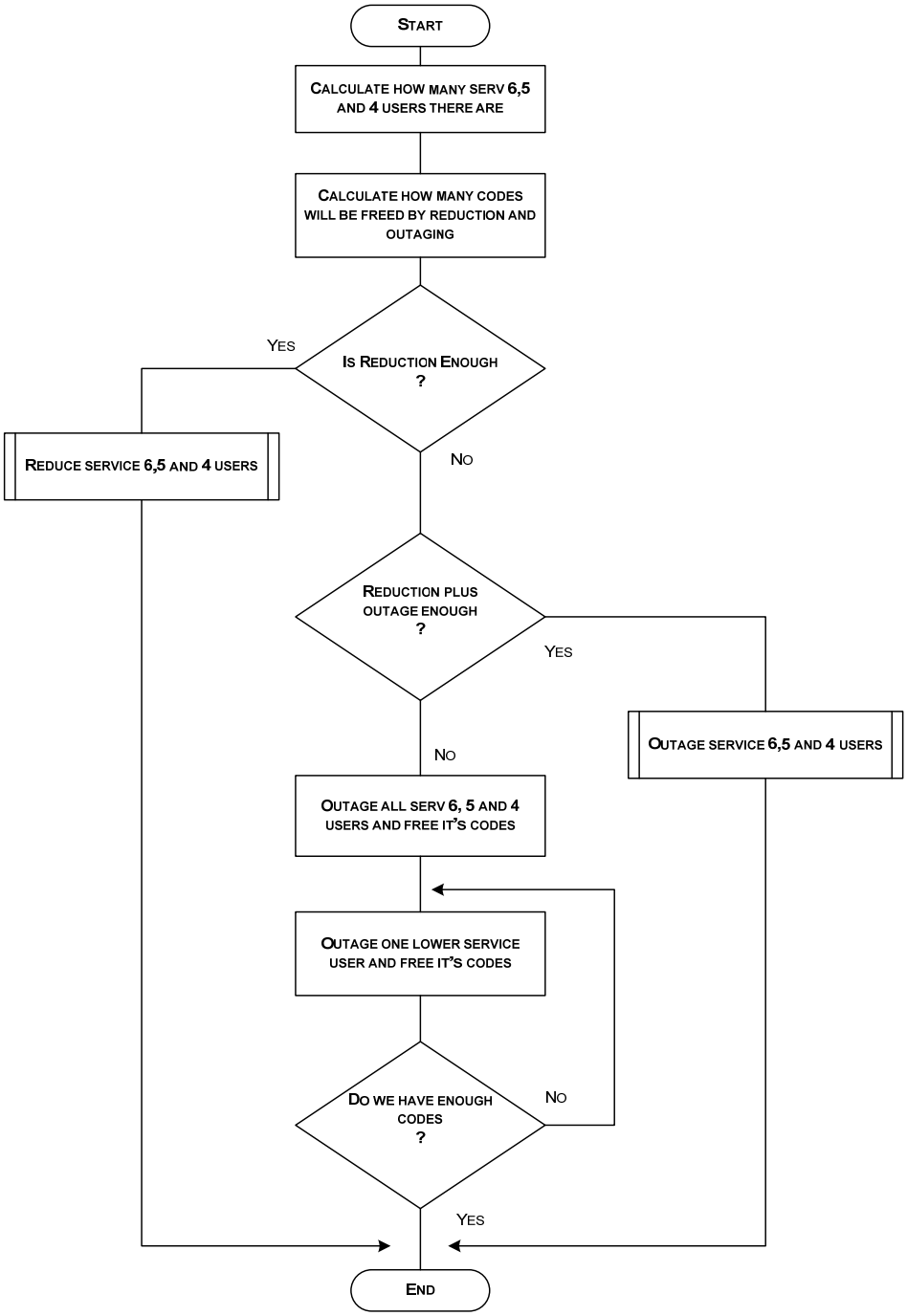

Figure C.16 – MT reduction and outage algorithms.

Figure C.17 shows the algorithm for the reduction steps of services 6, 5 and 4 bit rates.

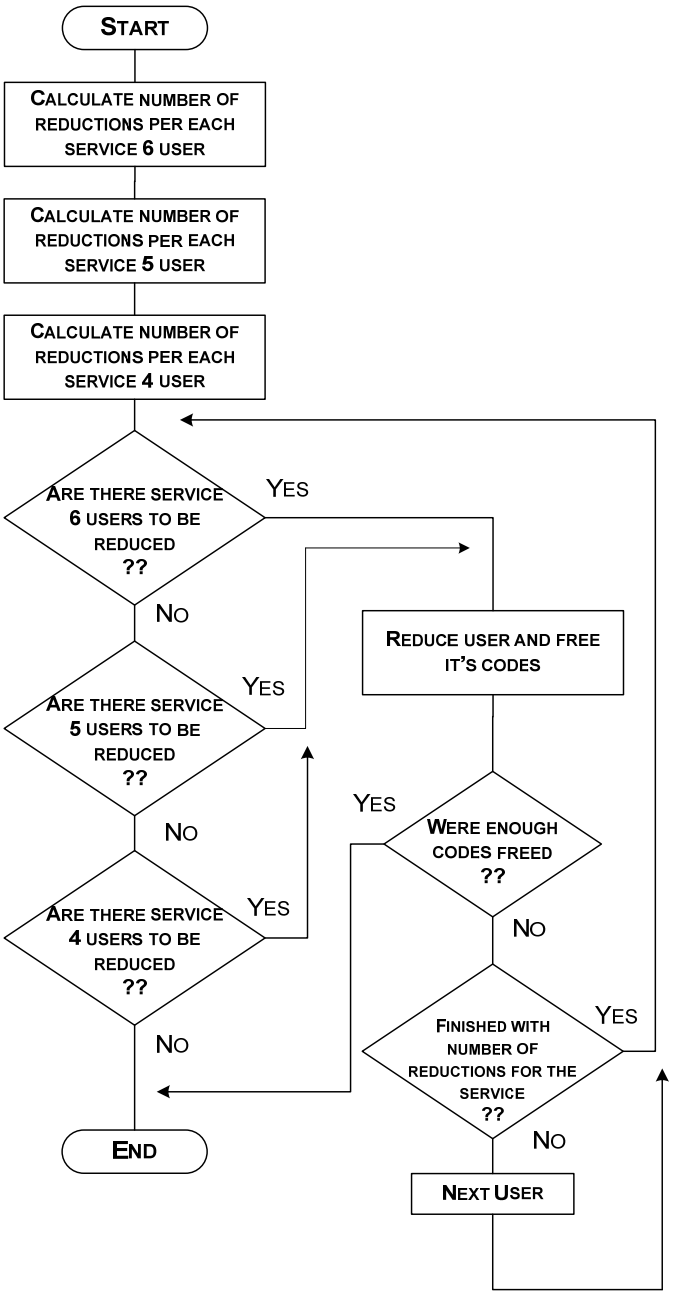

Figure C.17 – Reduce service 6, 5 and 4 MTs.

Figure C.18 shows the algorithm for the reduction steps of services 6, 5 and 4 bit rates.

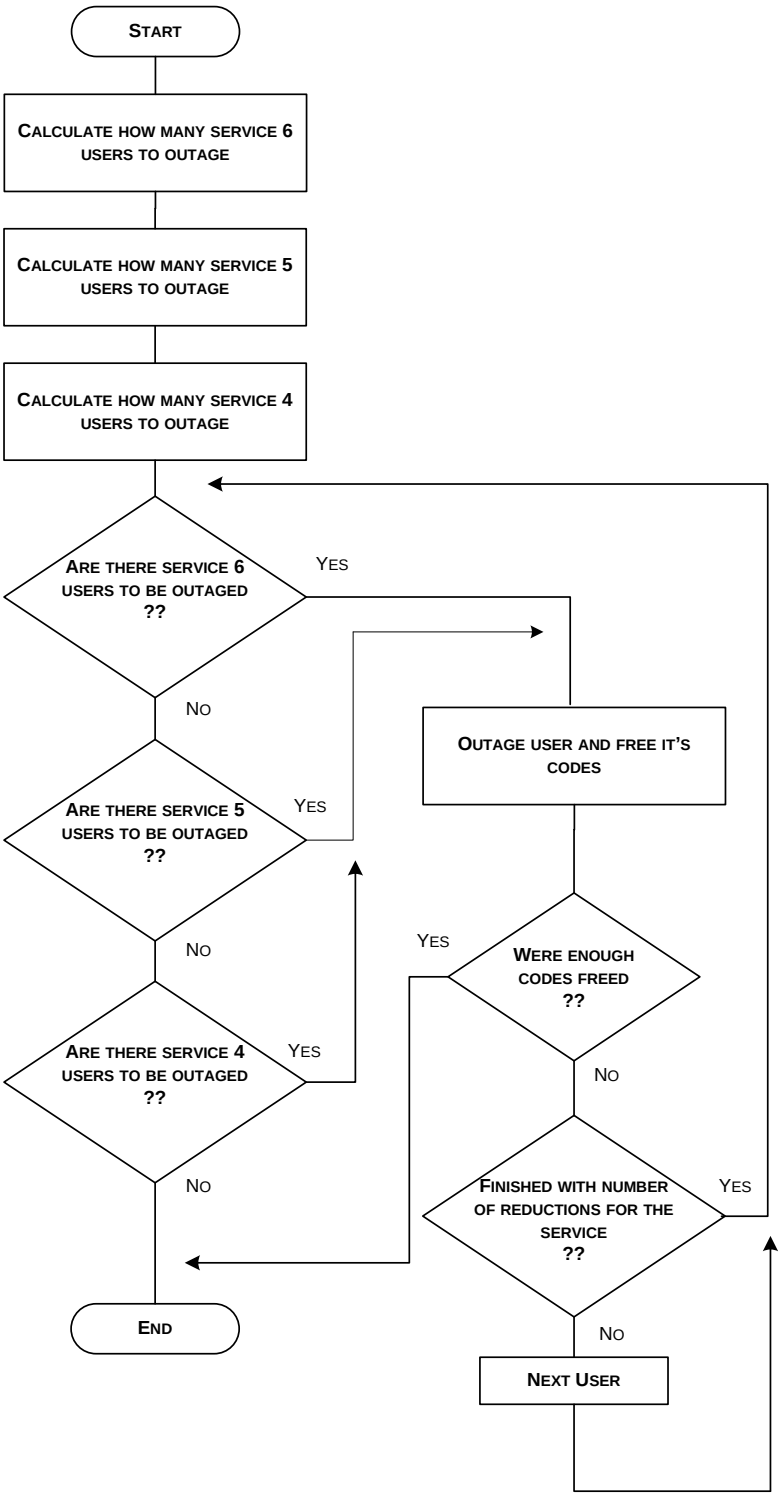

Figure C.18 – Outage service 6, 5 and 4 MTs.

Annex D

Validation of TDD Simulator

Every simulator's results must be evaluated and validated. In the present annex, the necessary validations of TDD simulator are presented.

All the presented simulator results cover only the TDD simulator developed, as FDD simulator validation was already made in [SeCa04]. The validations are separated in two types: general validations, which cover the general behavior of the simulator and interference-specific validations, which cover interference calculations within the developed simulator.

D.1 General Validations

These validations cover general aspects of the theory behind the development of the simulator. It is important to notice that, whenever present, general network performance indicators, e.g., delay or blocking probability, are purely indicative and their values may not be realistic. The validations have the objective to generate results over specific indicators and not over general network performance indicators.

Regarding the validations, the first information that must be held is the number of codes needed for each service. The several values can be found in Table D.1.

Table D.1– Number of codes per service.

Service bit rate [kbps]	Needed codes
16	2
64	5
128	10
384	28
1920	140

The first step of the validation is to make sure that the simulator calculates the correct number of needed codes per each service. Practical values refer from now on to the values obtained in the simulator. Theoretical values, whenever applied, refer to values obtained through calculations. The test scenario for the subsequent simulations is a network composed of a single BS, a total of 3000 MTs in the network with varying service according to the simulation results needed. The BS location was carefully chosen so that, at least 1000 MTs would be covered. In the current scenario, from the total 3000 MTs, the BS covers 1200 MTs.

The first results from the simulator had to be the ones related with the number of codes that the simulator allocates to each service. Figure D.1 shows these first results. As seen, the simulator correctly allocates the needed codes per service.

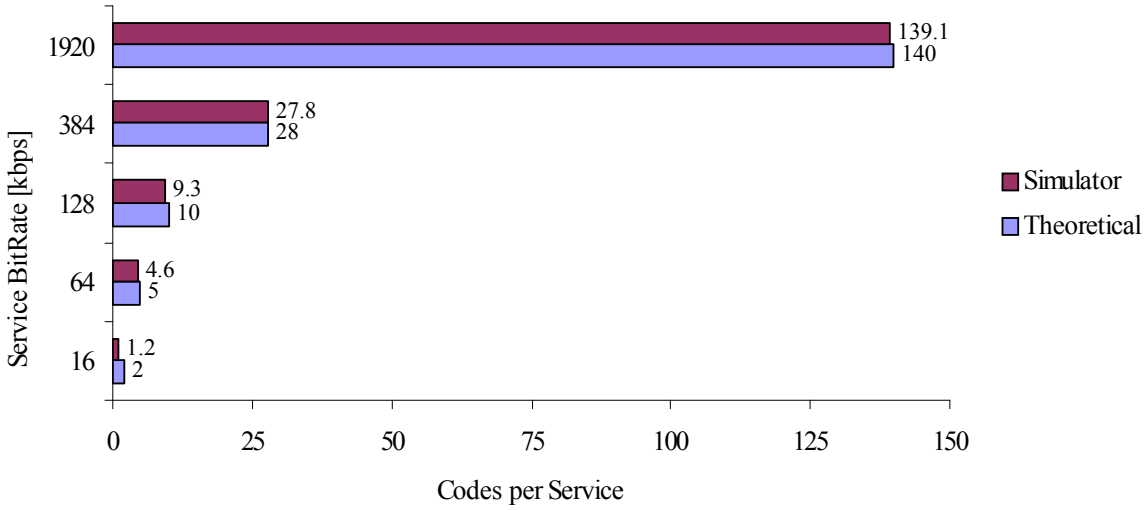

Figure D.1 – Number of needed codes per service.

These calculations were made accordingly to Table D.1.

This is step one in all the simulator validation and must be working correctly before going further in TDD simulator development. Knowing that each TS has a total of sixteen codes to allocate, one can find the number of MTs that can be servicing at the same time in one TS. The number of MTs is calculated knowing how many codes are necessary for each service. As so, the second validation to be made was to make sure that TDD simulator correctly allocates the codes of one TS for the several services, resulting in the maximum number of MTs of each service that a single TS can sustain. Figure D.2 shows the results of the simulator.

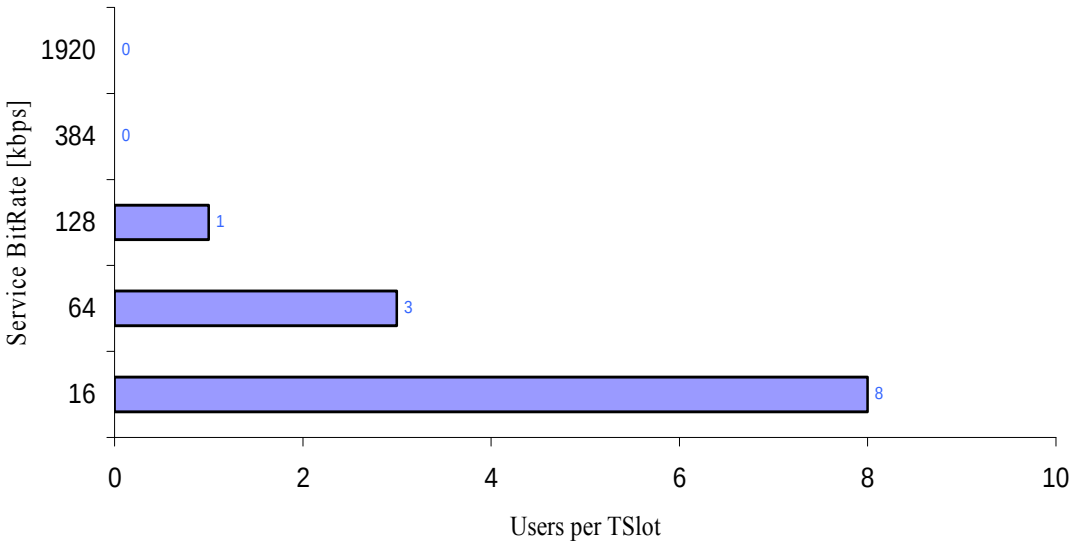

Figure D.2 – Maximum number of MTs that a TS can sustain.

As seen, the maximum number that the simulator allocates in single TS follows the theoretical

calculations. For a service of 16 kbps, which consumes two codes, there can only be a maximum of eight MTs in one TS, because eight MTs using two codes each sum up to the maximum available sixteen codes per TS. As the service bit rate increases, the maximum number of MTs that can be allocated in a single TS drops, as expected. In the limit case, the services with a bit rate equal to 384 or 1920 kbps do not have enough codes to allocate, at least, one MT in a TS.

With the confirmation that the simulator is correctly allocating MTs in each TS accordingly to each service requirements, the next step was to check if the simulator could correctly find the number of TS that an MT of each service would require.

The theory states that to find the number of TS needed for each service, the relation between the codes needed for each service and the maximum codes per TS should be determined.

As the service bit rate increases, the number of codes also does and the number of TS needed for one MT of each service also increase. For services with bit rates lower then 128 kbps, one TS is enough to make sure that one MT is servicing. For the service of 384 kbps, due to the fact that the number of needed codes is superior to sixteen, it is necessary to use more than one TS to allocate one MT of this kind of service, namely three TSs. For the service with the highest bit rate, 1920 kbps, nine TSs are necessary. This is why the recommended frame asymmetry has, at least, nine TS in DL. If less then nine TS are reserved for the DL, it is impossible to have 1920 kbps MTs servicing. This theory is confirmed by the simulator results, as seen in Figure D.3, and validates the simulator in this aspect.

The asymmetry of TDD frame is very important in what regards the network capacity. TDD is suitable for highly asymmetrical services, which means that considerable differences must exist in the UL and DL. As so, it is expected that, as the frame tend to be symmetrical, the services present some kind of degradation. This is a theoretical aspect that would be very important to confirm with some simulator results.

The theory state that as TDD frame becomes symmetrical, the number of DL MTs become progressively less while in the UL the opposite happens. This leads, in the limit, to an excessive load in the UL, which is more limited then the DL. In UL the maximum allowed load is 50 %, while in DL is 70 %.

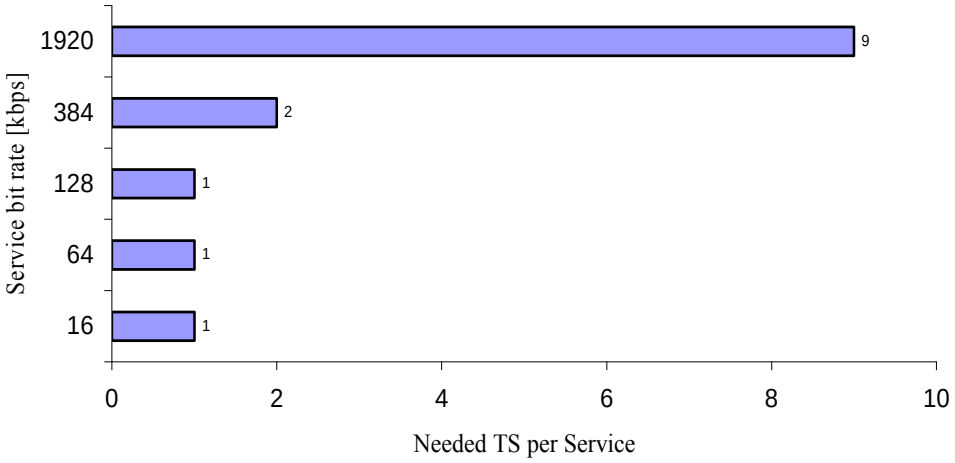

Figure D.3 – Number of TSs needed for one MT of each service.

These values needed to be confirmed by the simulator to validate the effects of frame asymmetry in the simulator results.

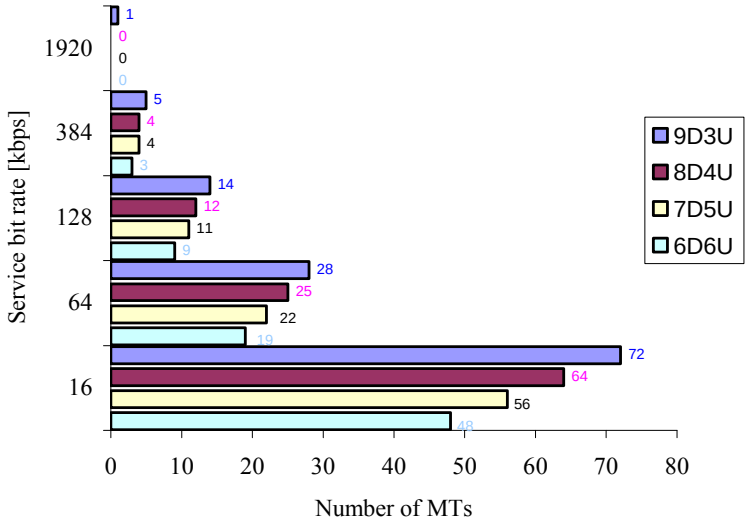

Figure D.4 – Maximum MTs in DL per bit rate for different frame asymmetries.

As seen in Figure D.4 as the frame becomes more symmetric, the number MTs drop rapidly as well as the services performance. For example, a limit situation occurs when the frame is completely symmetric, six TSs UL and six TSs DL, leading to a mean reduction of the number of MTs of 34 %. The results of the simulator confirm the theory, and the services degradation becomes greater as the frame becomes more symmetric. This is a very important aspect that needed to be proven and validated in the simulator because one of the greatest sources of interference in TDD is the different asymmetries of TDD frames between BSs, as seen in Chapter 3.

As referred before, UL suffers an increase of load as the frame becomes symmetric. As more TSs are allocated in UL, there are more MTs servicing over that link, and the network load increases rapidly in a link where the opposite should happen. As expected and shown in Table D.5, the number of MTs in UL becomes higher as more TSs are allocated in that link. This leads to an excessive load in UL and the overall network performance drops. The results from the simulator can be seen in Figure D.5 and follow the theory.

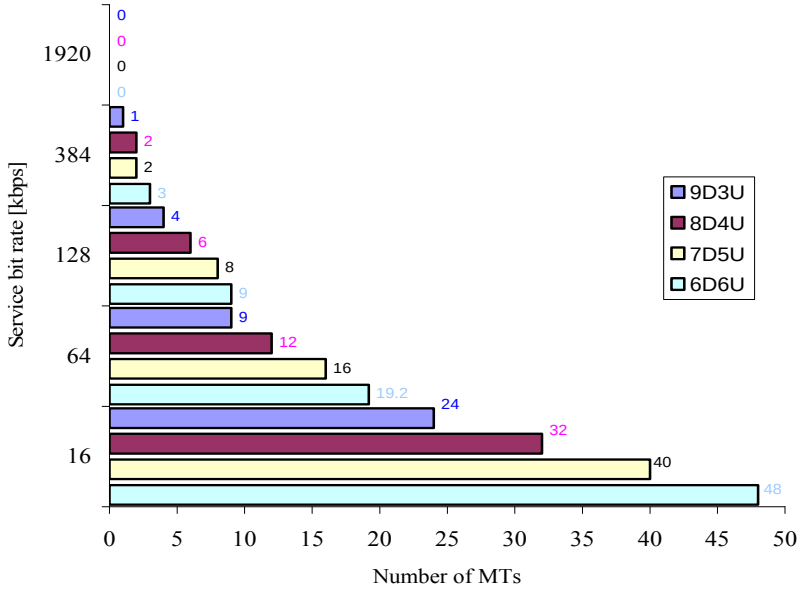

Figure D.5 – Maximum MTs in UL per bit rate for different frame asymmetries.

This validation is very important because in order to correctly evaluate the effects of frame symmetry on interference, it is necessary to be sure that the simulator works correctly with different frame symmetries. This validation was successful and allows future simulations without having doubts if the frame symmetry is working correctly.

A closer look to the codes allocation scheme shows that the number of codes given to each service may, eventually, lead to what was defined as bit rate leakage. The bit rate leaked is defined as the difference between the necessary bit rate for each service, defined as target bit rate, and the bit rate available from the codes allocated, defined as network bit rate. For example, the 16 kbps service needs two codes to work. Two codes mean that two times 13.8 kbps is allocated, i.e., 27.6 kbps, for a service that only needs 16 kbps. The bit rate leakage here is 27.6 kbps – 16 kbps = 11.6 kbps.

The comparison between the theoretical values (network bit rate) and the simulator results are show in Figure D.6. As expected, the values are not completely equal because the simulator makes the calculations based on the number of codes allocated for each service bit rate. Yet,

this inequality allows the appearance of the bit rate leakage, which is an interesting parameter to consider. The bit rate leakage is lower as the bit rate of the service becomes closer to an integer multiple of the base bit rate of 13.8 kbps.

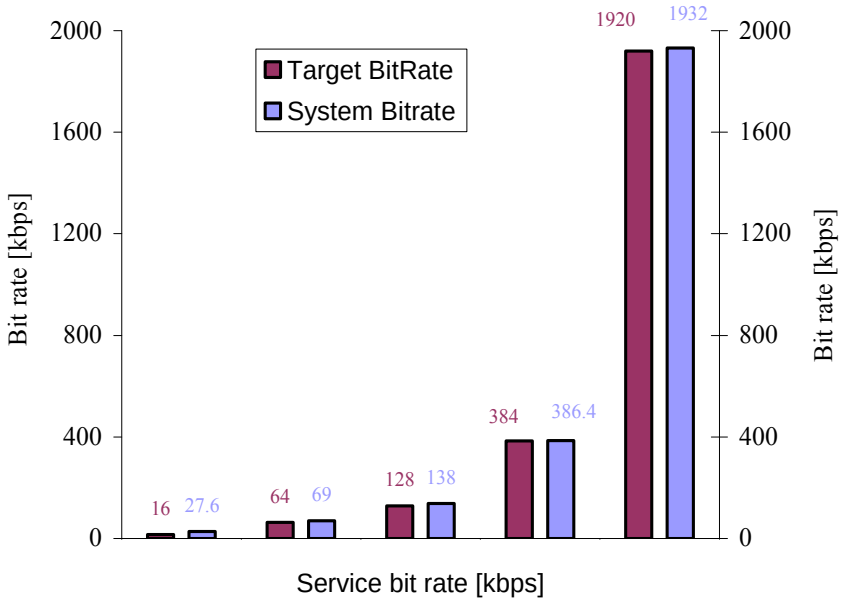

Figure D.6 – Comparison between network and target bit rates.

Figure D.7 shows the simulator results for the values of bit rate leakage per service. These two figures allow the validation of the simulator in what concerns the bit rate per service calculations.

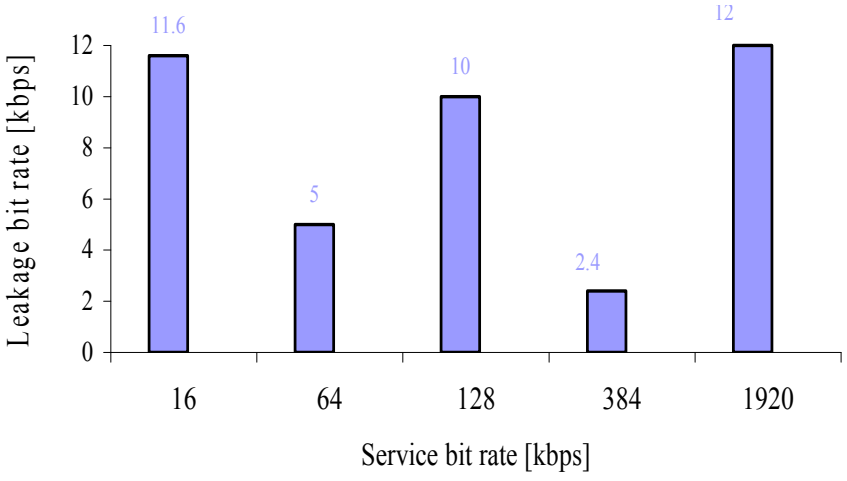

Figure D.7 – Bit rate leakage per service bit rate.

One of the most important parameters that must be analysed in the network is the load. In TDD the load concept is analysed in a per – TS basis. Thus, any TDD simulator must be able to correctly calculate the load per TS as a function of the different existing services. In that

way, it is important to validate the simulator results in what concerns the maximum load that TS can impose onto the network and the number of MTs that generate that load. It is important to analyse the maximum load that a single MT of each service imposes on one TS. As so, theoretical values of the load that one MT creates over one TS were calculated and crosschecked with the ones created by the simulator. This comparison is very important because it validates the simulator in what concerns load calculations per TS. The results are shown in Figure D.8. In order to find the maximum values, the simulations and calculations were made considering the scenario as vehicular.

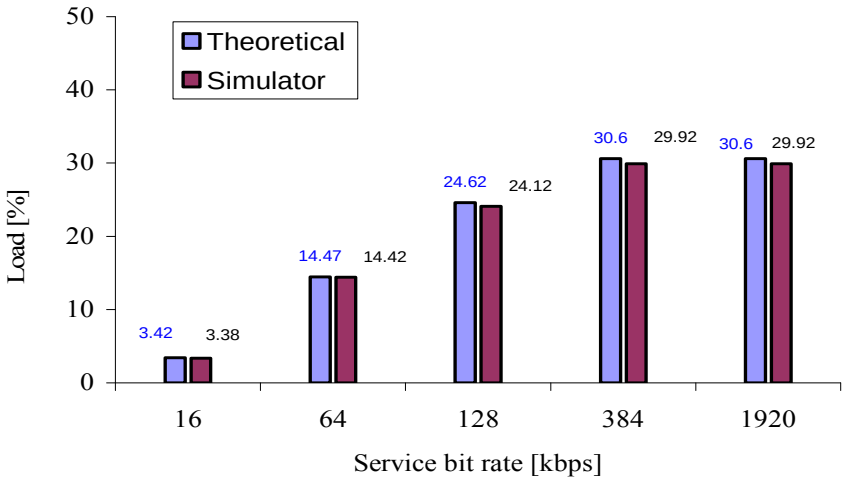

Figure D.8 – Maximum load that an MT can generate on one TS in DL.

It can be seen that the maximum load that a single MT can create on a single TS is 30.6%. This means that a single MT of 1920 kbps sets the maximum load on any TS, which is far from the maximum of 70 % in DL. It may be expected that when the TS has a mixture of several MTs the load increases.

In UL, the comparison between the results of the simulator and the theoretical values can be seen in Figure D.9. Again, the maximum load that a single MT can create on one TS is 19.3%, far from the maximum of 50 % in the UL. After having the results of the load of one MT, the next analysis is to find the maximum load that a certain service would create on a single TS and the number of MTs that would cause that value. The results shown in Figure D.10 refer to the maximum DL load that the several services cause on single TS and also the number of MTs needed to cause that load.

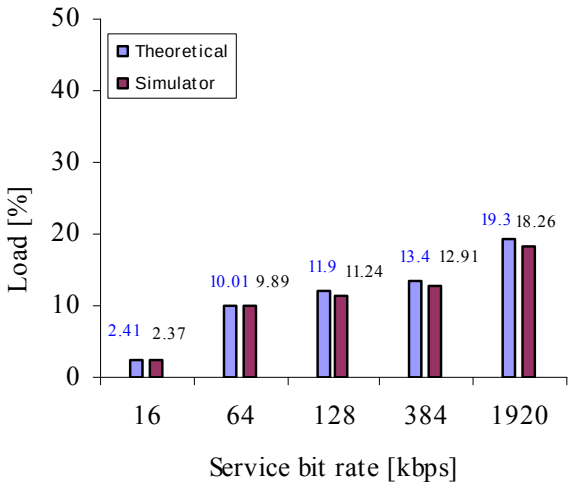

Figure D.9 – Maximum load that an MT can generate on one TS in UL.

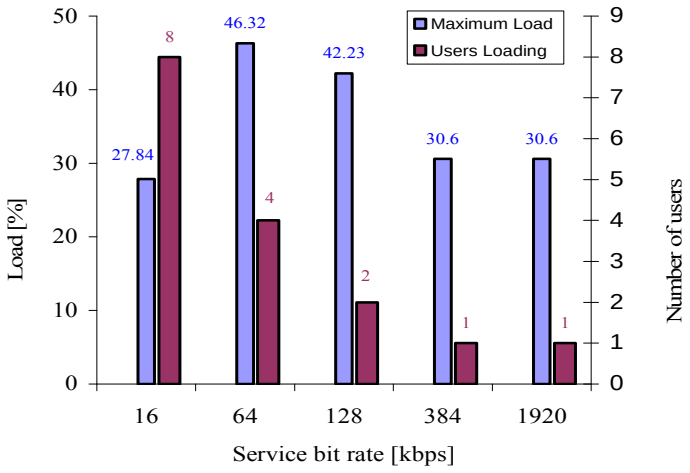

Figure D.10 – Maximum DL Load in one TS.

For example, eight MTs of a 16 kbps service cause a maximum load of 27.84 % on one TS. Four MTs of 64 kbps cause a maximum load of 46.32 % on one TS. To note that the fact that four 64 kbps MTs being allocated in one TS is not strange, when the maximum supported MTs is three. This happens because with three MTs in TS, there is still 1 code remaining. As another MT enters the network, it sees one of its five codes allocated in the TS and the other four in the following TS. This other code has its contribution to the total load in the TS and, thus, the maximum load can be determined.

Per TS, the maximum load that is observed is 46.32 %, far from the maximum of 70 %. To note that a single MT of 1920 kbps causes a load of 30.6 % on one TS. In the UL, the load is expected to be smaller than in DL. The maximum UL load per TS is shown in Figure D.11 and confirms the expected behavior of the simulator.

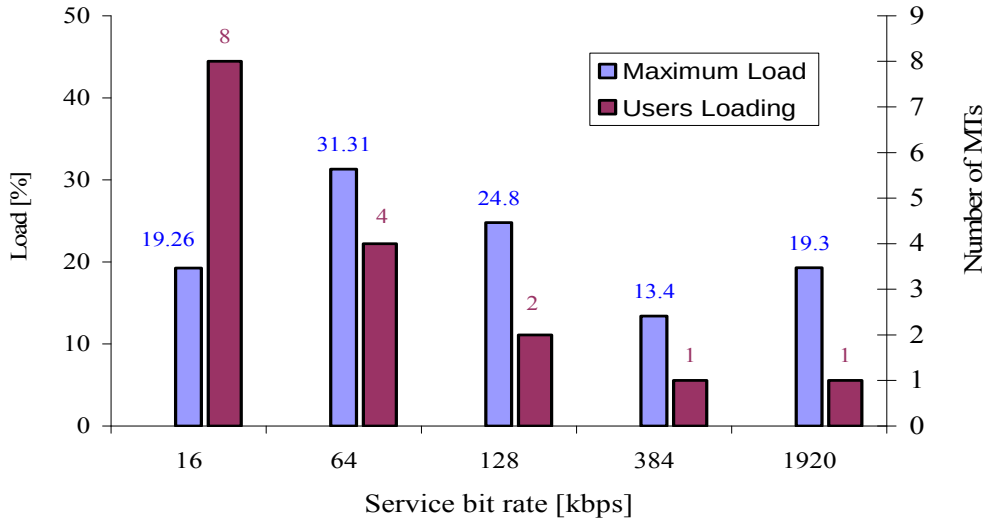

Figure D.11 – Maximum UL Load in one TS.

The MTs definitions determine that there are three different scenarios available: pedestrian, indoor and vehicular. Each one has its own distinct characteristics and a comparison is made between them to analyse the expected differences. Figure D.12 shows the simulation results for the load calculations of one MT considering the three different scenarios it can be in. It can be seen that the indoor and pedestrian scenarios have almost no differences due to very similar characteristics among them. The vehicular service presents higher loading as a result of higher values of E_b/N_o.

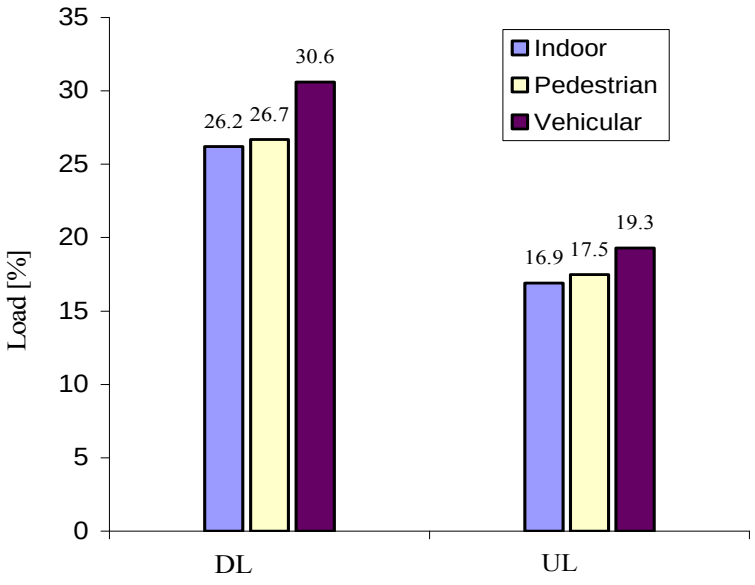

Figure D.12 – Load in the DL and UL for one MT and several scenarios.

As expected, in the same conditions and scenarios, the UL load is smaller than in DL. This theoretical aspect is completely confirmed by the simulation results.After having the presented values of the several simulations, additional network simulations were made in order to discover if the simulator was working as supposed. The objective was to see the performance of the simulator and obtain some of the most important network indicators as served and uncovered MTs and uncovered and delayed probabilities. The simulation conditions include a total of 1000 VoIP MTs (16 kbps), within a pedestrian scenario and the network varies from one to a total of thirty BSs.

The first result is shown in Figure D.13 and refers to the number of served MTs. As expected, as the number of BSs is increased, the number of served MTs also increases. In what concerns the uncovered MTs, as the number of BSs increases, the number of MTs without coverage decreases, as expected. To note that with only one BS the number of uncovered MTs is approximately 800, which is explained by the fact that a TDD cell has a smaller radius when compared with FDD cells.

In what concerns the uncoverage delay probabilities, shown in Figure D.14, it was expected that as the network BSs increase and the number of uncovered MTs decreases, the uncoverage probability decreases, as well as the delay probability. The scenario was chose as pedestrian so that the results could, at this point, be the most realistic possible, when several scenarios are not considered. As the major part of MTs is servicing under a pedestrian scenario, it was assumed that this was a good tested.

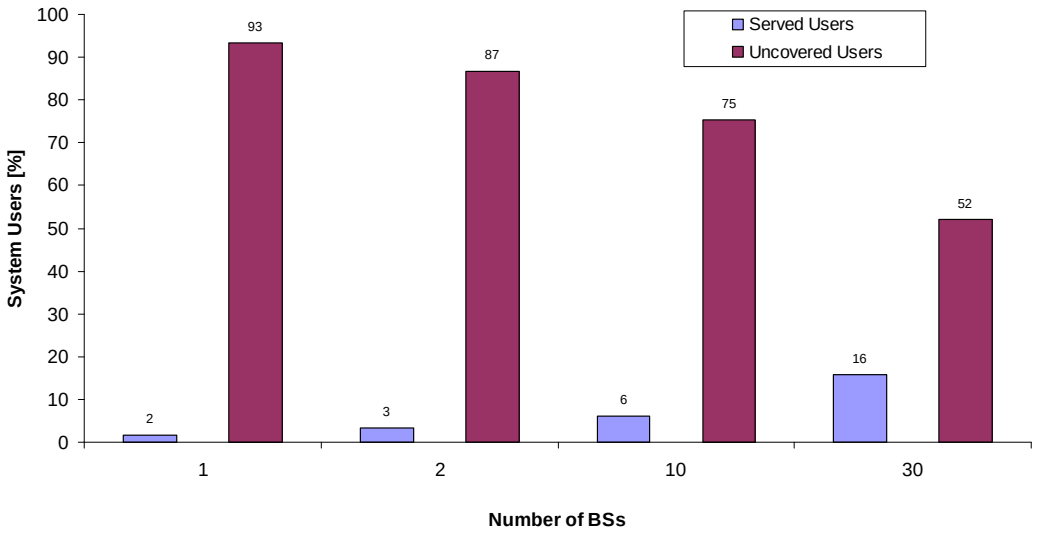

Figure D.13 – Served and uncovered probability as a function of the number of BSs.

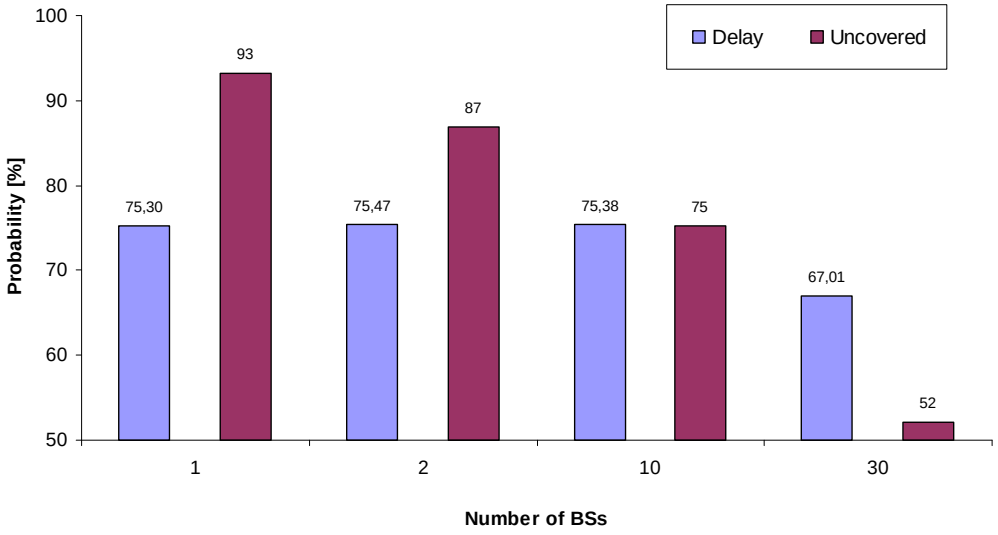

Figure D.14 – Delay and uncoverage probability as a function of the number of BSs.

D.2 Interference-Specific Validations

After having the general validations successfully concluded there is the need to validate the core of this work, which is the interference calculation algorithm.

These validations were made with basic test scenarios consisting of one and two BSs and 50 and 2000 VoIP and Location MTs. The main goal is to analyse the intra- and inter-interference in the cells and therefore, conclude about the correctness of the interference algorithms. Because the actual operation mode is TDD, all the calculations and validations concern a single TS and not all of them, except when clearly referred.

The first test that had to be done was to see in which way the BS transmitting power (seen as interference power from the MT point of view) varies as the MT increases or decreases its distance to its own BS. Only one BS is considered, thus, allowing testing only two interference scenarios.

The theory states that, as MT's distance increases, its receiving power is progressively lower. Figure D.15 shows the result of that study, as MT's distance to its own BS is increased. The simulator behaves as expected which allows proceeding to additional validations.

Taking into consideration that in DL, intra-cell interference in an MT is seen as the sum of the transmitted power to all servicing MTs minus his received power, it is expectable, as MTs increase the distance to their servicing BS, that suffered interference increases considering

that the other MTs are kept still. Refer to (D.1).

This is an important test as it consists on the first evaluation of the interference calculation algorithm.

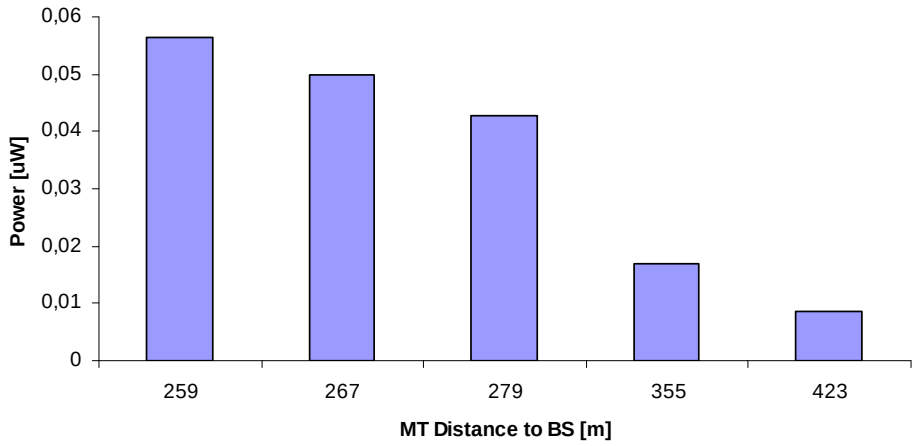

Figure D.15 – MT received power from BS as function of its distance.

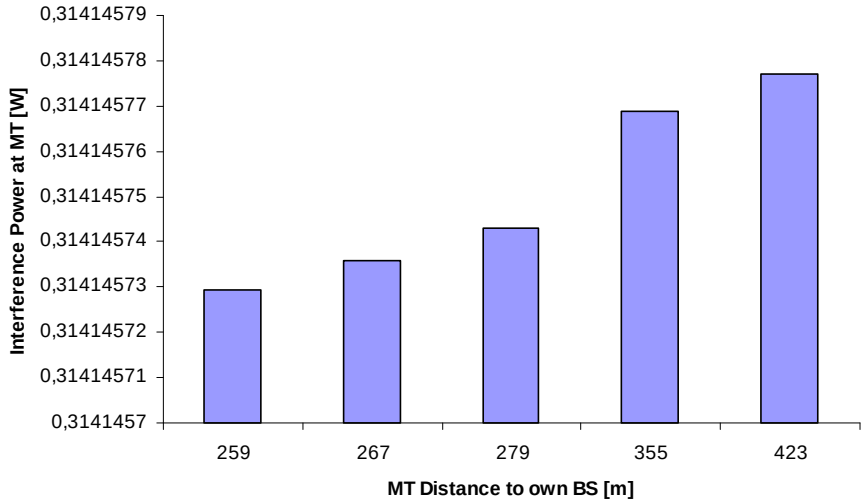

Figure D.16 – MT received interference from BS as function of its distance.

As can be seen from Figure D.16, the received interference from its own BS increases as an MT moves towards its cell border.

The next study referred to UL. In this link interference suffered by the BS is the sum of all the signals from all the transmitting MTs inside it. As so, it is expectable that as the number of servicing MTs increases interference at the BS also does. Refer also to (3.28). This happens because additional MTs are transmitting to the BS, adding up its signal to the main interference count. The study, therefore, consisted in varying the number of MTs and also

their distance to the BS. The MTs were placed at concentric distances with radius of 40, 90, 140 and 190m from the BS.

As Figure D.17 shows, as an MT moves away from the BS, it causes less interference in UL, as the total arriving interference power at the BS decreases with the distance.

This behavior is maintained when the number of MTs varies. The only difference is the amount of interference that more MTs cause on their own BS. As expected though theory, more MTs create more interference over their own BS in the UL. Figure D.17 also shows that, at a certain distance, all MTs are blocked and no additional interference exists in the UL.

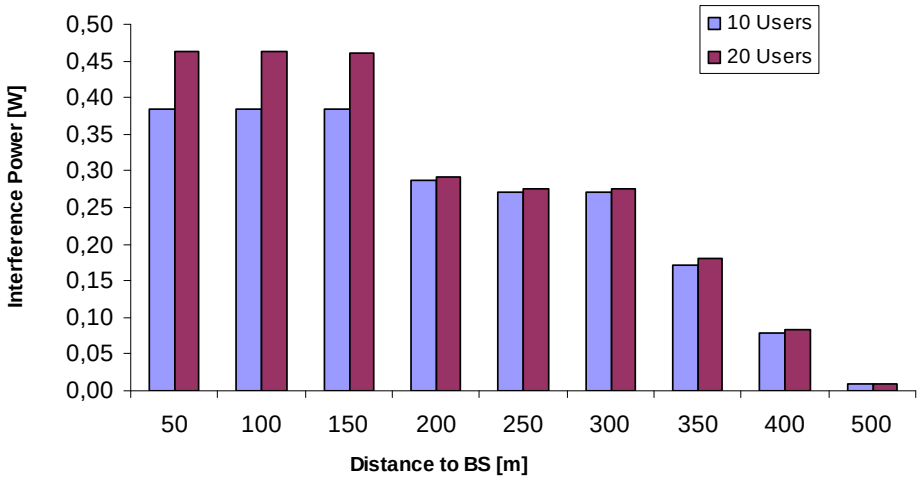

Figure D.17 – Interference suffered by BS as function of MTs distance to BS.

The simulation with only one BS allows other validations that are not suitable to be shown in the form of a graphic. When only one BS exists, there is no inter-cell interference, thus, intra-cellular interference impacts over the delay probability and cell radius can be analysed. The next validation study consisted of looking at the delay probability and cell radius first without considering interference and secondly, considering the existence of intra-cell interference. The scenario is comprised of 50 VoIP MTs and a single BS, again. From these 50 MTs, the BS covered only 41.

When no interference is considered, 25 MTs are servicing. When intra-cell interference is considered, for each MT the new E_b/N_o is calculated and matched against the target value for that service. From the 25 servicing MTs, only 5 are now servicing, which raises the delay probability to a value of 20 %. This allows confirming the following theoretical aspects: the cell radius decreases and delay probability increases when interference is considered. It is shown that all MTs beyond 100m of distance from the BS were delayed, thus, increasing the

delay probability. Again, it is important to state that the delay probability values are not supposed to be accurate and realistic. The objective here is to validate the interference algorithms and their related indicators.

Due to the fact that the DL and UL transmitting powers are similar (23 dBm and 21 dBm, respectively, for data and non-EIRP) major differences between the delay blocking probabilities in DL and UL are not found. Also, considering that in DL the E_b/N_o is greater than the one in UL, any MT that sees its target value achieved in DL also has its value big enough to allow UL servicing.

The following tests and validations were made with a different scenario. This time, to be able to have all the four interference scenarios the validations were made with two BSs in the network and 2000 VoIP and Location MTs. When referred, additional tests were made with other services.

The first test had the objective of testing the effects of the inter-cell interference on a single MT. The theory states that MTs closer to their cell edge suffer more interference from the adjacent BS, as the received signal from it is greater. Also, as MTs move away from the adjacent cell, on the contrary, it is expected to suffer less inter-cell interference. The result of the test is shown in Figure D.18. It can be seen that, as an MT approaches its cell edge, it approaches the adjacent cell and suffered inter-cell interference increases. Again, practical values confirm the theory that MTs closer to its cell edge suffer the most inter-cell interference in the DL.

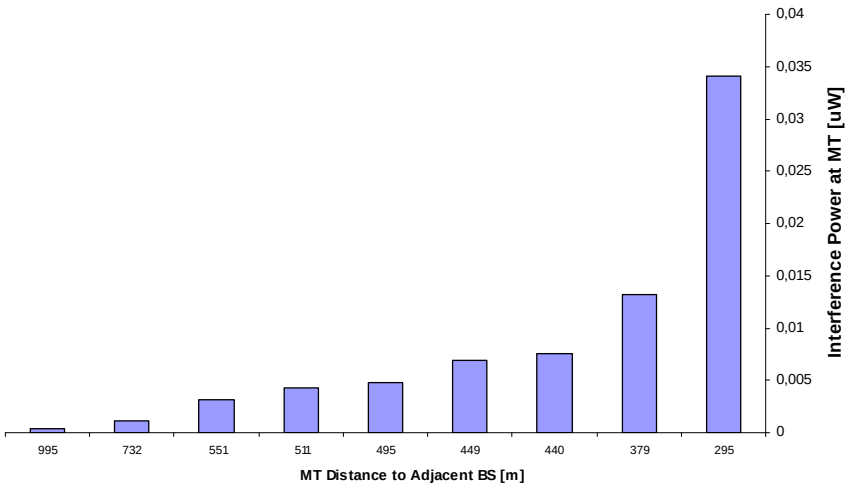

Figure D.18 – Inter-Cell interference in DL as function of the MT distance to adjacent BS.

Also, it would be interesting to see what happens on the UL. As an MT approaches its cell

edge, it causes more interference in UL over the adjacent cell, as expected. This theory states that MTs at the cell boundaries are the ones who interfere the most over adjacent BSs. Figure D.19 shows the results of this test. As an MT moves to its cell edge, becoming progressively closer to the adjacent BS, the amount of interference power that arrives to that BS increases. As so, inter-cell interference in UL increases as the MT is closer to its cell boundaries.

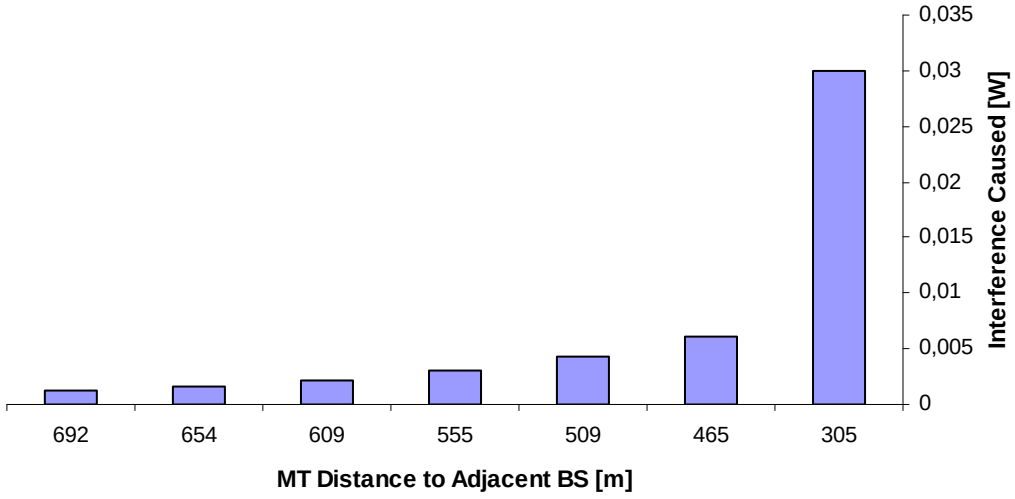

Figure D.19 – Inter-Cell interference in UL as a function of MT distance to adjacent BS.

Taking into account that the simulator has multiple services, it would be interesting to see the difference between two or more services, in what concerns the amount of interference generated. And so, the study goal was to compare the results of interference between the Voice and Location services. In theory, the more the service bit rate, the more interference power it generates due to the fact that the transmitting powers increase. Figure D.20 shows the results of the comparison between the intra-cell interference generated by the two services. It can be seen that, as expected, the location service creates greater values of interference due to the fact that its bit rate is greater and, thus, the transmitting powers involved.

The same results are found if inter-cell interference is considered. As shown in Figure D.20, as MT's bit rate increases, generated interference also increases. This kind of behavior is expected to all services as the bit rate increases. The behavior of MT-generated interference when it moves to its cell boundaries is aggravated by increasing the service bit rate.

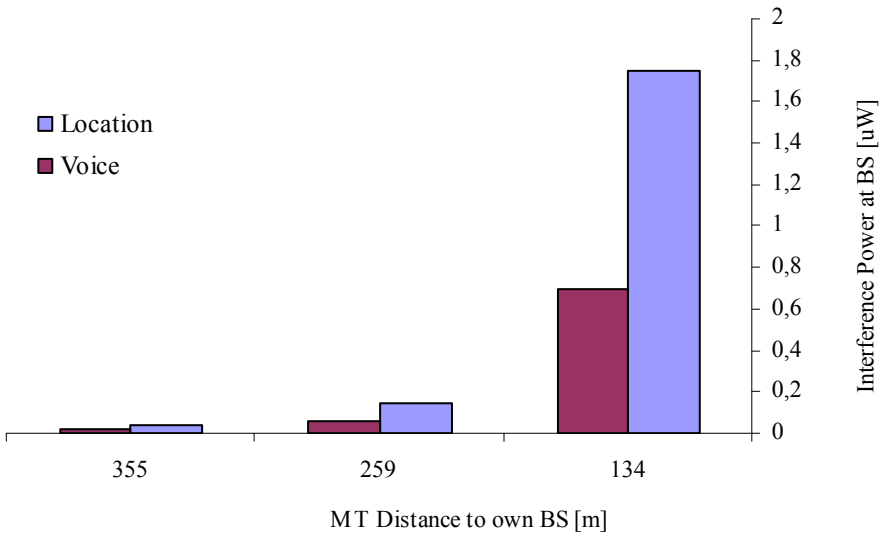

Figure D.20 – Intra-Cell interference in UL as a function of MT distance to own BS.

As MTs move closer to their BS, generated interference rises. This validates the theory that states that, in intra-cellular interference, MTs closer to BSs are the ones who most contribute to the total interference inside the cell. MTs that are further away from the BS do not generate as much interference and so, contribute less to the intra-cell interference. These are not significant for the intra-cell interference but are to the inter-cell interference, as seen below. Regarding the opposite, please refer to Figure D.16.

An MT that moves to its cell boundaries generates less intra-cell interference, but greater inter-cell interference, as seen in Figure D.21.

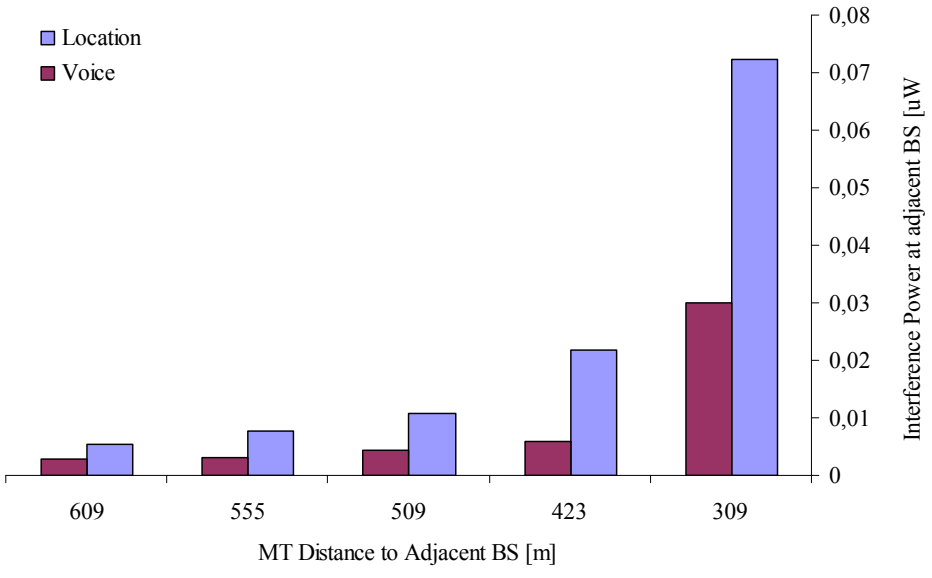

Figure D.21 – Inter-Cell interference in UL as a function of MT distance to adjacent BS.

At this point there is still one interference scenario to be studied and evaluated. The next interference study allows the validation of the algorithm that calculates the interference that MTs cause on each other. As can be seen from (3.27), this interference mode only exists when considering inter-cell interference, due to the existence of an offset between adjacent cells synchronism. In this test it was assumed that an offset exists, without a value being specified because the objective was to analyse the impact that MTs have on a single MT from an adjacent cell. The frame offset value models this impact, making it higher as the offset value increases.

The first test consisted in a certain MT that was fixed at a certain distance from its BS. The interference that the interfering MTs from adjacent cell cause on it was found. The MT was fixed at a distance of 113 meters from its BS. The interfering MTs were located at several distances in the adjacent cell. It can be shown from the results in Figure D.22 that as the adjacent MTs move away from the MT in the other cell, the interference that they cause on that MT decreases.

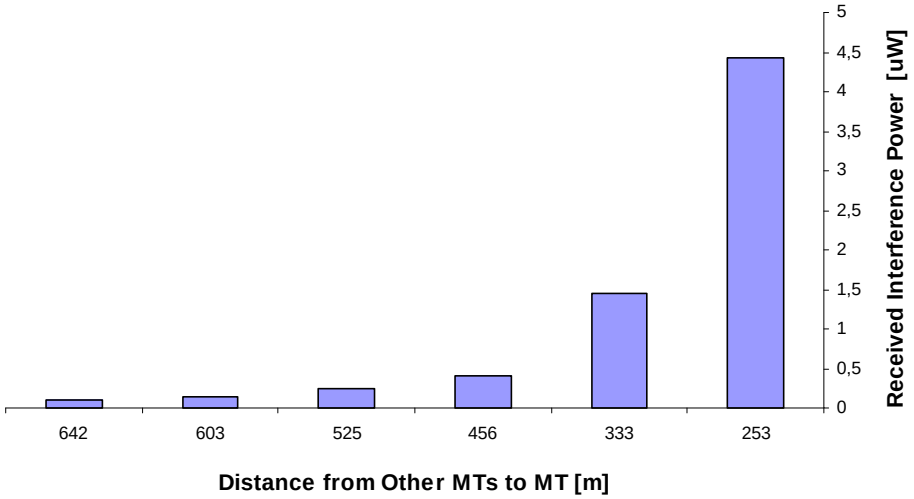

Figure D.22 – Inter-Cell interference caused by adjacent MT over one MT.

On the other hand, it can be seen that as the other-cell interfering MTs move closer to the fixed MT the interference that they cause on him increases. This validates the theory that when an MT is in a fixed location MTs located at the adjacent cell edges cause more interference on it, than MTs further away from adjacent cell edges. MTs closer to its BS suffer less interference from other cell's MTs, thus, less inter-cellular interference exists.

This annex presented the several validations made to TDD simulator. Several theoretical calculations were made so that the simulator results could be cross-checked with them. TDD

simulator shows a good performance, and the TS allocation engine and the interference calculation algorithms results allow the assumption that the simulator is working properly, accordingly to expected.

Annex E

Additional Scenario Statistics

This annex presents the statistics of the several parameters analysed in order to find the reference scenario for TDD and also the statistics for the reference scenario itself.

This annex is divided in two different parts. The first one presents all the additional parameters and simulation results referred to the study that was made until finding the reference scenario. The subsequent sub-sections present the additional statistics to the several parameters that were varied to test the scenario performance.

E.1 Several Scenarios Comparison Study

The following tables and graphics present the parameters comparison between the several scenarios that were analysed. Mean values from 10 simulations are presented for each scenario on the following figures.

Table E.1 – MTs statistics after initial RRM and without interference for all scenarios.

Users statistics without interference accounted				
Scenario	Network MTs	Outaged MTs (RRM) [%]	Puc [%]	MTs servicing without interference [%]
1	3279	2.9	0.95	97.1
2	3300	7.8	0.94	92.2
3	3379	17.9	0.92	82.1
4	3880	21.3	0.80	78.7
5	3364	33.1	0.92	66.9
6	3398	41.0	0.91	59.0

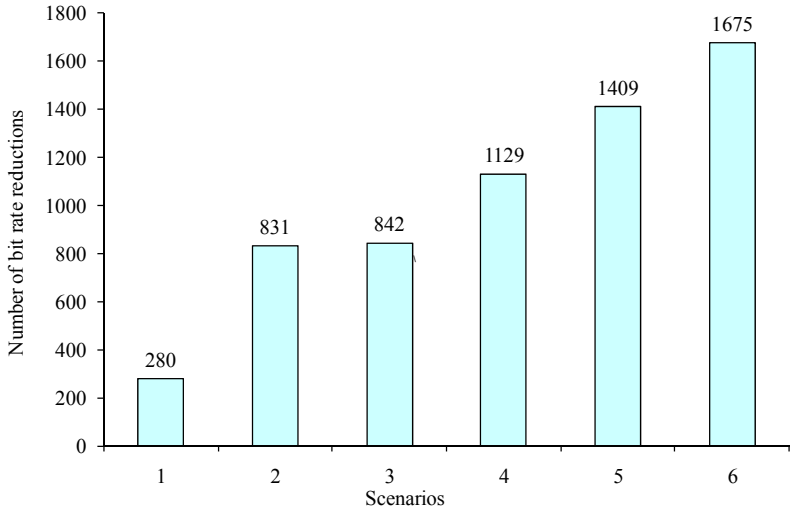

Figure E.1 – Number of reductions in the network due to RRM.

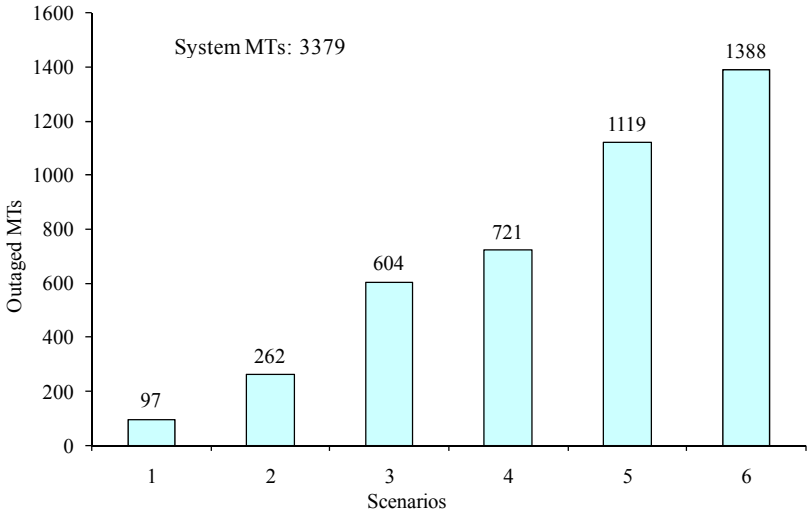

Figure E.2 – Number of Outaged MTs in the network due to RRM.

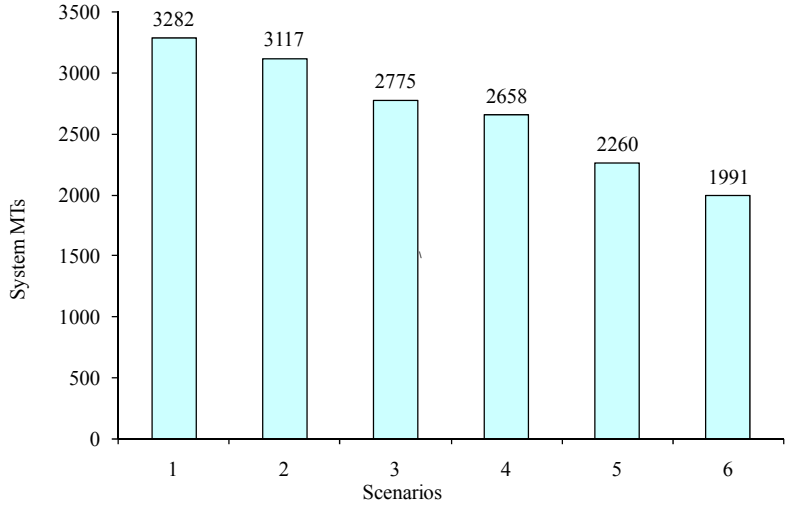

Figure E.3 – Number of MTs servicing after RRM and without considering interference.

Regarding services, it is interesting to see how the RRM algorithm effects are noticeable. As so, the following tables present some parameters variations that allow a deeper understanding of the RRM algorithm effects over the different services, Tables E.2 and E.3.

Table E.2 – Effective bit rate per service after RRM.

Scenario	Efective bit rate [kbps]					
	VoIP	VideoTel	MMS	Email	Video streaming/File download	Web browsing
1	16.0	64.0	64.0	121.9	174.5	506.2
2				67.4	176.4	705.3
3				60.6	176.4	705.3
4				60.6	186.9	877.4
5				60.6	167.1	904.3
6				60.6	163.9	807.4

Table E.3 – Percentage of the bit rate that the services have after RRM.

Scenario	Bit rate usage [%]					
	VoIP	VideoTel	MMS	Email	Video streaming/File download	Web browsing
1	100.0	100.0	100.0	95.2	45.4	26.4
2				52.6	45.9	36.7
3				47.4	45.9	36.7
4				47.4	48.7	45.7
5				47.4	43.5	47.1
6				47.4	42.7	42.1

It can be seen that due to RRM the HBR services are highly penalised. For instance, Web Browsing MTs that should be servicing, theoretically, at 1 920 kbps only service at 26 to 47% of that value, corresponding to a minimum of 505 kbps to a maximum of 907 kbps. Tables E.4, E.5 and E.6 show additional results and considerations.

Table E.4 – Bit rate reduction after RRM compared with the theoretical values.

Scenario	Bit rate reduction [%]					
	VoIP	VideoTel	MMS	Email	Video streaming/File download	Web browsing
1	0.0	0.0	0.0	4.8	54.6	73.6
2				47.4	54.1	63.3
3				52.6	54.1	63.3
4				52.6	51.3	54.3
5				52.6	56.5	52.9
6				52.6	57.3	57.9

Table E.5 – MTs statistics considering interference for all scenarios.

MTs statistics without interference accounted					
Scenario	MTs servicing without interference	MTs delayed due to interference UL/DL [%]	MTs servicing with interference [%]	Reduced MTs due to E_b/N_o <target and more than 1 TS DL [%]	Reduced MTs due to E_b/N_o <target and more than 1 TS UL [%]
1	3185	28.1	71.9	18.3	3.1
2	3041	31.6	68.4	26.7	4.6
3	2773	26.9	73.1	26.4	5.2
4	3054	28.1	71.9	28.1	4.9
5	2251	41.2	58.8	52.6	8.8
6	2005	45.2	54.8	62.9	9.7

Table E.6 – Number of interferent MTs and BSs over one BS in the network.

Scenario	Mean		Max		Min	
	Interfering BSs	Interfering MTs	Interfering BSs	Interfering MTs	Interfering BSs	Interfering MTs
1	4	47	12	140	1	1
2		44		133		
3		33		95		
4		34		107		
5		34		99		
6		33		101		

The percentage of code losses due to interference rises as the scenario progresses. As interference rises, HBR MTs begin to see its bit rate reduced partially or totally and the used codes in the network drop below the number of used codes without the presence of interference.

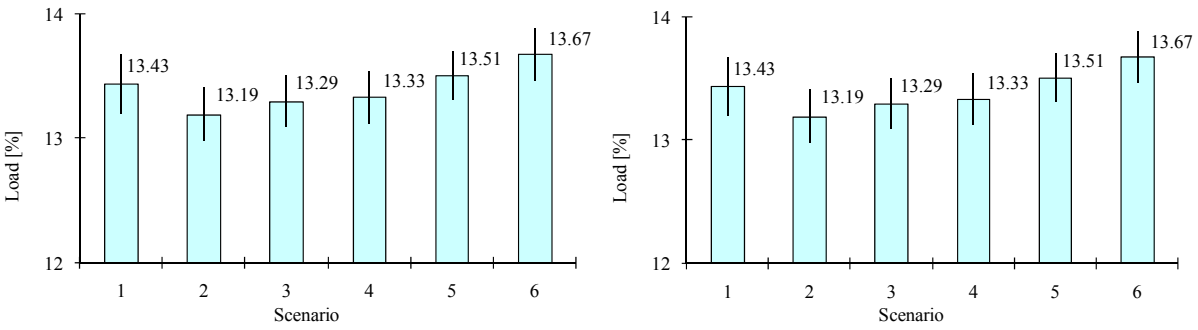

(a) Without interference. (b) With interference.

Figure E.4 – UL Load.

Looking at Figure E.4, although it may not appear, the UL load without interference is smaller than when interference is considered. The reason for this not to be so noticeable is, as explained in Chapter 5, that the interference power rise in the UL is of a few micro Watt, not noticeable when summed up with the MT power without interference accounted.

Annex F

Frame Asymmetry Statistics

This annex presents additional statistics for the frame asymmetry study that was presented in Chapter 5.

Figures F.1 and F.2 show the offered codes before interference and the existing number of codes after interference is considered. The bit rate presents exactly the same behavior scale by a value of 13800 in order to present the number of codes in the form of bit rate.

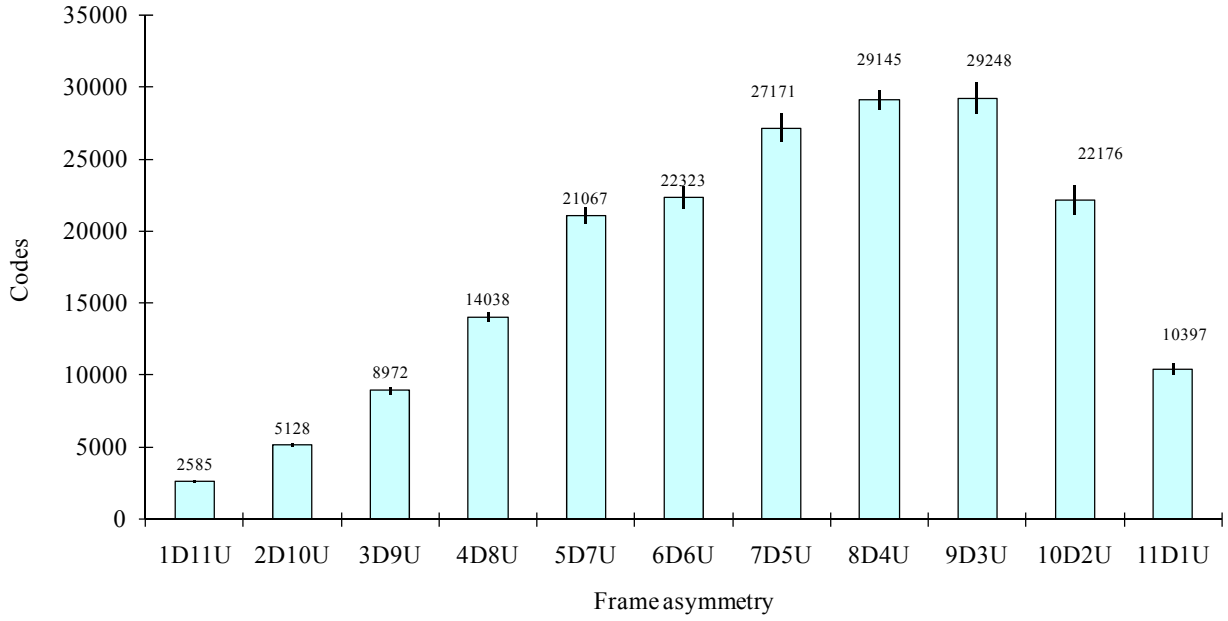

Figure F.1 – Number of offered/existing codes before interference.

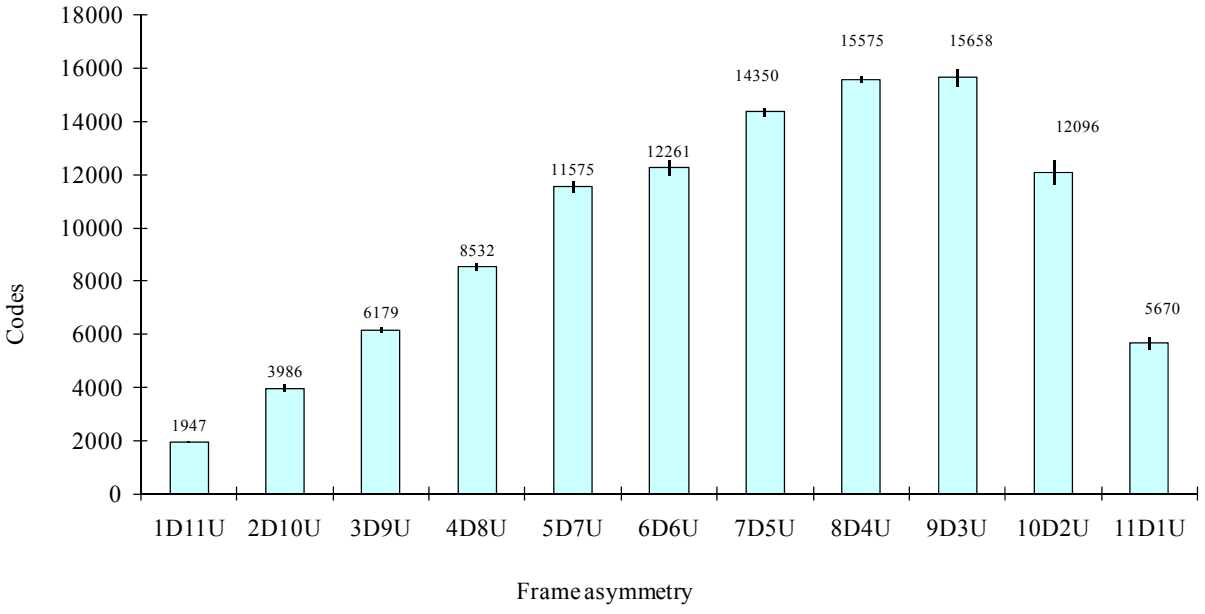

Figure F.2 – Number of carried/existing codes after Interference is accounted.

Regarding the occupancy, it can be seen that as the number of DL TS increase the number of used codes also increases and the number of free codes decreases. For extreme cases, the number of used codes is very low due to the fact that one or two TS in each greatly reduces the number of servicing MTs. Figures F.3 and F.4 show code occupancy without and with

interference considered, respectively. Code reduction can be analysed from Table F.1.

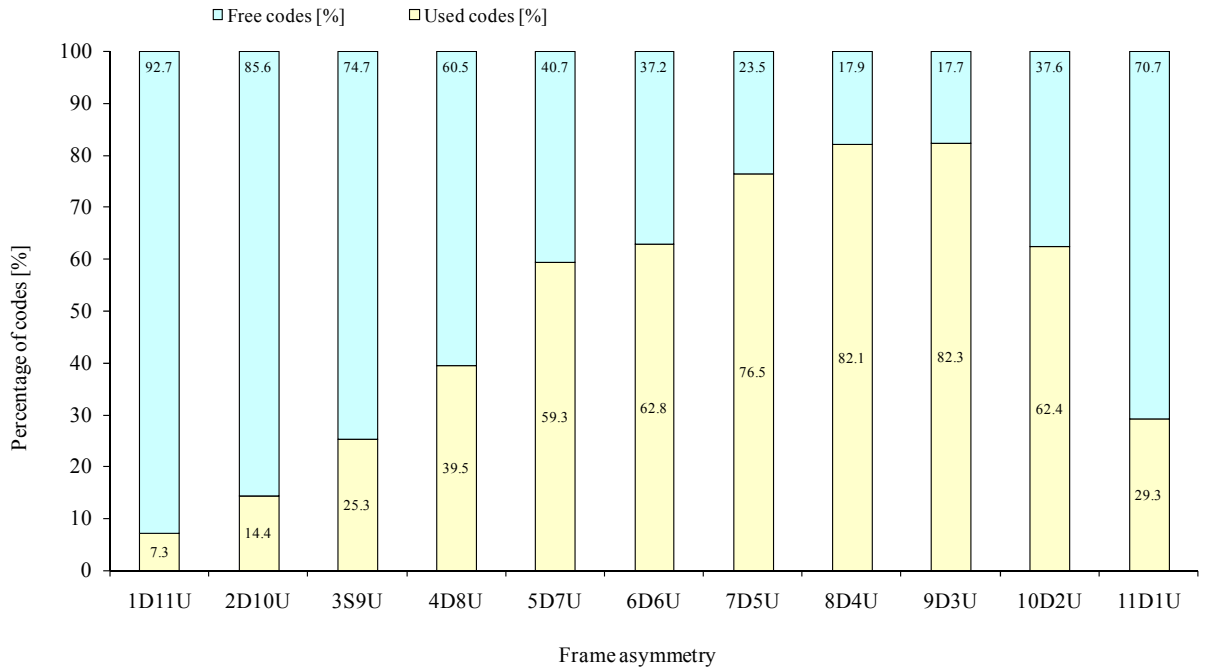

Figure F.3 – Absolute code occupancy when interference not considered.

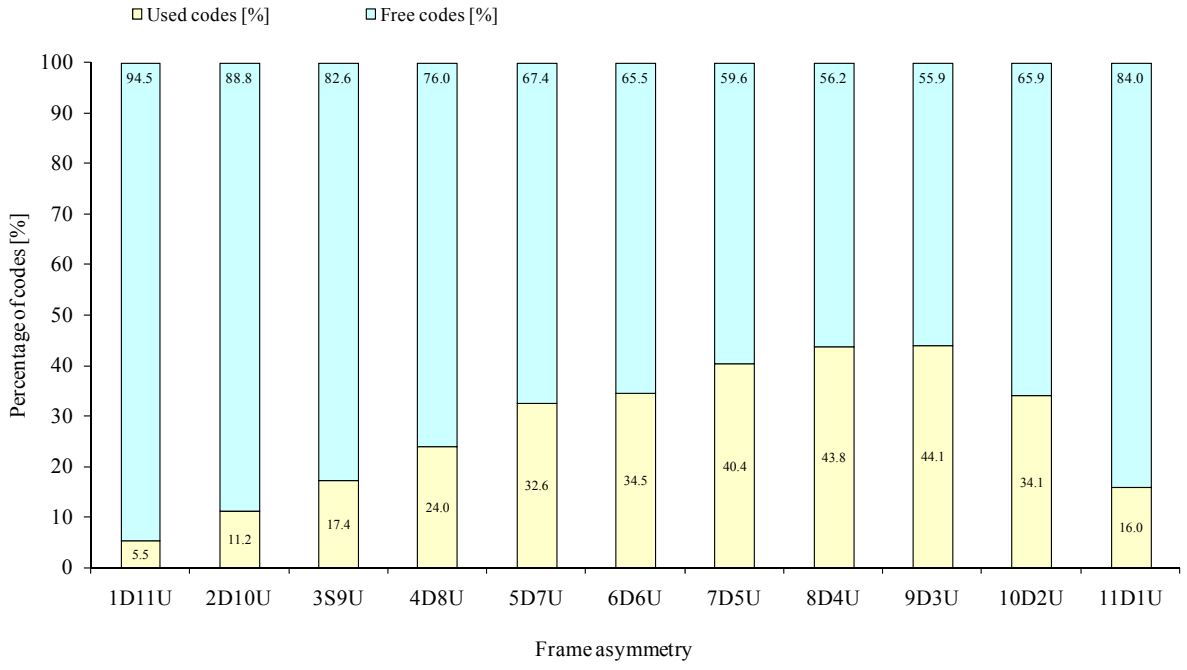

Figure F.4 – Absolute code occupancy when interference effects are considered.

Table F.1 show the percentage of bit rate reduction due to interference. At a first glance it can be seen that only the three most HBR services suffer bit rate reduction. It can be seen that as the DL TS increase, the reduction in the email and streaming service is lower, while it is higher in the Web Browsing case. Interesting to see that in 10D2U there are no reduction on

the Email service and all the reduction on the Streaming/FTP service than in the 9D3U case and only around 3 % more in the Web Browsing case. This may well present an advantage of the 10D2U symmetry over the 9D3U.

Table F.1– Code reduction per service.

Frame asymmetry	Code reduction per service due to interference [%]					
	VoIP	VideoTel	MMS	Email	Streaming/FTP	Web Browsing
1D11U	0.00	0.00	0.00	48.53	75.00	0.00
2D10U				25.59	67.37	0.00
3D9U				9.25	54.62	75.63
4D8U				3.17	41.24	76.52
5D7U				3.39	24.97	76.34
6D6U				1.08	18.52	75.78
7D5U				1.56	15.37	76.06
8D4U				0.64	9.41	75.70
9D3U				0.96	8.39	74.63
10D2U				0.00	3.92	71.90
11D1U				0.00	2.30	73.89

Regarding the probability of low access, it can be seen that as more HBR MTs are entering the network, the probability of bit rate reduction due to interference increases, Figure F.5. The maximum observed value is 47.1 % for the 8D4U and the leveling seen in the values owns itself to the RRM algorithm.

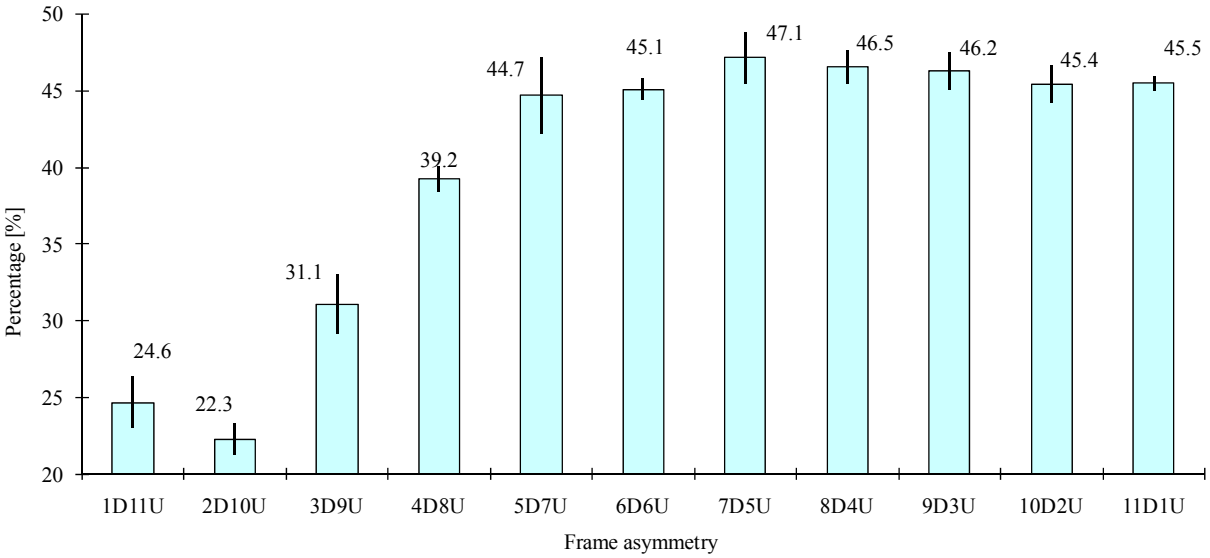

Figure F.5 – Probability of low quality Access due to interference.

As seen before, the RRM algorithm has a high level of influence on the global network results. RRM algorithm effects over MTs must be analysed in order to understand how deep

that influence goes. As it can be seen from Figure F.6 as more DL TSs are available the less outage MTs exist due to RRM algorithm, because there are more resources available in the network. Conversely, the number of MTs servicing after RRM algorithm also increase with the increase of the available DL TSs. In the extreme cases, when only one TS is available in one of the links, the RRM algorithm can outage 40 % of the network's MTs.

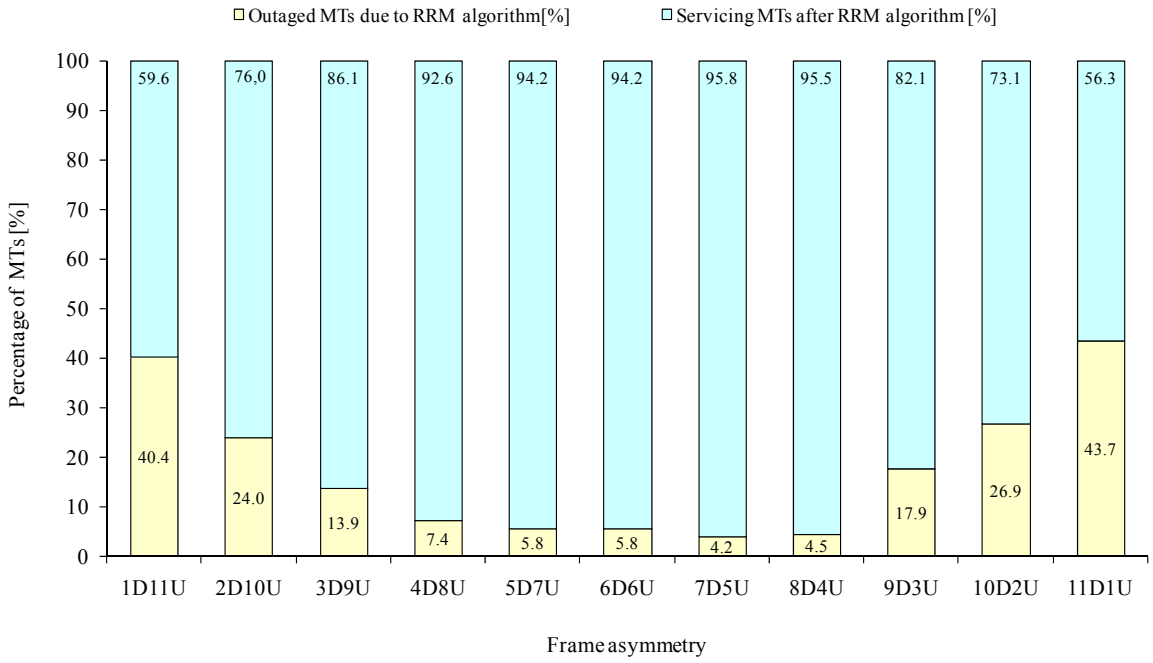

Figure F.6 – Effects of the RRM over the MTs prior to interference effects.

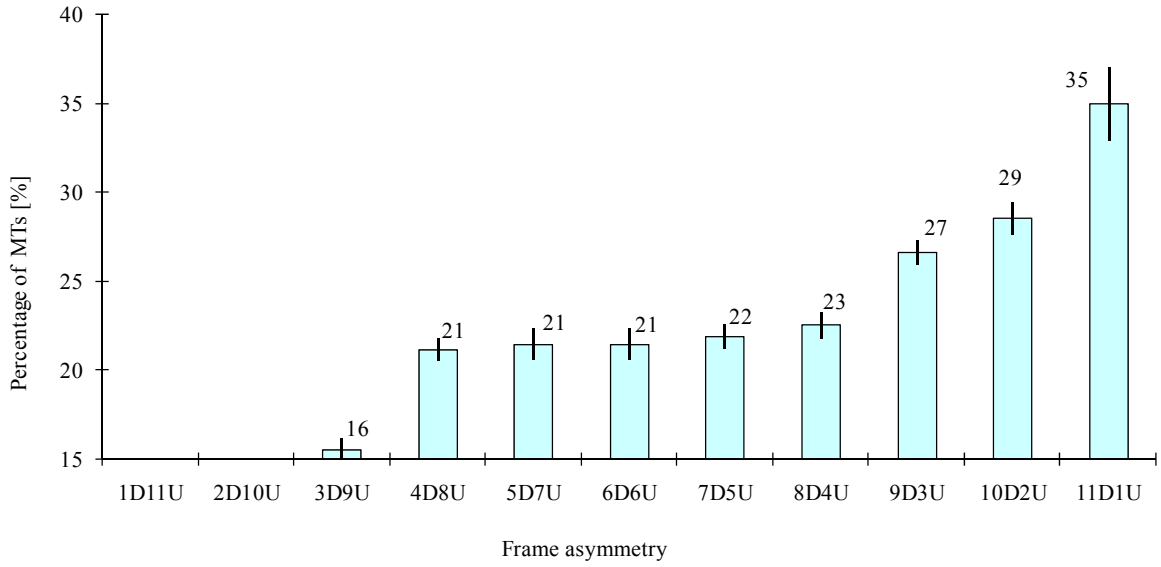

Figure F.7 – Reduced MTs due to E_b/N_o below target when using more than one TS DL.

Figures F.7 and F.8 show reduced MTs due to non-destructive interference effects for both links. As it can be seen the number of reduced MTs increases as the number of DL TS

increase, allowing more MTs in the network and also higher interference effects on the MTs.

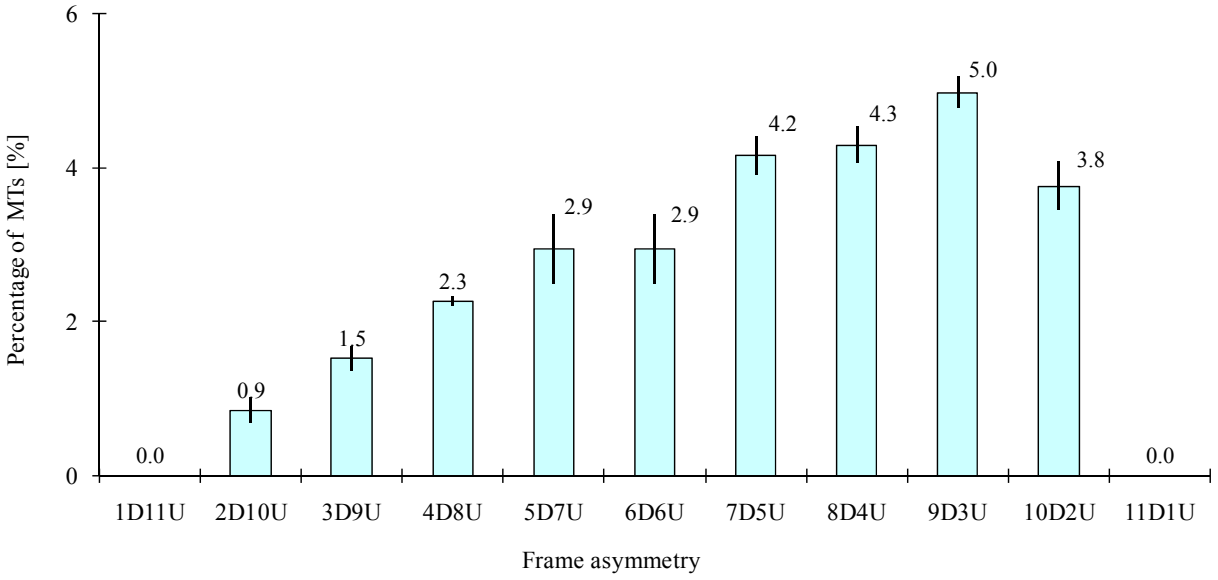

Figure F.8 – Reduced MTs due to E_b/N_o below target when using more than one TS UL.

In UL the behavior is the same, as more MTs are allocated in each TS, creating higher values of interference, leading to an increase of reduced MTs per BS in the network.

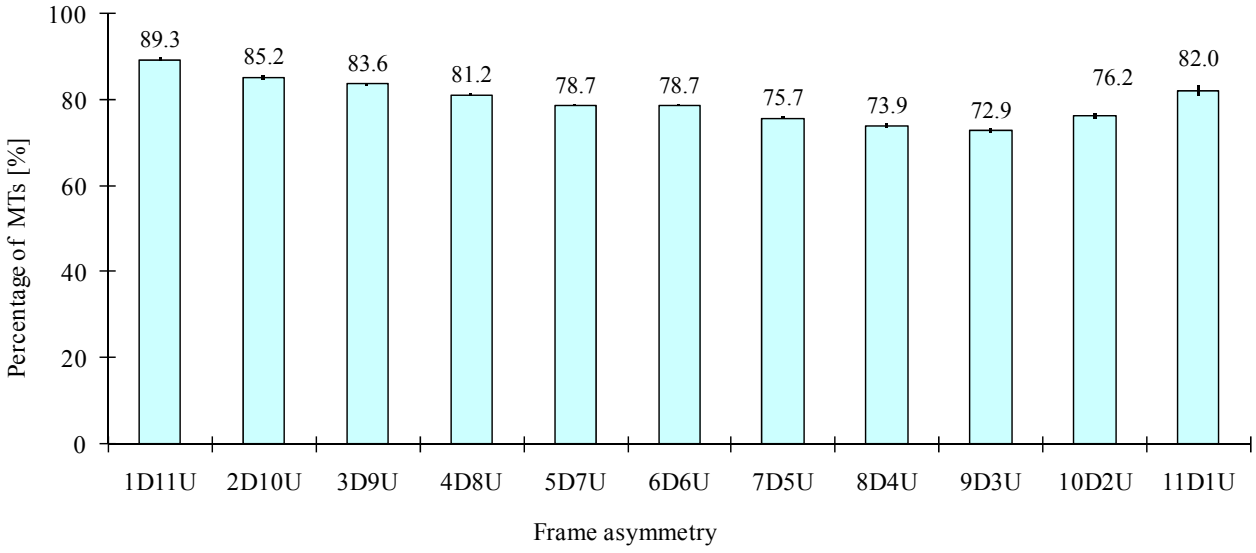

Figure F.9 – Percentage of MTs servicing after considering interference effects.

Intimately related to the probability of forced termination, it can be seen that for the asymmetries were 1920 kbps and 384 kbps MTs can start servicing in DL, the rise of interference results in higher values of P_{ft} and lower number of MTs servicing in the whole network, Figure F.10. As the number of TS for the UL start to be insufficient the number of HBR MTs drops and also interference, allowing more MTs servicing due to the decrease of

global network interference.

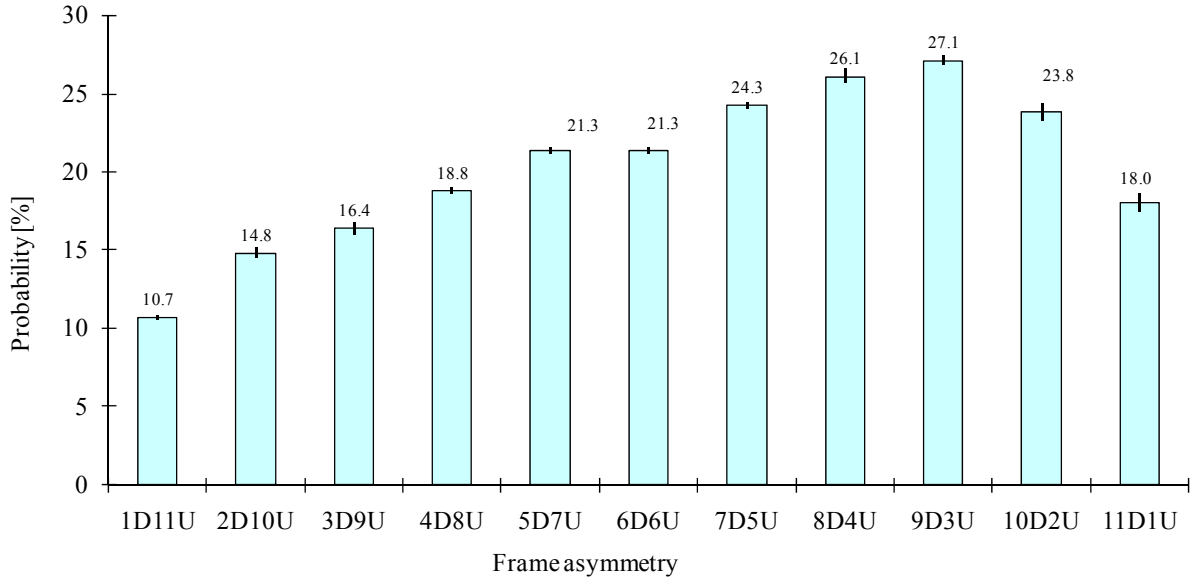

Figure F.10 – Probability of forced termination due to interference.

As more TS are available in DL the number of MTs servicing per BS increases, as well as the total interference inside the cell, Figure F.11. As more MTs are allocated in the TS, the higher is the interference power. One notices that the 9D3U and 10D2U asymmetries are the ones that present smaller values of intra-cell interference, being the asymmetries that make sense consider. This is due to the fact that higher HBR MTs start servicing, namely the 1920 kbps MTs, rising the interference levels and creating higher values of P_{ft}, resulting in a lower intra-cell interference power. The same behavior is valid for the UL and also for the inter-cell interference in both links, as seen in the following figures.

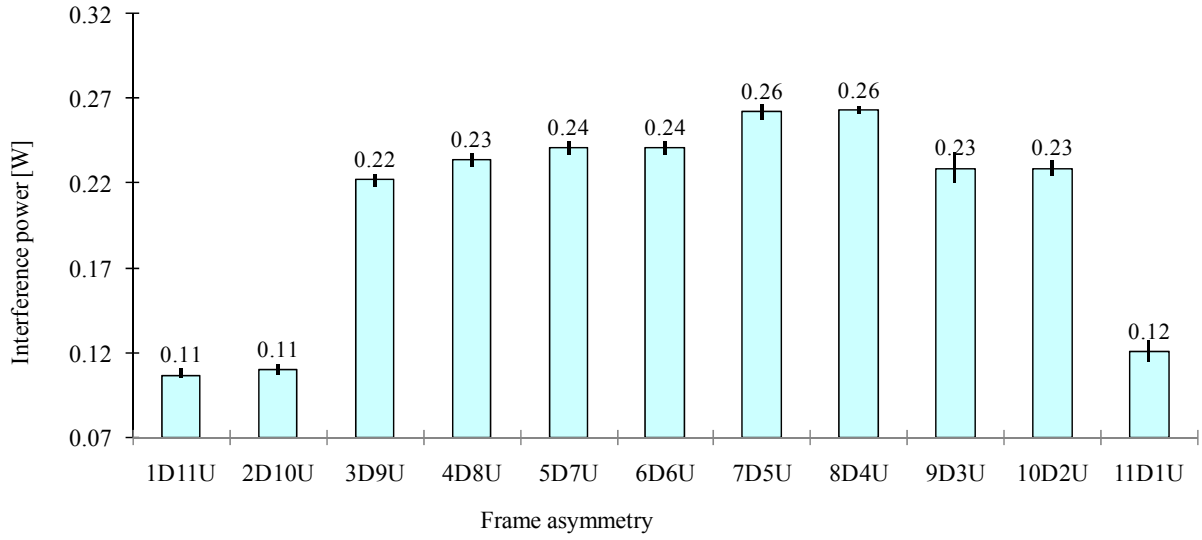

Figure F.11 – Intra-cell interference in DL.

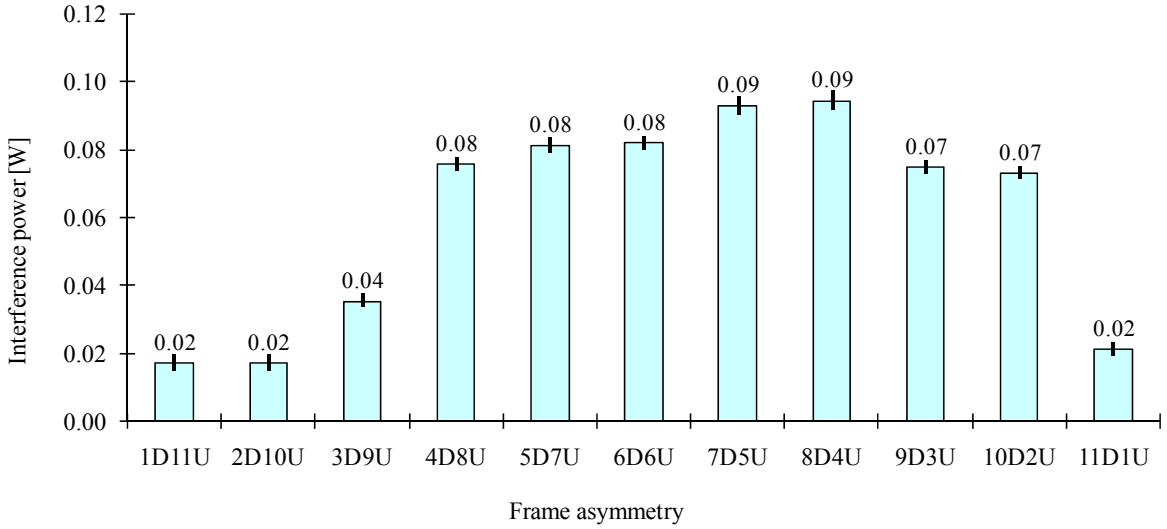

Figure F.12 – Intra-cell interference in UL.

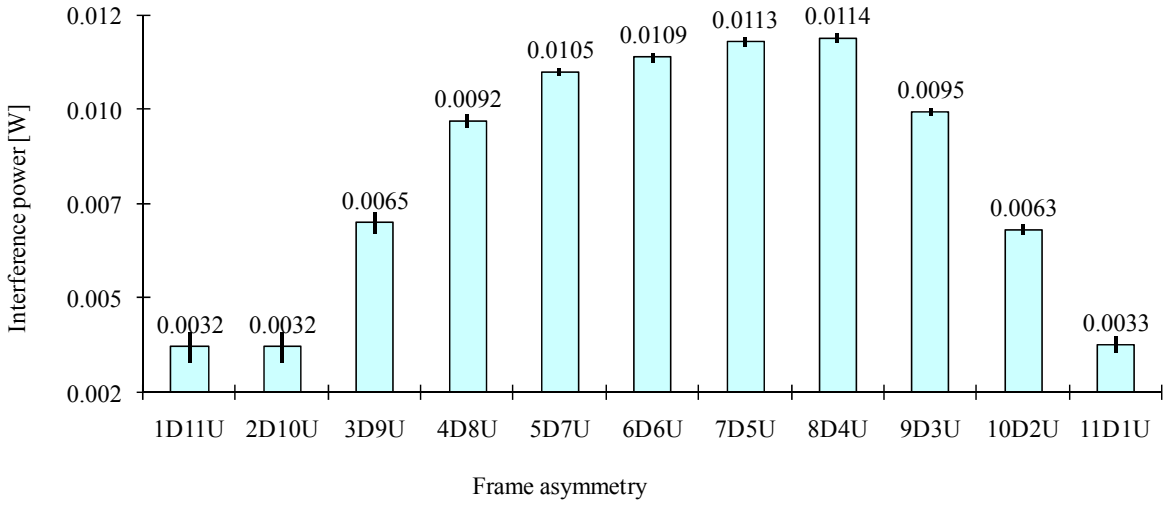

Figure F.13 – Inter-cell interference in UL.

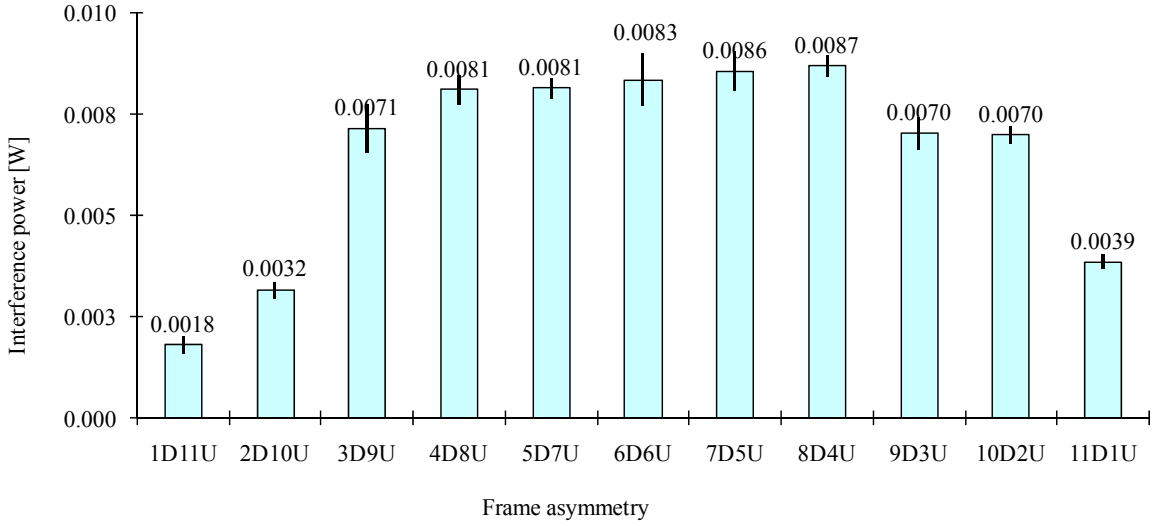

Figure F.14 – Inter-cell interference in DL.

Figures F.15 and F.16 show the weight of each interference component in the whole network's interference. In DL the intra-cell interference is the major part of the whole interference, as expected. In the UL case, although the inter-cell interference rises, the intra-cell interference still remains as the majority of the interference of the whole network in the UL.

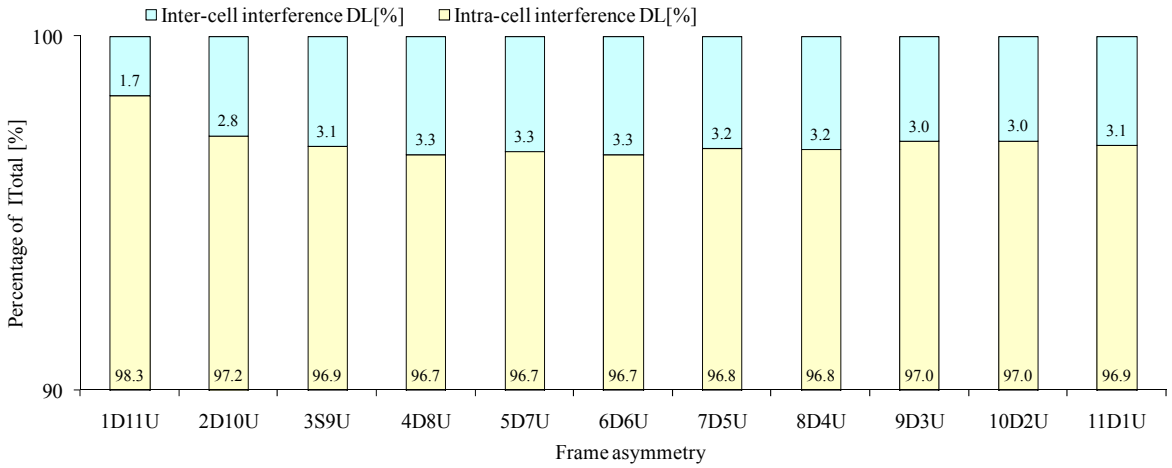

Figure F.15 – Intra- and Inter-cell interference contribution to global interference in DL.

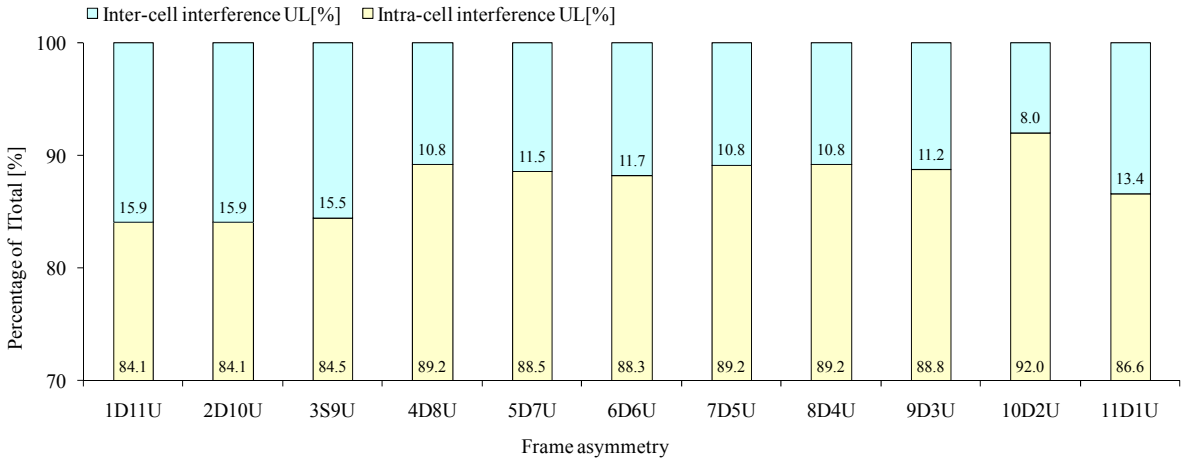

Figure F.16 – Intra- and Inter-cell interference contribution to global interference in UL.

Annex G

Network Asynchronism Statistics

This annex presents the additional statistics to the study of network asynchronisation as presented before in Chapter 5.

Figure G.1 presents the number of MTs servicing after considering the effects of interference for the different values of the asynchronism factor. Figure G.2 shows the number of reduced MTs due to non destructive interference. It can be seen that, from an MTs point of view, that until an asynchronism factor of 5 %, the number of MTs servicing does not rise, indicating that until that asynchronism factor the capacity gain is not noticeable. For asynchronism factors higher than 5 % it can be seen that the number of servicing MTs increases to a mean value of 84 %, representing a total of 10 % more MTs servicing in the network.

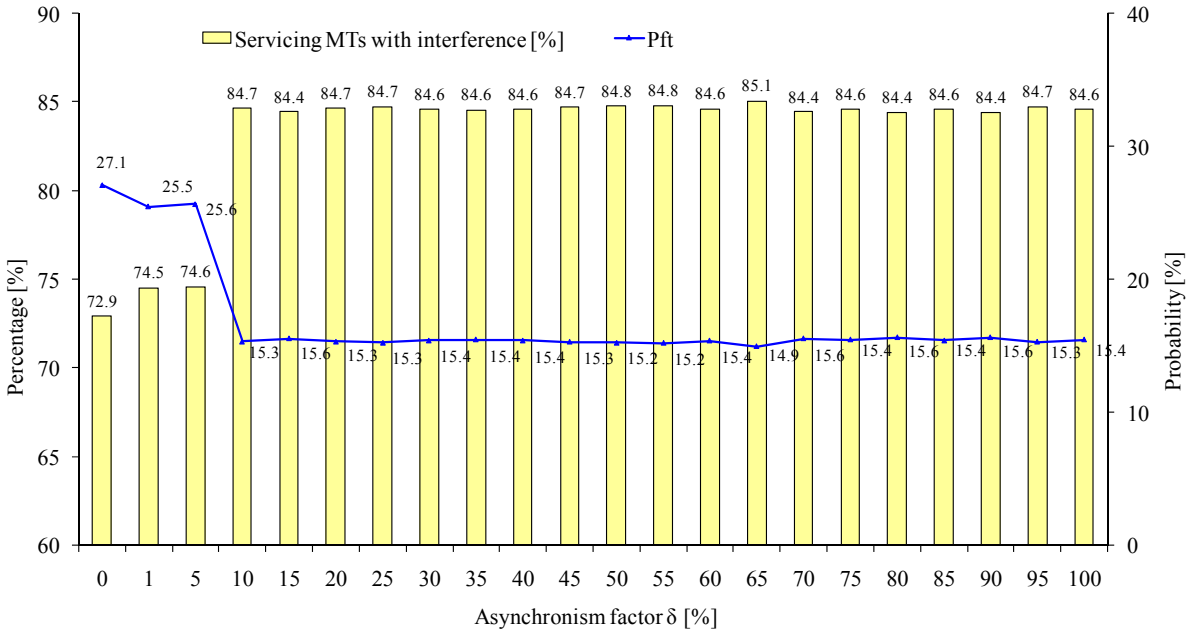

Figure G.1 – Influence of δ_{offset} on the probability of forced termination and servicing MTs.

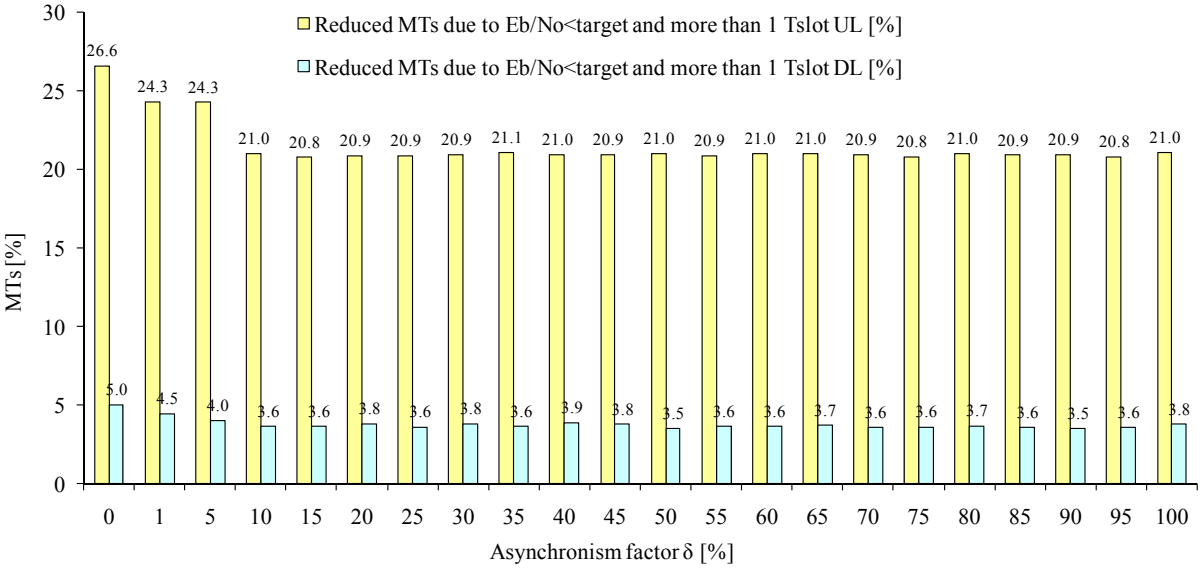

Figure G.2 – Influence of δ_{offset} on non-destructive interference.

As for the P_{ft}, naturally, it drops about 12 % when compared with the asynchronism result of 27.1 % P_{ft} for the 9D3U asymmetry. Also, it can be seen from Figure G.2 that the number of reduced MTs drops 6 % in the DL and 1.5 % in the UL, when compared with the synchronism case.

Figures G.3 and G.4 show interference behavior between adjacent BSs and between MTs and BSs, respectively, when synchronism offset is considered.

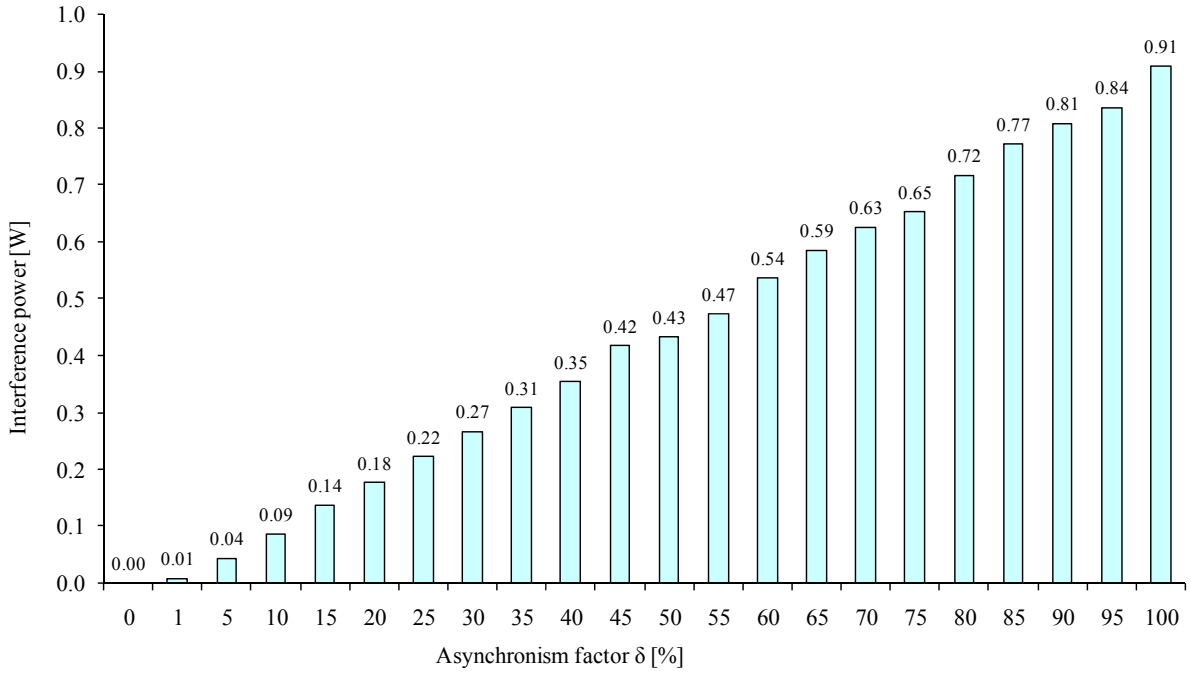

Figure G.3 – Influence of δ_{offset} on the inter-cell interference power between BSs.

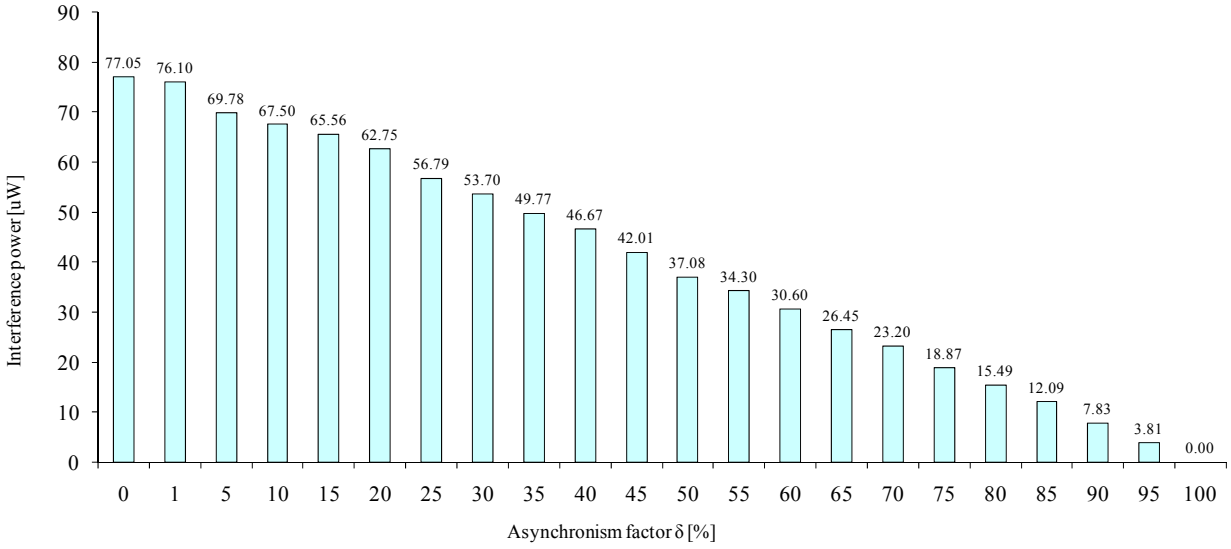

Figure G.4 – Influence of δ_{offset} on the inter-cell interference power between MT and BS.

As seen from Figure G.4, as expected from the theoretical interference model, the interference between the MTs and BS in UL reduces as δ_{offset} increases.

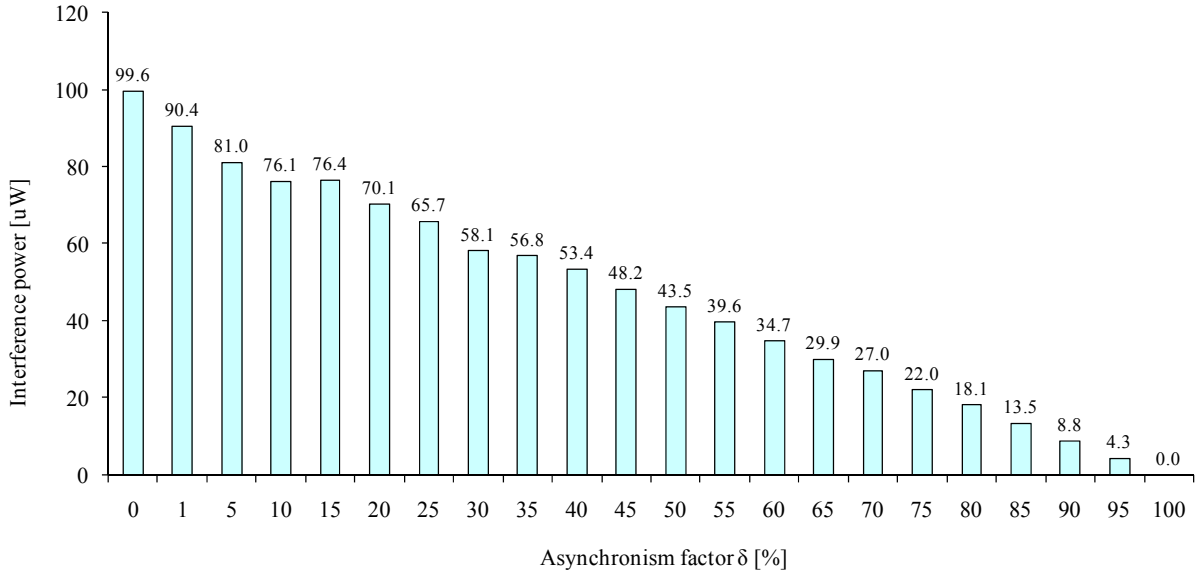

Figure G.5 – Influence of δ_{offset} on the inter-cell interference power between BS and MTs.

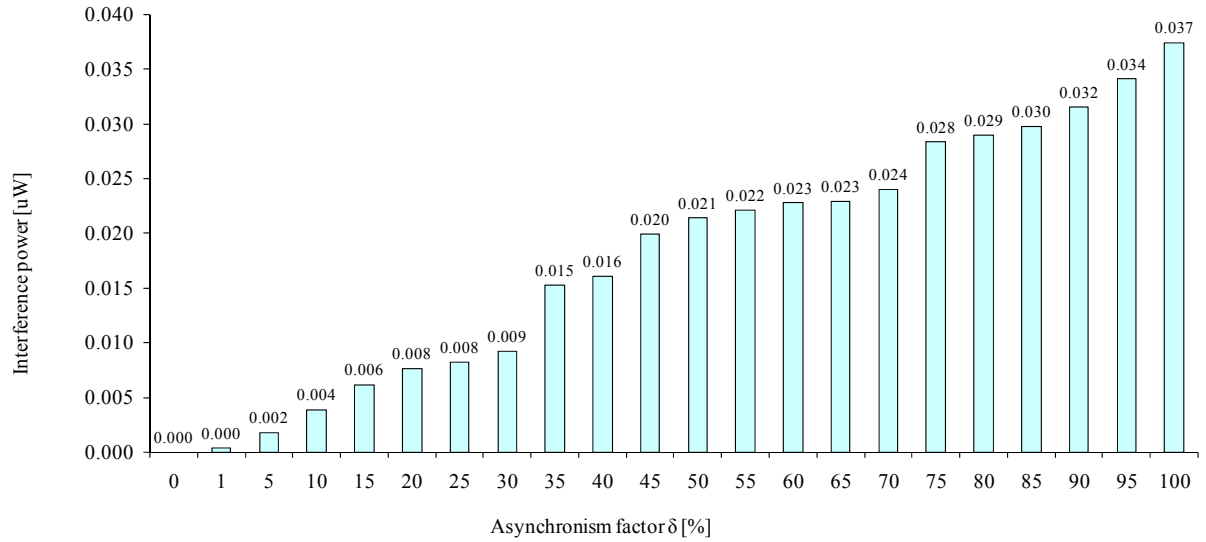

Figure G.6 – Influence of δ_{offset} on the inter-cell interference power between MT and MT.

In UL, the interference between the BS and MTs drops, as expected, while the interference between MTs increases. As seen before, taking into consideration that interference between MTs is 10^3 times lower than the interference between MT and BS; its effects are not noticeable as were the effects of the interference rise between BSs in the DL. Figure G.7 presents the intra-cell interference in both links.

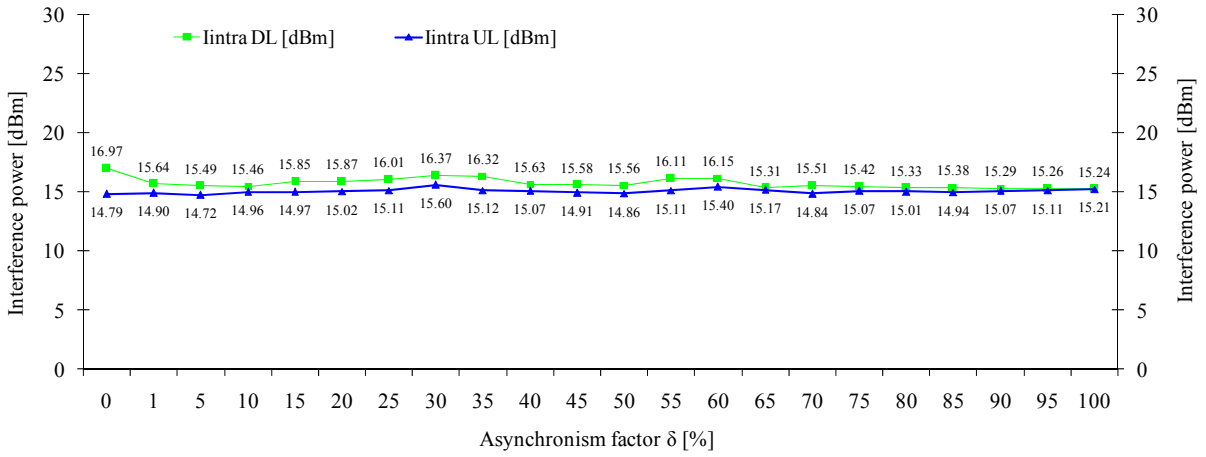

Figure G.7 – Intra-cell interference in UL and DL.

Note that the intra-cell interference does not depend on the value of δ_{offset}. Its behavior does not depend on δ_{offset} but it is still presented for the several values of δ_{offset} in order to relate them to the total interference values. The intra-cell interference in the UL and DL is quite similar, even in the values of interference power, due to the fact that MTs and BSs have the same transmission power, are fixed from each point of view between it selves, and to the fact that the propagation model used in both links is similar. This leads to losses and interference power levels very close to each other.

Annex H

Software User's Manual

This annex presents MT's manual for the developed simulator taking into account that TDD of operation was created from the start and added to the existing simulator.

This MT's guide focuses only on the windows used to configure the simulator for operation on TDD and also to configure the interference algorithm parameters. For the correct configuration of FDD refer to [SeCa04].

The first step consists in importing demographical data. This data is comprised of three files, two of them related to the characteristics of the terrain and districts and the last one related to non-uniform MT distribution over that terrain. Figure H.1, shows the window that allows importing these files.

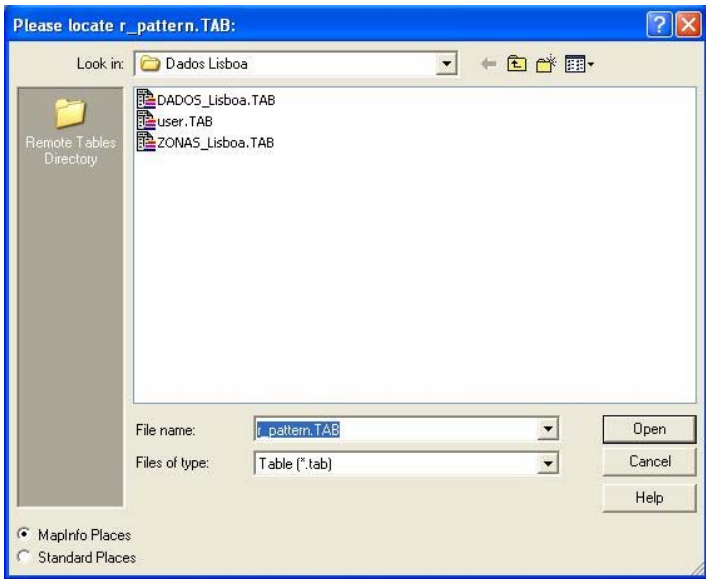

Figure H.1 – Window for importing the demographic data files.

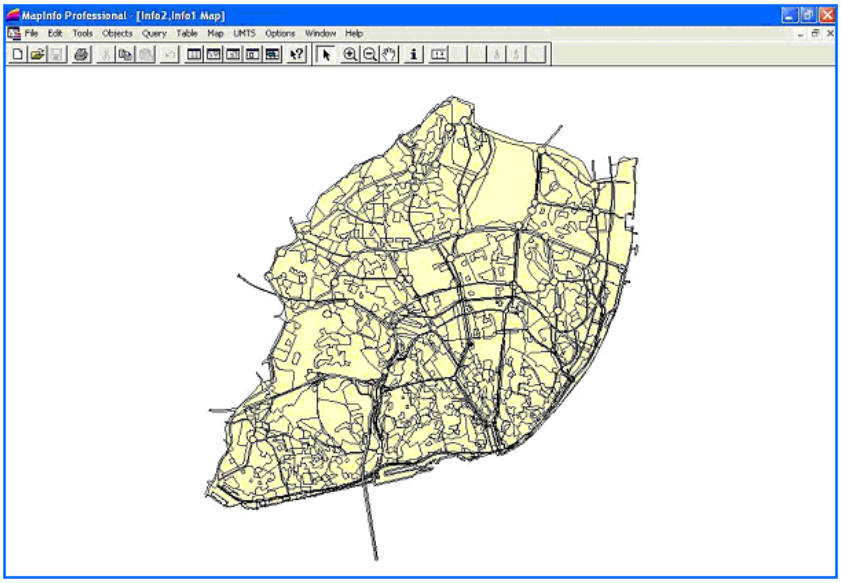

Figure H.2 – Simulator aspect with map of Lisbon

Figure H.2 shows the simulator main window after the demographic files are all read, displaying the terrain and the area of interest.

Figure H.3, presents the window where the configuration of the services penetration rates can be made.

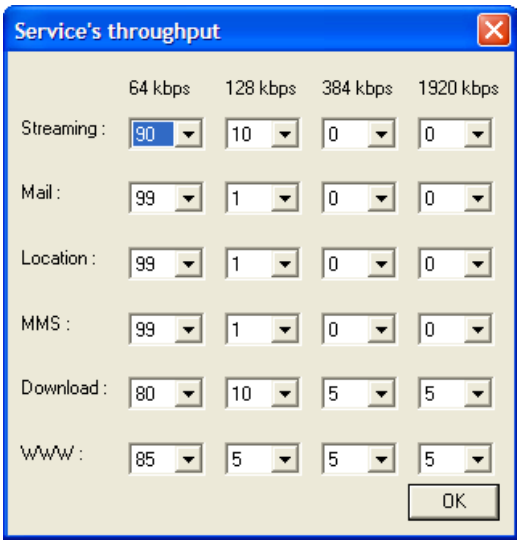

Figure H.3 – Service's throughput window.

In order to visually represent MTs in the map and easily relate them to each service, the window show in Figure H.4 allows assigning a color to each existing services. Note that values presented are not the ones of the reference scenario, being merely indicative.

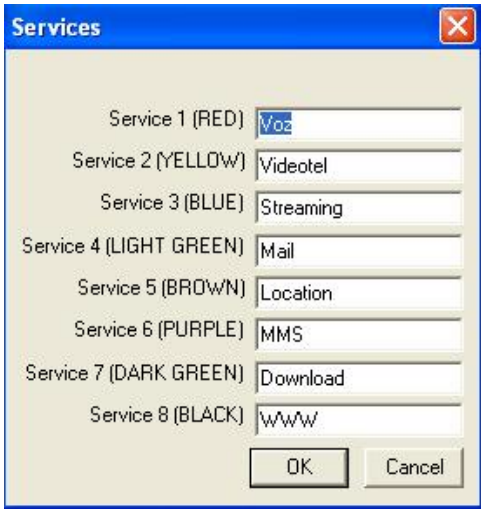

Figure H.4 – Relationship between map colors and MT services.

Figure H.5 shows the result of importing the terrain and MTs data and also the outcome of the relationship between the colors and services as defined in the window of Figure H.4. Also Figure F.5 presents the result of the configurations made on the penetration rates as shown in Figure H.3.

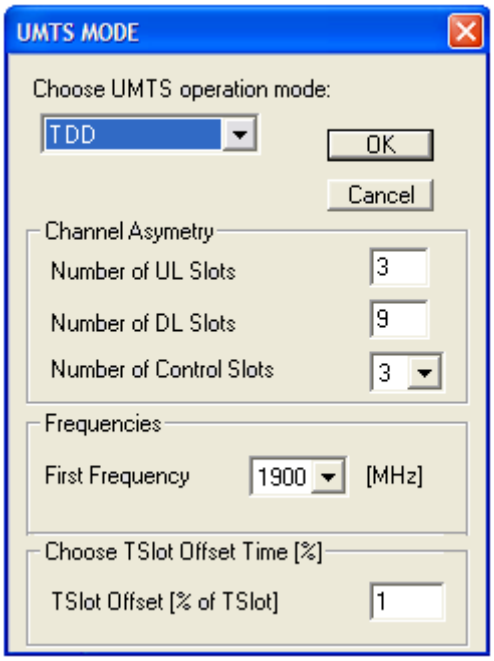

Figure H.5 – Configuration window for UMTS mode and interference algorithm.

Figure H.6 shows the results of inserting MTs in the region of interest. It is possible to associate the different colors with the different services, as configured in the window of Figure H.4.

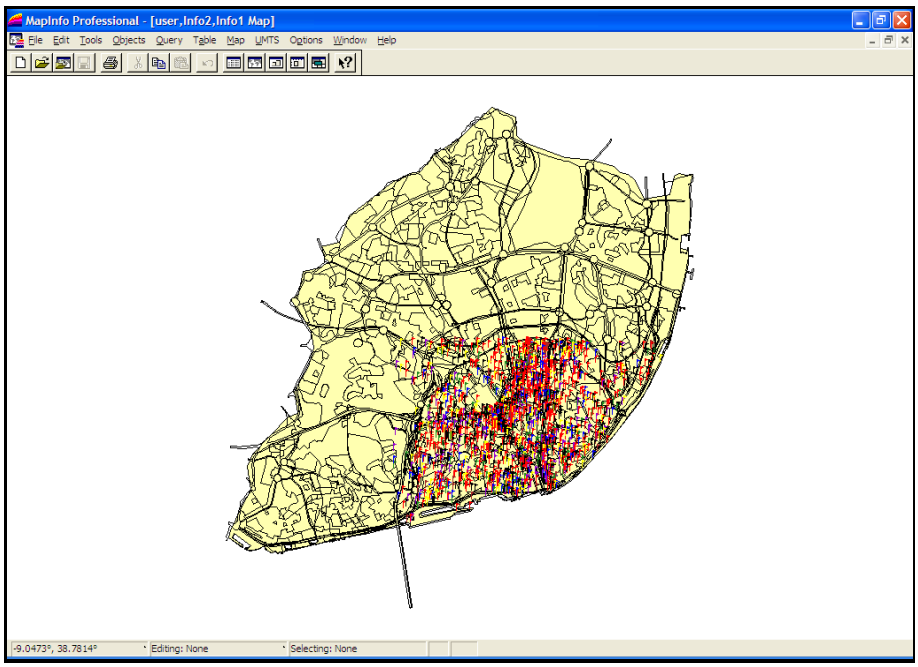

Figure H.6 – Reference scenario (Lisbon map) with TDD MTs inserted.

Figure H.7 shows the propagation model configuration window and its default parameters.

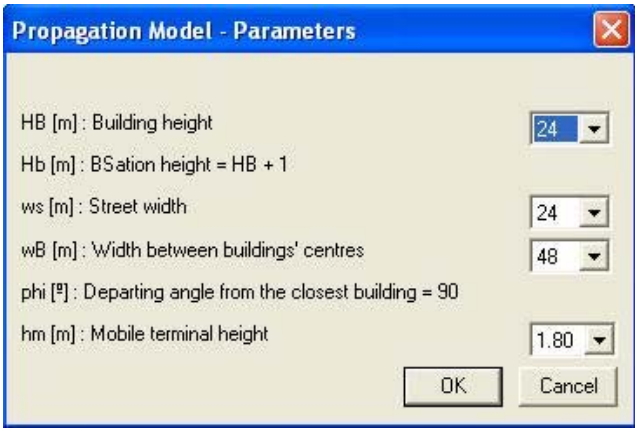

Figure H.7 – Configuration window for propagation model.

Figure H.8 shows the network coverage for TDD after inserting the 185 BSs and the region of interest for TDD analysis, centred in downtown Lisbon.

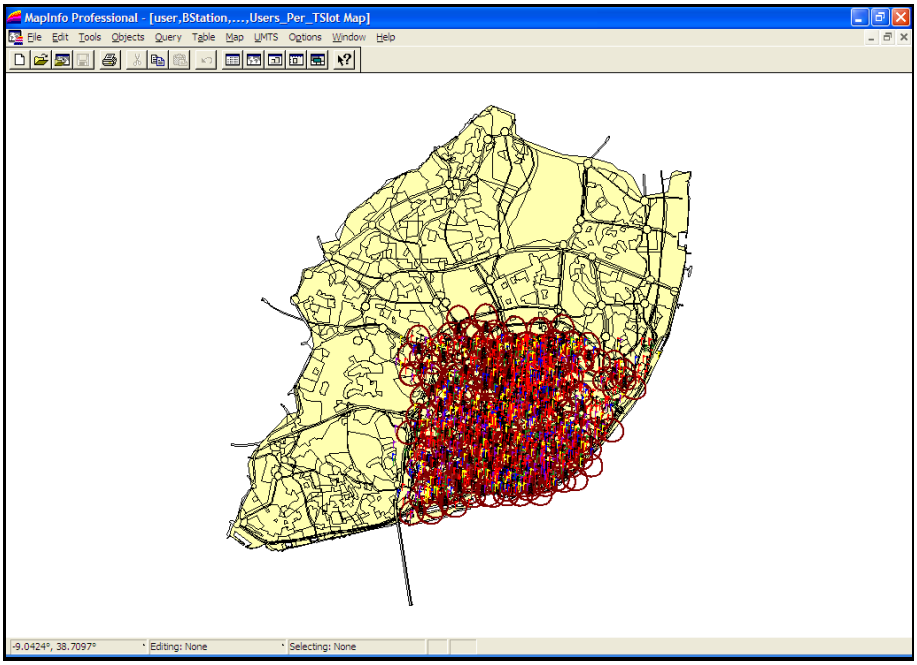

Figure H.8 – Coverage map of downtown Lisbon for TDD .

Figure H.9 presents an output window with several result and statistics of TDD parameters for all BSs. It is possible to have five different parameters in each of the fifteen TSs of the selected BS. These parameters can be found in greater detail in section 4.6 in Chapter 4.

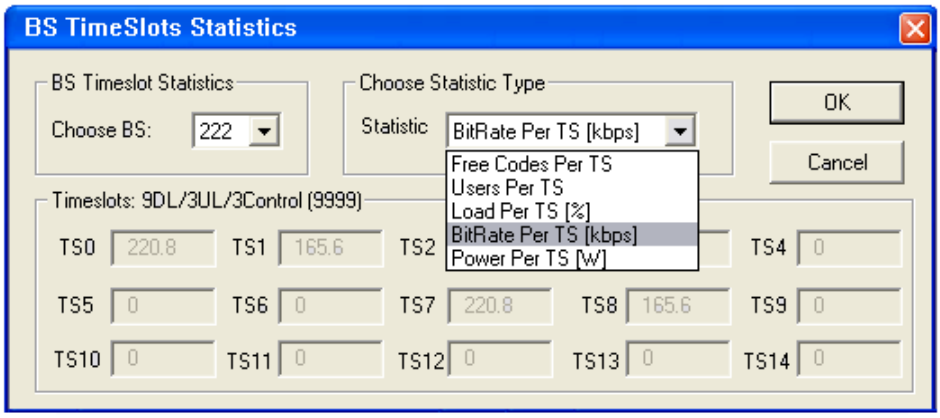

Figure H.9 – BS TS statistics in the end of simulation.

The developed simulator generates a set of output files. Each one of them has distinct contents from the others.

For the DL:

- *DL_IBS1MS1.stat*: interference between the BS and MTs of cell of interest;
- *DL_IBS2BS1.stat:* interference between BSs of adjacent cells;
- *DL_IBS2MS1.stat:* interference between the BS and MTs of adjacent cells;
- *DL_IMS2MS1.stat:* interference between MTs of adjacent cells.

For the UL statistics, one has the following output files:

- *UL_IBS1MS1.stat:* interference between the BS and MTs of cell of interest;
- *UL_IBS2BS1.stat:* interference between BSs of adjacent cells;
- *UL_IBS2MS1.stat:* interference between the BS and MTs of adjacent cells;
- *UL_IMS2MS1.stat:* interference between MTs of adjacent cells.

Other files and statistics:

- *BS_Interference.stat:* Interference statistics on every BS;
- *RB_TS_TDD.stat:* Bit Rate per TS;
- *Users_TS_TDD.stat:* Users per TS;
- *GerirRecursos.stat:* Results of the first RRM algorithm;
- *Codes_TS_TDD.stat:* codes per TS;
- *Load_TS_TDD.stat:* Load per TS;

With asynchronism considered the additional output files are:

- *TOFF _IBS1MS1.stat:* interference between the BS and MTs of cell of interest;
- *TOFF _IBS2BS1.stat:* interference between BSs of adjacent cells;
- *TOFF _IBS2MS1.stat:* interference between the BS and MTs of adjacent cells;
- *TOFF _IMS2MS1.stat:* interference between MTs of adjacent cells.

References

[3GPP00a] 3GPP, *UTRAN Overall Description*, Technical Specification, TSG 25.401, v.3.2.0, Mar. 2000

[3GPP00b] 3GPP, *QoS Concept and Architecture*, Technical Specification, Report No. 23.107, v.3.2.0, Mar. 2000

[3GPP03a] 3GPP, *User Equipment (UE) radio transmission and reception (FDD)*, Technical Specification, Report No. 25.101 v.6.3.0, Dec. 2003

[3GPP03b] 3GPP, *User Equipment (UE) radio transmission and reception (TDD)*, Technical Specification, Report No. 25.102 v.6.0.0, Dec. 2003

[3GPP03c] 3GPP, *Spreading and modulation (FDD)*, Technical Specification, Report No. 25.213 v.6.0.0, Dec. 2003

[3GPP03d] 3GPP, *Physical channels and mapping of transport channels onto physical channels (FDD)*, Technical Specification, Report No. 25.211 v.6.0.0, Dec. 2003

[3GPP03e] 3GPP, *Physical layer - General description*, Technical Specification, Report No. 25.201 v.6.0.0, Dec. 2003

[3GPP04] 3GPP, *RF System Scenarios*, 3GPP Technical Specification Group Radio Access Networks, Report No. 25.942 v.6.3.0, Mar. 2000.

[CMLi06] Câmara Municipal de Lisboa (*Lisbon Town Hall*), Urbanism and Planning Division, 2006.

[Corr99] Correia,L.M., *Mobile Communications – Parts I and II* (in Portuguese), Course Notes, Instituto Superior Técnico, Lisbon, Portugal, Mar. 1999.

[DaCo99] Damosso,E. and Correia,L.M. (eds.), *Digital Mobile Radio Towards Future Generation Systems – COST 231 Final Report*, COST Office, Brussels, Belgium, 1999.

[DaMo97] Das,K. and Morgera,D., "Interference and SIR in Integrated Voice/Data Wireless DS-CDMA Networks - A Simulation Study", *IEEE Journal on Selected Areas Communications*, Vol. 15, No. 8, Oct. 1997, pp. 1527-1538.

[ETSI98] ETSI, TR 101.112 v3.2.0, *Selection procedures for the choice of radio transmission technologies of the UMTS*, 1998.

[FeCS00] Ferreira,L., Correia,L. M. and Serrador,A., *Characterisation Parameters for UMTS Services and Applications*, IST-MOMENTUM Project, Deliverable D1.2, IST-TUL, Lisbon, Portugal, Mar. 2000.

[HoTo01] Holma,H. and Toskala,A., *WCDMA for UMTS*, John Wiley & Sons, Chichester, UK, 2001.

[HoTo06] Holma,H. and Toskala,A. (eds.), *HSDPA/HSUPA for UMTS*, John Wiley & Sons, Chichester, UK, 2006.

[HSLT00] Holma,H., Heikkinen,S., Lehtinen,O., and Toskala,A., "Interference considerations for the time division duplex mode of the UMTS terrestrial radio access", *IEEE Journal on Selected Areas in Communications*, Vol.18, No. 8, Aug. 2000, pp. 1386-1393.

[KwWa95] Kwok,M. and Wang,H., "Adjacent cell interference analysis of reverse-link in CDMA cellular radio systems", *6th IEEE International Symposium on Personal, Indoor and Mobile Radio Communications,* Toronto, Canada, Oct. 1995.

[LaWN02] Laiho,J.,Wacker,A. and Novosad,T. (eds.), *Radio Network Planning and Optmisation for UMTS*, John Wiley & Sons, Chichester, UK, 2002.

[LKCW96] Lee, D., Kim,D., Chung,Y. and Whang,C., "Other-cell interference with power control in macro/microcell CDMA networks", *46th IEEE Vehicular Technology Conference*, Atlanta, CA, USA, Apr. 1996.

[MOME04] MOMENTUM, *Models and Simulations for Network Planning and Control of UMTS*, IST-MOMENTUM Project. http://www.zib.de/projects/telecommunication/MOMENTUM/

[NgDa03] Nguyen,T. and Dassanayke,V., "Estimation of Inter-cell Interference in CDMA Macro Cells", *Australian Telecommunications, Networks and Applications Conference*, Melbourne, Australia, Dec. 2003.

[Pires07] Pires, L., *Optimisation of UMTS-TDD Base Stations Location for Non-Uniform Traffic Distributions*, M. Sc. Thesis, IST-Technical University of Lisbon, Lisbon, Portugal, Dec. 2007.

[QiWD00a] Qingyu,M., Wenbo,W. and Dacheng,Y., "An investigation of inter-cell interference in UTRA-TDD system", *52nd IEEE Vehicular Technology Conference*, Boston, MA, USA, Oct. 2000.

[QiWD00b] Qingyu,M., Wenbo,W. and Dacheng,Y.,"An investigation of interference between UTRA-TDD and FDD system", *International Conference on Communication Technology Proceedings*, Beijing, China, Aug. 2000.

[SeCa04] Sebastião,D. and Cardeiro,J. *Modelling and Dimensioning Traffic in UMTS Radio Interface* (in Portuguese), Graduation Project, Instituto Superior Técnico, Technical University of Lisbon, Lisbon, Portugal, Nov. 2004.

[SLHW02] Staehle,D., Leibnitz,K., Heck,K., Schröder,B., Weller,A. and Tran-Gia P., *An Approximation of Othercell Interference Distributions for UMTS Systems using Fixed-Point Equations*, Report No. 292, University of Würzburg, Würzburg, Germany, Jan. 2002.

[Thom03] Thompson,D.E., "Modelling Adjacent Channel Interference in 3G Networks", *5th European Personal Mobile Communications Conference*, Glasgow, UK, Apr. 2003.

[Xia97] Xia, H.H., "A simplified analytical model for predicting path loss in urban and suburban environments", *IEEE Transactions on Vehicular Technology,* Vol. 46, No. 4, Nov. 1997, pp. 1040-1046.